

SOFTCOPY PHOTOGRAMMETRIC TECHNIQUES FOR MAPPING
MOUNTAINOUS TERRAIN: GREAT SMOKY MOUNTAINS NATIONAL PARK

by

THOMAS R. JORDAN

(Under the Direction of Dr. Roy A. Welch)

ABSTRACT

Softcopy photogrammetric techniques were adapted for use in the establishment of a seamless digital geographic information system (GIS) database and vegetation maps for Great Smoky Mountains National Park in the southern Appalachian Mountains – an area of approximately 2000 square kilometres. This difficult mapping project presented a number of challenging problems resulting from extreme terrain relief, the near-continuous canopy cover and the lack of roads and cultural features that precluded the use of conventional methods for identifying and measuring the coordinates of ground control points (GCPs). Issues addressed included generation of ground control using analytical aerotriangulation and differential rectification of vegetation overlays to correct for displacements caused by relief in aerial photographs.

As part of a cooperative agreement between the Center for Remote Sensing and Mapping Science, The University of Georgia, and the National Park Service, softcopy photogrammetric procedures were employed with approximately 1000 large-scale color-infrared aerial photographs corresponding to 17 U.S. Geological Survey (USGS) 1:24,000-scale topographic quadrangles in the Park. Ground control points identified on USGS Digital Orthophoto Quarter Quadrangles with elevations extracted from USGS Digital Elevation Models were employed with analytical aerotriangulation methods to compute the X, Y, Z ground coordinates of over 4300 GCPs and pass points - enough to permit differential rectification of the aerial photographs and associated overlays. The $RMSE_{XY}$ error at 1195 GCPs used in the aerotriangulation adjustment was ± 12.6 m.

The photo coordinates of the GCPs were mathematically registered to photo interpretation overlays using fiducial marks and employed to orthorectify the overlays. The vegetation polygons on the raster overlays were then converted to vector format and transferred to the GIS database where they were edited, edge-matched with adjacent overlays and assigned attributes according to the vegetation classification system.

INDEX WORDS: Softcopy photogrammetry, Digital mapping, Natural resources, Vegetation mapping, Aerotriangulation, Orthophotos, Geographic information systems, Great Smoky Mountains National Park

SOFTCOPY PHOTOGRAMMETRIC TECHNIQUES FOR MAPPING
MOUNTAINOUS TERRAIN: GREAT SMOKY MOUNTAINS NATIONAL PARK

By

THOMAS R. JORDAN

B.S., The University of Georgia, 1979

M.A., The University of Georgia, 1981

A Dissertation Submitted to the Graduate Faculty of The University of Georgia in Partial
Fulfillment of the Requirements for the Degree

DOCTOR OF PHILOSOPHY

ATHENS, GEORGIA

2002

© 2002

Thomas R. Jordan

All Rights Reserved

SOFTCOPY PHOTOGRAMMETRIC TECHNIQUES FOR MAPPING
MOUNTAINOUS TERRAIN: GREAT SMOKY MOUNTAINS NATIONAL PARK

By

THOMAS R. JORDAN

Approved:

Major Professor: Roy A. Welch

Committee: Hamid Arabnia
Rex Clark
Thomas Hodler
Clifton Pannell

Electronic Version Approved:

Gordhan L. Patel
Dean of the Graduate School
The University of Georgia
May 2002

DEDICATION

This dissertation is dedicated to my wife, Mary.

ACKNOWLEDGMENTS

I would like to thank my wife, Mary Mayes, and our two sons, Charles and Ben, for sticking with me, supporting me and encouraging me through this long process – especially for the last difficult months. They are the best! My parents, Bob and Sandy Jordan, made it financially possible for me to pursue the Ph.D. – they thought it was a good idea all along. I also like to thank Joe and Virginia Mayes and Cathie and Hugh Hudson for letting me use vacations and other family times to worry about writing.

This dissertation reports on a portion of a larger project undertaken by the Center for Remote Sensing and Mapping Science and I could not have collected the massive amounts of data required for this work without help from people who work there. I would like to especially thank Qiqi Lu, Chris Watson and John Dolezal for finding points on all those hundreds of photographs. My friend, Marguerite Madden, was there every day, working with me on the project and providing moral support as I finally got going on the writing. Thanks, too, to Phyllis Jackson and Thom Litts for being there whenever I had questions I couldn't answer about trees or esoteric ARC/INFO operations.

Finally, I'd like to recognize Dr. Roy Welch, major professor, boss, partner and friend, for all he has done to help me earn this degree. I literally could not have done it without his help.

Funding for this project was provided by the U.S. Department of Interior, National Park Service, Great Smoky Mountains National Park (Cooperative Agreement No. 1443-CA-5460-98-019).

TABLE OF CONTENTS

	Page
ACKNOWLEDGEMENTS	v
LIST OF TABLES	viii
LIST OF FIGURES	ix
PREFACE	xiv
CHAPTER	
1 INTRODUCTION	1
Objectives of the Dissertation	1
Great Smoky Mountains National Park	2
Geographic Information Systems for Park Management.....	8
The Great Smoky Mountains National Park Vegetation Mapping Project	10
Organization of the Dissertation	12
2 NATURAL RESOURCE MAPPING IN AREAS OF HIGH RELIEF.....	14
Types of Mapping Tasks.....	14
Mapping Project Requirements and Considerations.....	16
Mapping From Aerial Photographs	20
Rectification of an Aerial Photograph	29
Aerotriangulation	55
Vegetation Mapping Projects in National Park Lands.....	66

3	CONTROL EXTENSION TECHNIQUES AND RECTIFICATION	
	PROCEDURES REQUIRED FOR GIS DATABASE DEVELOPMENT	79
	Data Sets	79
	Photointerpretation Overlays, Control Extension and Rectification	
	Procedures Employed to Create the Database	88
4	SOFTCOPY PHOTOGRAMMETRY AS THE FOUNDATION FOR GIS	
	DATABASE DEVELOPMENT.....	133
	Control Extension and Aerotriangulation	133
	Development of the Vegetation Maps and GIS Database	146
5	SUMMARY AND CONCLUSION	161
	Summary	161
	Future Mapping of National Parks.....	163
	Conclusion	166
6	REFERENCES	167
	APPENDICES	177
	A. Camera Calibration Data for Wild RC20 Camera SN# 5132	177
	B. List of USGS Quadrangles, NPS abbreviations, Revision Dates	178
	C. Photo Center, GCP and Pass Point Maps.....	179

LIST OF TABLES

Table 2-1.	Displacements due to earth curvature and atmospheric refraction for aerial photographs at 2000 m AGL.....	25
Table 2-2.	Relief displacement calculated for a photograph exposed with a standard mapping camera (f=152.4 mm) from a flying height (FH) of 2000 m above mean terrain (AMT)	28
Table 2-3.	NPS Vegetation Mapping Project. Completed and partially completed National Monuments (NM), Seashores (NS), Historical Sites (NHS) and Parks (NP)	74
Table 3-1.	Data sources used in the map/database development for Great Smoky Mountains National Park.	81
Table 3-2.	Color-infrared photographs for the Great Smoky Mountains National Park vegetation mapping project	89
Table 3-3.	USGS topographic quadrangles in the Great Smoky Mountains National Park and the number of photographs in each.....	92
Table 3-4.	Abbreviated PC GIANT report (GIANT.OUT).....	115
Table 3-5.	Over 38,000 individual polygons have been mapped in 17 quadrangle areas in Great Smoky Mountains National Park.....	132
Table 4-1.	Summary of aerotriangulation results by quadrangle	136

LIST OF FIGURES

Figure 1-1.	Location of Appalachian Mountains chain and Great Smoky Mountains National Park in eastern United States.....	3
Figure 1-2.	The Great Smoky Mountains are named after the blue haze that often covers the landscape	4
Figure 1-3.	The climate of the area surrounding the Great Smoky Mountains National Park is characterized by mild temperatures and moderate rainfall	5
Figure 1-4.	Perspective view of Great Smoky Mountains National Park looking east across a mosaic of SPOT multispectral images draped over a DEM	5
Figure 1-5.	Three of the major vegetation communities found in the Great Smoky Mountains National Park.	7
Figure 1-6.	National Park Service map showing the roads and major cultural features in and around Great Smoky Mountains National Park	9
Figure 1-7.	Great Smoky Mountains National Park is covered by 25 USGS 1:24,000-scale topographic quadrangles	11
Figure 2-1.	A Wild RC20 camera system similar to the one employed to record the photographs for the Great Smoky Mountains National Park mapping project	21
Figure 2-2.	The features of an aerial photograph	22
Figure 2-3.	Calibrated lens distortion curves of several modern mapping cameras.....	22
Figure 2-4.	The combined effects of earth curvature and atmospheric refraction.....	25
Figure 2-5.	Image displacement (de) due to relief in a vertical photograph for an object above a horizontal datum	27
Figure 2-6.	Relief displacement is radial from the center of a vertical photograph	27
Figure 2-7.	The elements of exterior orientation include three rotations angles omega, phi and kappa about the X-, Y- and Z-axes, respectively, and the coordinates of the exposure center (X_L , Y_L , Z_L).....	30
Figure 2-8.	Tilt causes scale variations across the photograph. In this example, the tilt direction is perpendicular to the direction of flight.....	30
Figure 2-9.	a) On standard 21 cm x 28 cm scanners, the full format of the aerial photograph, including all of the fiducial marks, cannot be scanned.....	33
Figure 2-10.	Epson Expression 836XL desktop scanner.....	34

Figure 2-11.	A digital image is structured as a matrix, or array, of digital numbers arranged in columns and rows	36
Figure 2-12.	GCPs should be well distributed throughout the entire photograph	39
Figure 2-13.	Detail of Thunderhead Mountain DRG file	41
Figure 2-14.	The layout of ten NAPP photographs relative to a typical 1:24,000 USGS 7.5-minute topographic quadrangle (photo centers falling within the quadrangle are marked by small black circles).....	43
Figure 2-15.	USGS 7.5-Minute DEM for the Thunderhead Mountain Quadrangle. a) Gray scale rendition where higher elevations are represented as lighter shades of gray. b) Hill shaded rendition of the Thunderhead Mountain DEM.....	45
Figure 2-16.	Image control points are digitized by zooming in on the image and clicking on the point location using the computer mouse.....	47
Figure 2-17.	Ground control points identified on both the image (scanned aerial photograph) and reference map are used to rectify an aerial photograph..	49
Figure 2-18.	Matrix of geometrically correct output pixels imposed on matrix of original, distorted input pixels	52
Figure 2-19.	The collinearity condition and definition of six exterior orientation elements for a single photo	53
Figure 2-20.	Schematic layout of a block of air photos showing nominal locations of GCPs (triangles) and pass points (circles)	58
Figure 2-21.	Aerotriangulation process flow.....	59
Figure 2-22.	a) The raw image coordinate system has its origin (0, 0) in the upper left corner of the image. The origin of the photo coordinate system (b) is at the center of the photo as defined by the intersection of the fiducial marks.....	61
Figure 2-23.	Spatial intersection enforces the collinearity condition to compute the X, Y, Z ground coordinates of pass points identified on two or more photographs.....	63
Figure 2-24.	Location map of Everglades National Park, Big Cypress National Preserve, Biscayne National Park, and Florida Panther National Wildlife Refuge.....	71
Figure 2-25.	Portion of the Everglades vegetation map database and corresponding photo showing an area along the south coast of Everglades National Park	72
Figure 2-26.	1:12,000-scale color-infrared aerial photograph of Glacier National Park recorded as part of the vegetation mapping project.....	76

Figure 3-1.	The Great Smoky Mountains vegetation mapping project requires the integration of mapping technologies to create a GIS database	80
Figure 3-2.	The organization of DOQQ within a DOQ.....	83
Figure 3-3.	Portion of the Clingmans Dome DRG showing the DLG transportation (red) and hydrography layers (blue) as overlays.....	86
Figure 3-4.	A representative large-scale color-infrared aerial photograph (# 10064) in the vicinity of Thunderhead Mountain	87
Figure 3-5.	Map of Great Smoky Mountains National Park study area showing the USGS quadrangle boundaries, flight lines and photo centers.....	90
Figure 3-6.	The photo index map for the Silers Bald Quadrangle shows the gridded pattern of photo exposure centers	91
Figure 3-7.	Diagram showing the relationships between photogrammetric, photointerpretation and GIS operations	94
Figure 3-8.	The photograph is placed on the bed of the scanner in preparation for scanning	96
Figure 3-9.	DMS point transfer dialog	99
Figure 3-10.	Point transfer graphics screen showing two images side by side	100
Figure 3-11.	A specific tree crown identified on 2 photos (indicated by the “X”) is selected as a pass point	101
Figure 3-12.	Pass points are numbered according to the photo frame number and position on the photo (01, 02, 03).....	103
Figure 3-13.	Point transfer procedure for measuring pass points along a flight line....	103
Figure 3-14.	An ideal pass point is one that is a well-defined geometric feature.....	104
Figure 3-15.	Tree crowns are frequently distorted by relief displacement when they are located near the edge of the photo	105
Figure 3-16.	Typical examples of GCP locations. a) A good quality GCP is located at a road intersection, driveway or some other distinct location. b) Indistinct points identifiable only by shape or implication make poor GCPs	107
Figure 3-17.	Elevations of GCPs are extracted from USGS DEMs using a bilinear interpolation algorithm.....	108
Figure 3-18.	Flight lines and photo centers for Great Smoky Mountains National Park. Flight lines 1 through 6 and 12 through 18 were recorded in October 1997. Photographs located in the central area of the park (flight lines 7-11) were recorded in October 1998. Photos for flight lines 19-27 (on the north side of the park) were recorded in May 1997.....	110

Figure 3-19.	The significant difference in the appearance between fall and spring photography made identification of pass points between flight lines 18 and 19 very difficult. a) The overlap area between photographs 18015 and 19015 (Luftee Knob Quadrangle) contains a river to help orientation, whereas b) there are no visual cues in the 18026/19026 photo pair (Mt. Guyot Quadrangle) to help identify common features ...	111
Figure 3-20.	The aerotriangulation process flow using PC Giant	113
Figure 3-21.	Distribution of control and pass points in the Noland Creek Quadrangle.....	122
Figure 3-22.	A portion of the Noland Creek digital orthophoto mosaic constructed from about 24 individual orthophotos.....	123
Figure 3-23.	The user interface of the GRSM Utility program for orthorectification of vegetation overlays	125
Figure 3-24.	The procedure employed for orthocorrection of vegetation overlays. After conversion to vector format, the vectors are transformed to the UTM coordinate system and imported to the GIS for editing, edge-matching and attributing	126
Figure 3-25.	(a) Raw unedited vectors for a portion of the Noland Creek Quadrangle showing the correspondence of corrected polygons from adjacent overlays (shown in blue, green, magenta and red). (b) Vectors for the same area after editing and edge-matching in ARC/INFO	130
Figure 3-26.	Final edited and attributed map coverage for the sample Noland Creek Quadrangle area	131
Figure 4-1.	Distribution of control points (triangles) and pass points (circles) identified and computed using aerotriangulation procedures for the Great Smoky Mountains National Park	134
Figure 4-2.	The accuracy of the aerotriangulation solution was higher in quadrangles containing roads and other cultural features that were for GCPs. Quadrangles with planimetric errors less than 20 m are shown in light green, while those with higher errors are shown in darker green on this map of Great Smoky Mountains National Park.....	138
Figure 4-3.	In contrast to the Mt Guyot quadrangle, the photo centers in the Luftee Knob quadrangle appear to be displaced from their correct locations. In addition, the orientation angles for many photos exceed the tolerance of ± 3 degrees tilt (as indicated by the graduated circles in red). Photo centers shown as green dots are within ± 3 degrees	140
Figure 4-4.	Distribution of photo centers, GCPs and pass points in the Calderwood Quadrangle.....	141

Figure 4-5.	The Calderwood DOQQs have been mosaicked to create a single image covering the entire quadrangle.....	142
Figure 4-6.	Distribution of photo centers, GCPs and pass points in the Thunderhead Mountain Quadrangle	144
Figure 4-7.	The Thunderhead Mountain DOQQ mosaic showing the locations of GCPs and pass points.....	145
Figure 4-8.	Distribution of photo centers, GCPs and pass points in the Gatlinburg Quadrangle.....	147
Figure 4-9.	Mosaic of approximately 25 large-scale aerial photos for the Gatlinburg Quadrangle.....	148
Figure 4-10.	Portion of photo mosaic from the Kinsel Springs quadrangle.....	149
Figure 4-11.	The raw vectors for vegetation communities in this portion of the Wear Cove quadrangle were converted directly from the overlays and displayed in register with the DOQQ.....	150
Figure 4-12.	The raw vectors corresponding to four photographs displayed over the DOQQ in the Calderwood quadrangle.....	152
Figure 4-13.	The edited vectors displayed over the DOQQ in the Mount Guyot quadrangle.....	153
Figure 4-14.	Wear Cove vegetation coverage after editing and resolving differences between adjacent photos	154
Figure 4-15.	Wear Cove vegetation map after final editing. Colors correspond to the dominant vegetation type in each polygon	155
Figure 4-16.	Portion of the completed Great Smoky Mountains National Park vegetation map including the junction between Wear Cove (upper left), Gatlinburg (upper right), Thunderhead Mountain (lower left), Silers Bald (lower right) Quadrangles	156
Figure 4-17.	A portion of the completed Calderwood vegetation map with dominant vegetation attributes	158
Figure 4-18.	A portion of the completed Gatlinburg vegetation map in the vicinity of Park headquarters at Sugarland. Attributes for dominant vegetation classes are shown	159
Figure 4-19.	The completed Thunderhead Mountain vegetation map	160

PREFACE

Patience and methodical analysis will rarely be unrewarded in this type of endeavor.

Analytical photogrammetry is notorious for using and generating massive amounts of data that seem to numb the mind.

- PC Giant User's Manual

CHAPTER 1

INTRODUCTION

In 1999, The Center for Remote Sensing and Mapping Science (CRMS) at The University of Georgia, Athens, Georgia began a cooperative agreement with the National Park Service (NPS) to produce a detailed vegetation map of the extremely rugged Great Smoky Mountains National Park in the southeastern United States (Figure 1-1). The goal of the project was to interpret the vegetation communities from 1:12,000-scale color-infrared aerial photos and produce a digital geographic information system (GIS) database that could be used to produce large-scale vegetation maps of Great Smoky Mountains National Park. This difficult mapping project presented a number of significant challenges that required the development of new and innovative techniques in digital photogrammetry. These techniques focused on the generation of ground control points (GCPs), correcting displacements in the aerial photographs and accurately transferring vegetation polygons to the GIS database.

Objectives of the Dissertation

The objective of this research is to adapt softcopy photogrammetric techniques for use in the establishment of a vegetation database and associated maps in the Great Smoky Mountains National Park. Issues to be addressed in this dissertation will include:

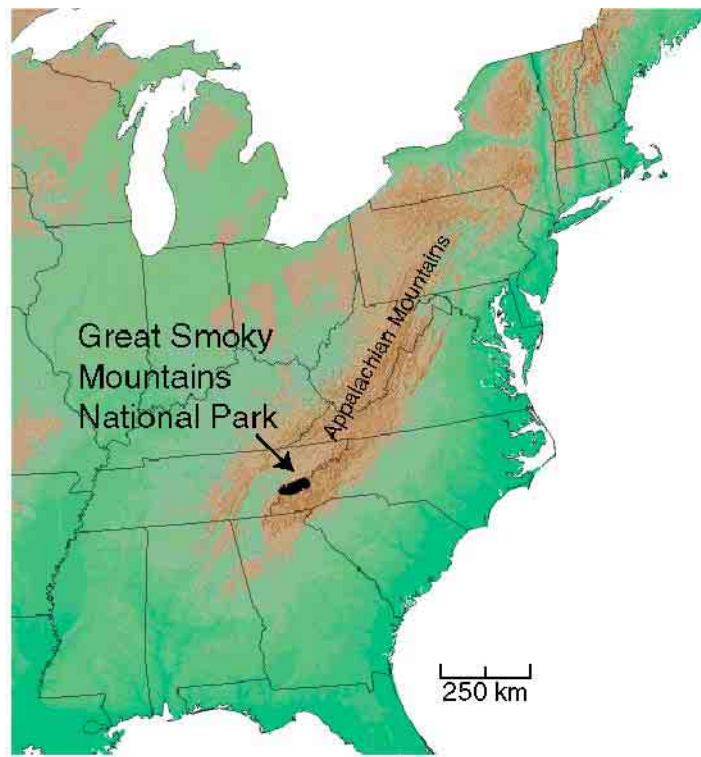
- a) techniques for generating ground control using analytical aerotriangulation;
- and

- b) methods for rectification of vegetation overlays to correct for displacements caused by relief in large scale aerial photographs.

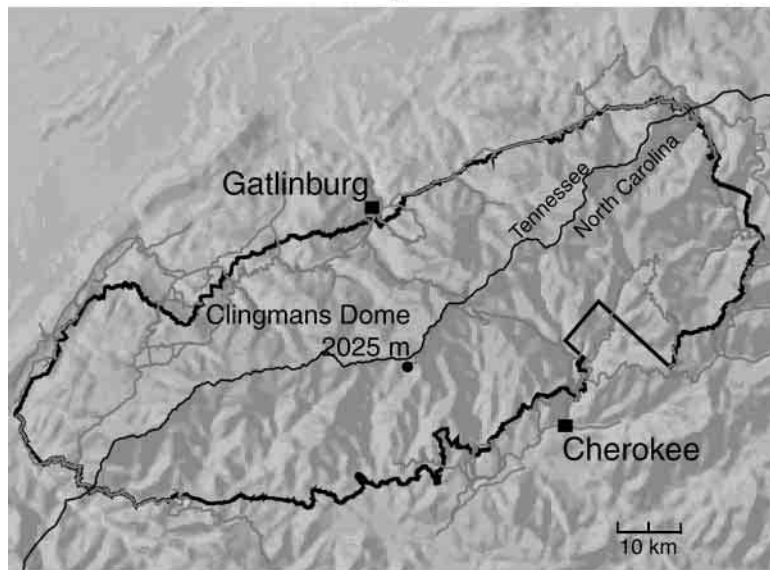
The results of this work will demonstrate the possibilities and advantages of using softcopy photogrammetric methods when compiling GIS databases of remote or rugged regions, and establish guidelines for creating vegetation and natural resource maps of other areas.

Great Smoky Mountains National Park

Great Smoky Mountains National Park, centered at 36° N latitude and 83° 30' W longitude, encompasses 209,000 ha in a region of the southern Appalachian Mountains straddling the Tennessee/North Carolina border (Figure 1-1). The Park is approximately 86 km long and averages 24 km in width, trending in a northeast-southwest direction along the ridgeline of the Appalachians (NPS, 1981). In the late 19th and early 20th centuries, logging companies began removing large tracts of timber from the area that later became the Great Smoky Mountains National Park. The practice of cutting all of the trees and clearing the land led to extensive forest fires, erosion and a severe degradation of the environment. By the time the Park was established to protect the area in 1934, only 60,000 ha of old-growth timber remained (Houk, 2000). While the vast majority of the Park is now reforested with stands of mature timber, the original old-growth tracts represent the largest area of undisturbed forestland in the eastern United States south of the Adirondack State Park in upstate New York (Nodvin *et al.*, 1993). In fact, the Great Smoky Mountains were named after the pervasive blue haze caused by high rates of evapotranspiration from the extensive forest (Figure 1-2; Cox, 2001).



a)



b)

Figure 1-1. Location of Appalachian Mountains chain and Great Smoky Mountains National Park in eastern United States.



Figure 1-2. The Great Smoky Mountains are named after the blue haze that often covers the landscape.

Within the Park are more than 900 km of streams and rivers that are fed by annual rainfall of over 200 cm, most of it falling in the summer months. Although extreme temperatures are not uncommon in any season, the weather in the Smokies is generally moderate with an average temperature of 20 degrees Centigrade in the summer and two degrees in the winter (Figure 1-3; Walker, 1991).

The Appalachian Mountains are among the oldest mountain ranges on earth. Believed to have been similar to the Alps or Himalayas in size and shape when they were formed as a result of uplifting and folding, 225 million years of erosion have carved the rock into the modern day Great Smoky Mountains (Moore, 1988). Elevations range from approximately 250 m above mean sea level (AMSL) at Fontana Lake to 2025 m AMSL at Clingmans Dome, the second highest point in the eastern United States (Figure 1-4). The average elevation in the Park is 730 m AMSL.

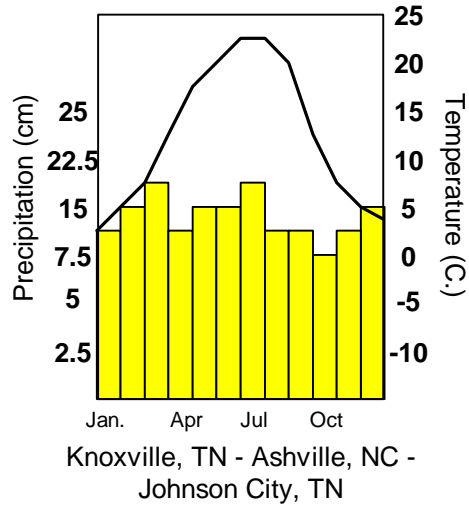


Figure 1-3. The climate of the area surrounding the Great Smoky Mountains National Park is characterized by mild temperatures and moderate rainfall (NCDC, 2002). The curve shows the average monthly temperature in degrees Centigrade. The vertical bars show the average monthly rainfall in centimetres.

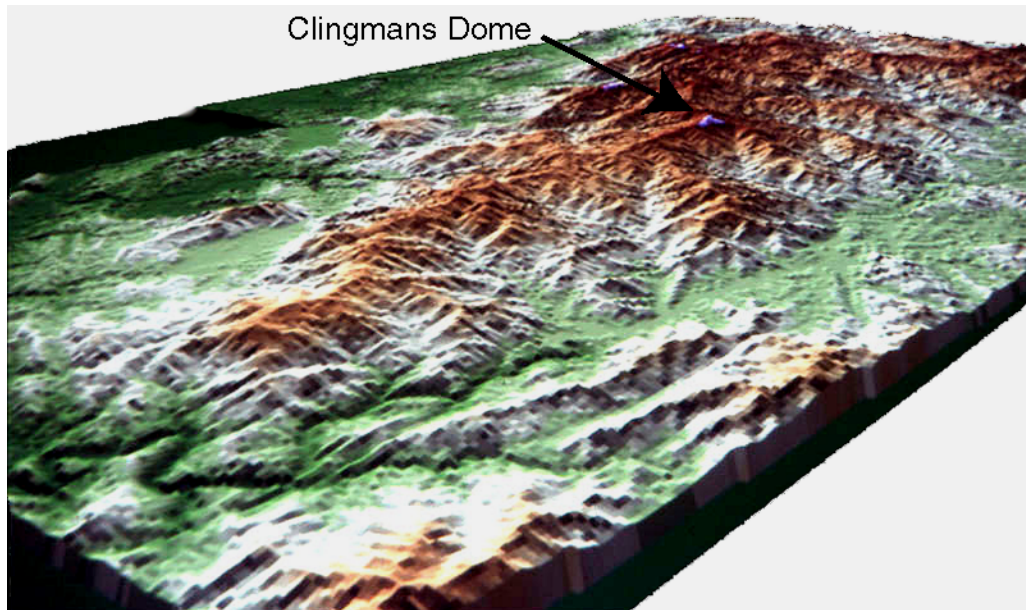


Figure 1-4. Perspective view of Great Smoky Mountains National Park looking east across a mosaic of SPOT multispectral images draped over a DEM. Elevations range from about 250 m to 2025 m AMSL.

The Smokies were never inundated by oceans or covered with glaciers, remaining as island refuges for plant species disrupted from other areas by periods of ice and flooding. The resulting diversity and millions of years of evolution have created a unique ecosystem that is the most biologically diverse in North America. This incredible diversity includes over 1500 species of flowering plants, among which are over 130 varieties of trees, and has led to its designation by the United Nations as one of only 43 International Biosphere Reserves in the United States, as well as a World Heritage Site and State Heritage Site in North Carolina and Tennessee (Kemp and Voorhis, 1993; Walker, 1991).

The terrain relief permits distinct forest types associated with elevation and rainfall regimes representing the range of major tree species and vegetation types in the eastern North American latitudinal gradient from the Deep South to southern Canada. The early successional yellow-poplar and mesic-oak-mixed hardwood communities are found at the lower elevations. Pine-oak communities occur in this same elevation range, but on drier slopes. At low and mid-elevations, up to about 1000 m AMSL, are the cove hardwood forests, extremely diverse communities unique to the southern Appalachian region. Montane red oak forests and northern hardwood forests occur at higher elevations (approximately about 1200 m). Grass and heath balds, also unique to these mountains, are found in these higher elevations. Finally, in the eastern part of the Park, the very highest elevations (above 1,700 m) are home to the spruce-Fraser fir community (Figure 1-5; Nodvin *et al.*, 1993; Whittaker, 1956).

There are very few roads and rivers in the Park and, consequently, access to the interior areas is difficult. In fact, most of the Park only can be reached via a 1280-km



a)



b)



c)

Figure 1-5. Three of the major vegetation communities found in the Great Smoky Mountains National Park: a) a grassy bald near Thunderhead Mountain; b) an example of the mesic-oak community; and c) dense underbrush in the cove hardwood community.

network of trails, including the Appalachian Trail which winds along the ridgelines (NPS, 2001). Within one and one-half days drive from two-thirds of the people in the U.S., there are approximately 9.1 million visitors to the Park each year. This makes it the most visited national park in the country. Many of the millions of annual visitors are hikers, campers and picnickers. The majority, however, are merely driving through the Park on U.S. Highway 441 running from Cherokee, North Carolina to Gatlinburg, Tennessee or are traversing the Blue Ridge Parkway (Figure 1-6).

The All-Taxa Biodiversity Inventory (ATBI) is underway to identify and catalog more than 8000 species of plants, animals and insects in the Great Smoky Mountains National Park (Kaiser, 1999). As scientists collect data, it is important for them to be able to plot the locations of the discoveries on a map base, along with information on terrain and vegetation communities (White and Morse, 2000). Thus, there is a requirement for a detailed spatial database that can be used by the Park managers and also by scientists recording ATBI data.

Geographic Information Systems for Park Management

Geographic information systems are becoming increasingly important for the management of national parks in the United States. In addition to national and regional GIS offices, more than 250 of the 356 national park units have their own GIS capability staffed by one or more person (NPS, 2000). On the local level, the role of the GIS coordinator is to manage spatial data about the park in such a way that intelligent decisions may be made with regard to management of resources. A primary component

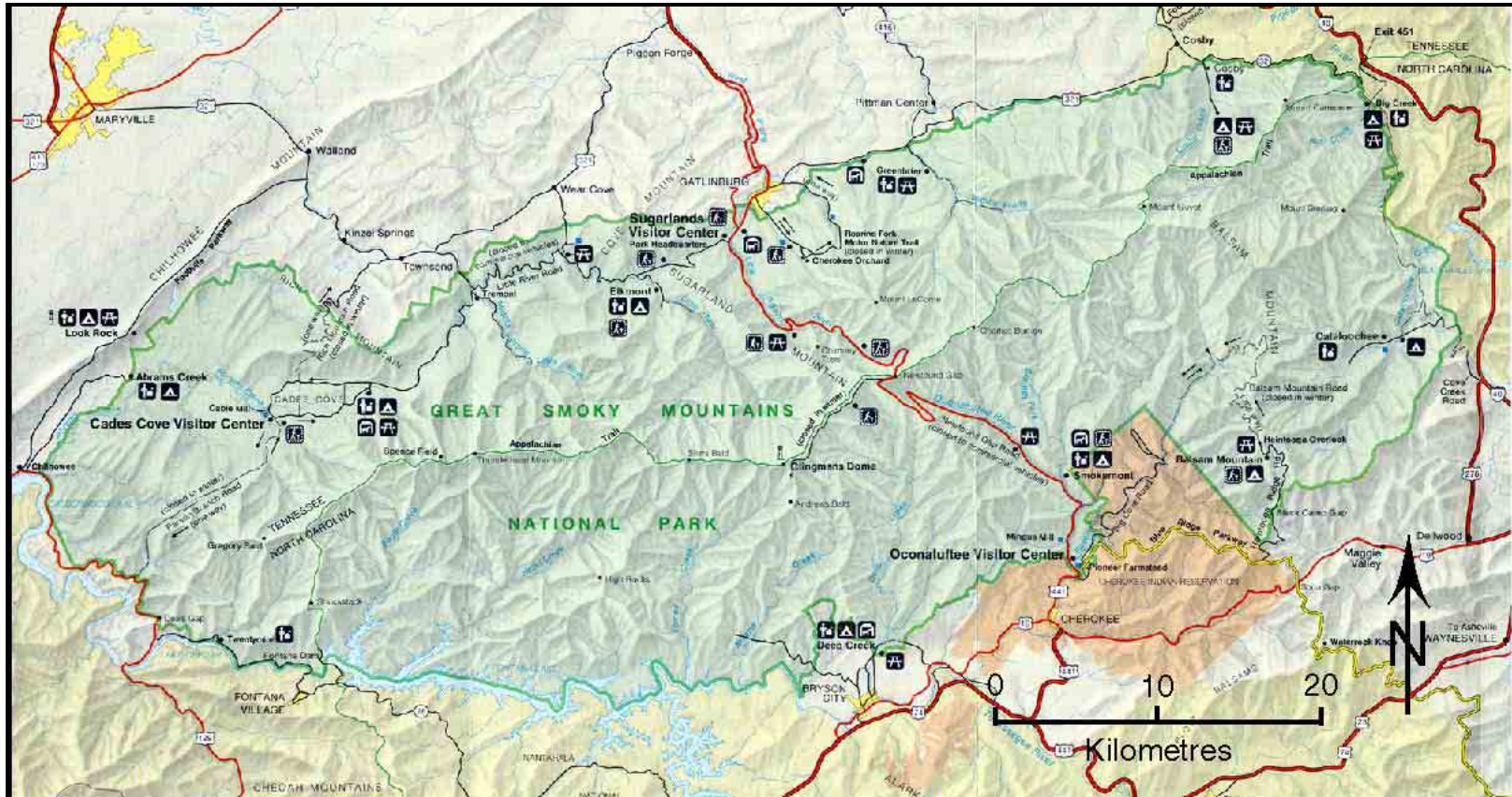


Figure 1-6. National Park Service map showing the roads and major cultural features in and around Great Smoky Mountains National Park (NPS, 1994). The major road through the Park connects the towns of Gatlinburg, Tennessee and Cherokee, North Carolina. Clingmans Dome, with an elevation of 2025 m, is the highest point in the Park. The Appalachian Trail follows the ridgeline along the Tennessee/North Carolina state border.

of the GIS is the base map layer. The base map provides the foundation upon which the rest of the data layers reside.

The U.S. Geological Survey (USGS) produced and updated 1:24,000 scale topographic maps of the Great Smoky Mountains during the 1960's and 1970's (Figure 1-7; Appendix B). These maps have been converted to digital format for use in a GIS as base map products. Unfortunately, they do not provide the detail that park managers require. With increasing pressures from fires, invasive exotic plants, insect infestations and recreational uses, it has become apparent that a more flexible and up-to-date system of maps is required (Dukes, 2001). These problems have led the USGS and National Park Service to sponsor a joint program under which detailed vegetation maps of all of the national parks will be produced (USGS, 2001a). The maps are to be developed from aerial photographs and organized in the form of a GIS database to permit the production of large-scale maps and change analyses (Welch *et al.*, 2000). Great Smoky Mountains National Park is one of the first parks in the eastern United States for which this mapping process has been authorized.

The Great Smoky Mountains National Park Vegetation Mapping Project

There were several major problems associated with the Great Smoky Mountains mapping project that had to be solved before work could proceed. First, was the problem of ground control. The Great Smoky Mountains are one of the most rugged areas in the eastern United States and exhibit an almost continuous canopy cover that precludes the

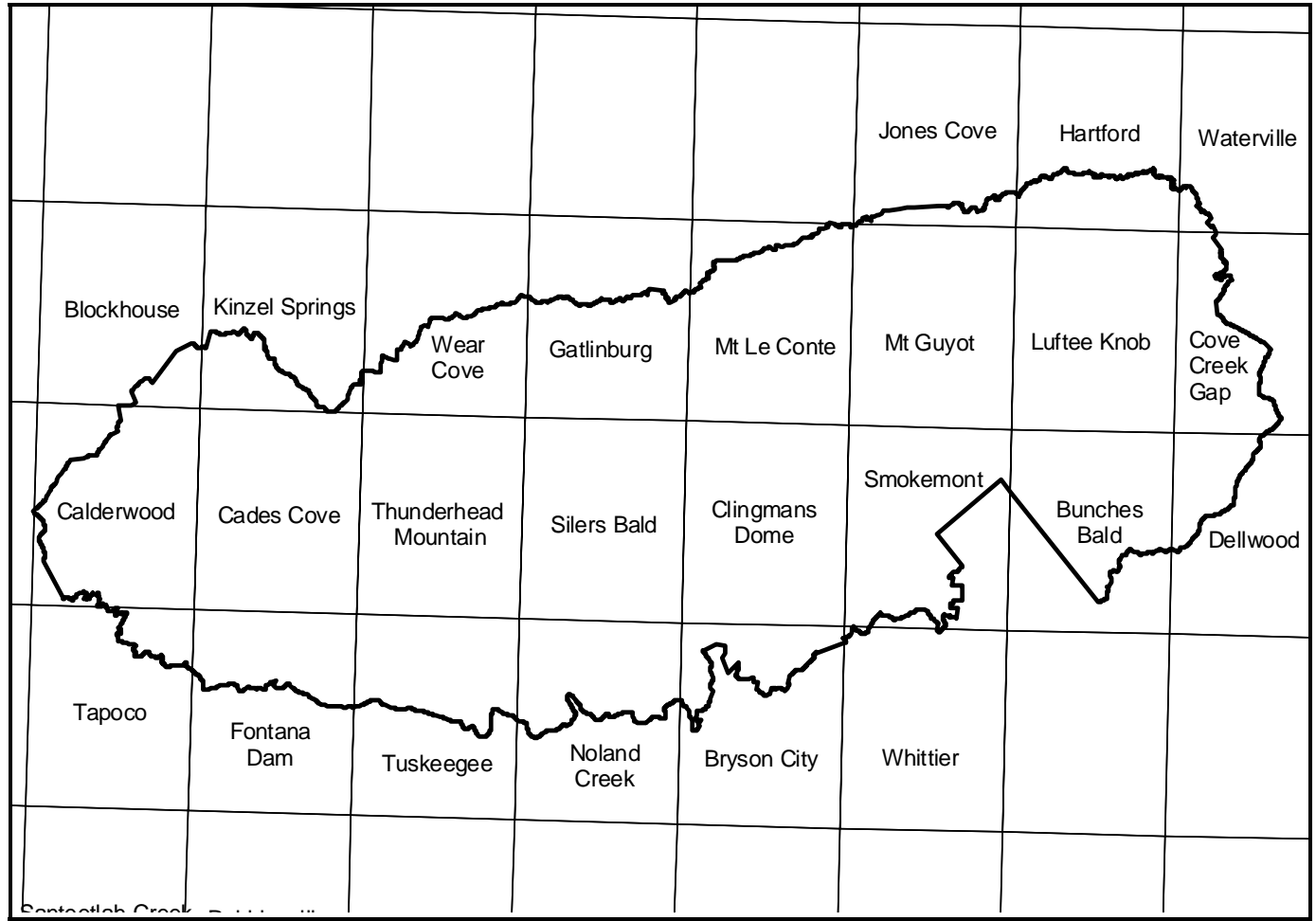


Figure 1-7. Great Smoky Mountains National Park is covered by 25 USGS 1:24,000-scale topographic quadrangles.

identification of control points of known coordinates required for rectifying aerial photographs. The second problem was to develop a mechanism by which data extracted from the aerial photographs could be efficiently rectified and transferred in digital format into the GIS database.

The enormity of the task is apparent when it is realized that over 1,000 aerial photographs cover the Park, that these photos were obtained during “leaf-on” conditions and, even more significantly, that terrain relief often exceeds 30 percent of the flying height from which the photos were recorded. While these photos are ideal for the photo interpreters whose job it is to delineate vegetation communities, the heavy canopy obscures most of the ground and even overhangs the few roads, making the identification of GCPs an extremely difficult task for the photogrammetrist. In addition, the displacements in the photos due to terrain relief dictate that a full photogrammetric solution be employed in the rectification process to permit the vegetation delineations to be properly aligned with the map coordinate system and with adjacent photographs.

Organization of the Dissertation

The focus of this dissertation is on the geometric aspects and methodologies for creating accurate map data. In Chapter 2, “Natural Resource Mapping in Areas of High Relief,” the possibilities for producing natural resources and vegetation maps of rugged terrain are reviewed, including requirements, specifications and some of the methods of

image restitution. In addition, a number of previous vegetation mapping projects for other areas are described.

The methods developed for this project for identification and measurement of pass points and control points as well as aerotriangulation and photo and overlay correction techniques are described in Chapter 3, “Control Extension Techniques and Rectification Procedures Required for GIS Database Development”. In Chapter 4, “Softcopy Photogrammetry as the Foundation for GIS Database Development,” the results of the work are presented and analyzed in relation to the individual topographic quadrangles covering the Park. Finally, in Chapter 5, the project is summarized and conclusions drawn for the possibilities of extending these procedures to other parks within the United States.

CHAPTER 2

NATURAL RESOURCE MAPPING IN AREAS OF HIGH RELIEF

The creation of a vegetation database for the Great Smoky Mountains National Park from large-scale aerial photographs presents a number of mapping problems that are common to remote areas of rugged terrain. The role of photogrammetry in natural resource mapping is in the transfer of information from an aerial photograph into a GIS database. In mountainous regions – especially in the eastern United States – this is not a trivial task due to a combination of factors, including the number of photos, the need for ground control and the presence of high relief and canopy cover. These factors compel the utilization of a range of mapping techniques in order to meet the project requirements. In this chapter, these requirements and the procedures supporting a satisfactory solution will be discussed.

Types of Mapping Tasks

Resource maps are required for applications such as planning, depicting vegetation and fire management. These maps can be stored in digital spatial database and displayed on a computer screen or plotted as hardcopy on a printer or plotter. In general, mapping tasks can be classed as planimetric mapping, topographic mapping, thematic mapping and map revision. A planimetric map represents point, line and polygon features in two-dimensions using their X, Y coordinates to define vectors or lines and boundaries.

Topographic maps depict terrain relief as well as planimetric features. Maps of this type typically represent the terrain as contours (a continuous line representing a single elevation) and spot heights (single point measurements with elevations). Other features such as buildings, roads and streams are included on the map according to their locations.

Thematic maps are normally planimetric maps depicting themes such as vegetation, soils and geology. In order to construct accurate thematic maps, it is necessary to have additional information called attributes associated with each feature to provide a mechanism by which features on the map may be represented and identified. To construct a thematic map, it is frequently necessary to have a knowledge of the topography, but elevations are not actually a component of the map.

A fourth major class of mapping tasks is that of map revision. A map must be revised when it is determined to be out of date because of changes in the landscape. In this case, new images are obtained with the goal of adding new information or correcting the existing data to make a map that more accurately represents current conditions in the area. Source materials for this task must be consistent with the type of data needs for the map revision, but are most typically recent aerial photographs (Newby, 1996).

The results of any of these mapping tasks are frequently integrated with additional information and map layers in a geographic information system (GIS). The GIS then provides the mechanism and tools for storing, cataloging and using the map data to aid in

planning or decision making processes. In this respect, the GIS database and associated map products are typically the desired end products of a mapping project.

Mapping Project Requirements and Considerations

Mapping projects are undertaken with certain requirements and expectations for accuracy that are normally specified in terms of accuracy standards. It is therefore important to define first, the final product requirements and then to plan the project with a goal of meeting those requirements. Considerations include level of detail of the information required and the characteristics of the aerial photographs that will be used to accomplish the project.

Accuracy Requirements

Accuracy requirements vary according to the type of map being produced. For example, the elevations and planimetric locations of features on a topographic map must be correct. A natural resource map, on the other hand, depicts topical information that may not have a well-defined location or boundaries. In this case, location is important but the accuracy of the thematic information – the attributes – may take precedence over the positional accuracy.

The United States government has established a set of standards for planimetric and topographic maps known as the National Map Accuracy Standards (NMAS). All maps produced by U.S. government agencies (e.g., the USGS) must meet these standards and, in practice, maps produced by other agencies and private contractors also use these standards as guidelines (U.S. Bureau of the Budget, 1947). These standards provide a

statement for positional accuracy of point details and topography but do not apply to thematic or resource maps. For maps of 1:20,000 scale and smaller, NMAS state that 90 percent of all well-defined points on a map must be located within ± 0.5 mm of their true location when measured at publication scale. For larger scale maps, these points must be plotted within ± 0.8 mm (ASPRS, 1980). Thus, a point meeting NMAS on a 1:24,000-scale map must be plotted within ± 12 m of its correct location. Typically, however, mapping accuracies are reported in terms of root-mean-square-error (RMSE), which is actually based on the 68 percent confidence level. The acceptable RMSE for a 1:24,000-scale map is ± 7.2 m.

In 1989, the American Society for Photogrammetry and Remote Sensing issued a revised set of proposed accuracy standards for large-scale maps that set coordinate accuracy requirements for Class 1 maps in terms of RMSE in ground units for a range of map scales. For example, the acceptable RMSE values for planimetric (X, Y) coordinates of well-defined points plotted on a 1:12,000 scale map is within ± 3 m. Two additional classes that are defined in terms of relaxed RMSE specifications were also described, in which the acceptable RMSE values were two and three times greater than for Class 1 maps, respectively (ASPRS, 1989).

According to the Geospatial Positioning Accuracy Standards published as part of the National Standard for Spatial Data Accuracy (NSSDA), a well-defined point

“represents a feature for which the horizontal position is known to a high degree of accuracy and position with respect to the geodetic datum. For the purpose of accuracy testing, well-defined points must be easily visible or recoverable on the ground, on the independent source of higher accuracy and on the product itself.”

The NSSDA standards also state that positional accuracy is to be estimated in terms of the RMSE value of check points measured from the map and compared to coordinates of the same points taken from an independent source of higher accuracy. Accuracy is to be reported, however, in terms of ground units at the 95 percent (two sigma) confidence level (FGDC, 1998). For example, if a map is found to have a RMSE of ± 5 m at independent check points, the accuracy of the map will be reported as being ± 10 m. This method of accuracy reporting is independent of scale and is better suited to digital data as it permits comparison of data sets of different resolutions and is consistent regardless of output scale.

Mapping Methods and Options

In general, photogrammetric mapping methods may be broken down into three general categories: analog, analytical and digital (Kraus, 1993). Analog methods work with the aerial photographs in film transparency or paper print formats using optical-mechanical devices. Similarly, analytical photogrammetry utilizes mathematical solutions for photographs in hardcopy format but employs computerized instruments for data collection. Digital photogrammetric methods, now commonly referred to as “softcopy photogrammetric methods,” utilize photographs in digital format and operate entirely in a computer domain that not only emulates operations performed on analog and analytical instruments but also permits an entire range of new functions to be performed. Although interpreting aerial photographs to delineate vegetation polygons is an analog operation, most of the tasks associated with building a digital GIS database fall into the realm of digital or softcopy mapping.

Most modern maps are created and managed in softcopy mapping systems or geographic information systems (GIS). Aerial photographs and information derived from them in analog format must be converted to digital format before they can be included in the map database. This conversion may be done by: 1) digitizing the map by hand using a digitizing table; 2) scanning the map and tracing the line work with heads-up digitizing methods in a mapping or GIS system; or 3) using raster-to-vector conversion software to automatically extract the line work from the scanned map (Welch, 1989; Lo and Yeung, 2002).

Known reference points called ground control points (GCPs) are employed to insure that the converted line work is referenced to the proper coordinate system and will fit into the larger map context. After incorporation into the final map database, the vectors from each individual photograph are edited and then edge-matched to the adjacent photos using digital editing software often included in the digital mapping/GIS package. Attributes describing details about a feature (e.g. vegetation type or percent canopy closure) are assigned as part of the editing process.

Map revision using digital techniques is also facilitated by the ability to superimpose an existing map in vector format over a new image to view the differences between the map and the image. Features in the map file can be updated interactively by adding, deleting or moving individual vertices or by digitizing new features into the database (Ormsby *et al.*, 2001). A digital map database produced as an end-product can be employed to plot hardcopy maps. The map is composed on-screen and then plotted on

a large format ink jet plotter. Smaller sized maps may be printed on a page-sized ink jet printer.

Mapping from Aerial Photographs

Knowledge of the characteristics of an aerial photograph is crucial to being able to produce an accurate map – it is not enough to simply trace features visible on the photograph and transfer them directly to a map base and call it “done.” An aerial photograph is exposed using a mapping camera with a 23 x 23 cm (9” x 9”) film format that is mounted in an aircraft such that the lens is aimed vertically below the aircraft. Although lenses of several different focal lengths are available, the majority of the cameras in commercial use are equipped with lenses having a nominal focal length of 152.4 mm (6 inches) (Figure 2-1).

The lenses in mapping cameras are of extremely high quality and are designed to optimize geometry and resolving power. A typical modern mapping camera has lens distortion of no more than eight to ten micrometres (ASPRS, 1980; USGS, 2000). Depending on the manufacturer of the camera (e.g., Leica, Wild or Zeiss), there are either four or eight fiducial marks located at the corners and midpoints of the film platen that serve to identify the geometric center of the photos, or the principal point, at the intersection of imaginary lines drawn between opposite fiducials. Information about the flying height AMSL, camera tilt, date and time of day at the instant of exposure is provided in a data block located on the side of the frame. Additional data on geographic position and exposure (shutter speed and f/stop) may also be found in the margin of the photograph (Figure 2-2).

Cameras are calibrated by the USGS Calibration Laboratory to measure the precise locations of the fiducial marks and the perspective center of the lens, as well as to quantify any distortions in the lens (Figure 2-3; Tayman, 1984; Light, 1992). These data are provided to the camera owner in the form of an aerial camera Report of Calibration (see Appendix A), which is subsequently made available to clients and end-users of the photographs. Data from the Report of Calibration is necessary to recover the interior orientation of the photograph as a precursor to making measurements from it. In analytical and softcopy photogrammetry, numerical corrections for lens distortion and film shrinkage are implemented, resulting in a much higher level of measurement accuracy.



Figure 2-1: A Wild RC20 camera system similar to the one employed to record the photographs for the Great Smoky Mountains National Park mapping project.

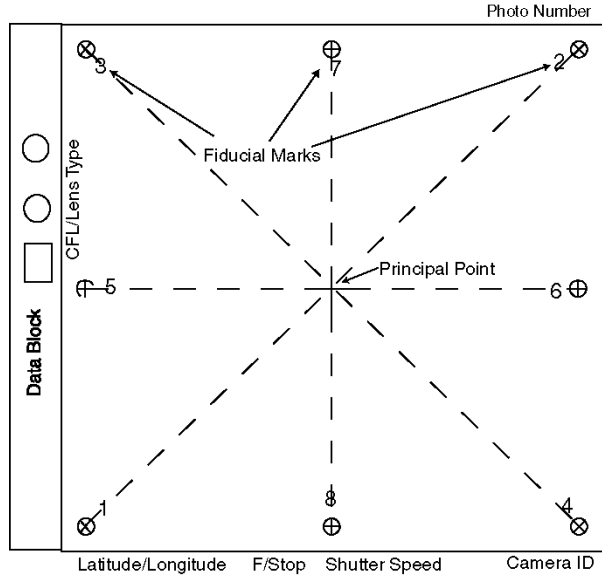


Figure 2-2. The features of an aerial photograph.

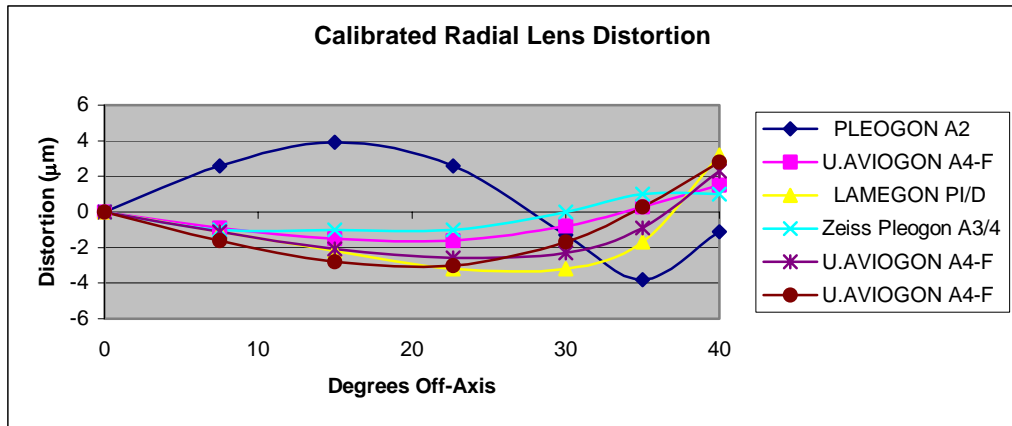


Figure 2-3. Calibrated lens distortion curves of several modern mapping cameras (Source: USGS Camera Calibration Report Database).

There are a large number of aerial film types manufactured by Kodak, Agfa and Fuji, that include black-and-white panchromatic, natural or true color and color-infrared (Kodak, 1992). Each type of film is well suited to specific applications. General mapping is performed using black-and-white film due to its higher resolution and lower cost when compared to color and color-infrared. Vegetation mapping is best conducted using color-infrared film such as the new Eastman Kodak Aerochrome III Infrared Film 1443 (EK 1443), which has resolution roughly double that of the older EK 2443. The infrared wavelengths are particularly sensitive to chlorophyll content in plants and can be used successfully to discriminate different plant species by their magenta or red color on the photograph. This capability can be enhanced further by careful planning of the acquisition date to take advantage of the autumn color changes in the deciduous trees (ASPRS, 1997).

Lens Distortion

Lens distortion causes imaged positions of points to be displaced from their ideal positions. Two major types of lens distortion are generally modeled: radial and decentering distortions. Of these, the radial component is the most important to consider (see Figure 2-3). Radial lens distortion, as the term implies, occurs radially from the principal point and is generally normalized to minimize its effects throughout the photograph. Lens distortion is manifested as a radial shift in the position of a feature in the image relative to its “correct” location. When an aerial photograph is scanned and converted to digital format, the effects of lens distortion are masked by the scanning

resolution (typically, 20 to 42 μm) and can generally be ignored except when precise photogrammetric computations are being performed (ASPRS, 1980).

In numerical (both analytical and softcopy) photogrammetry, corrections for lens distortion are applied before other corrections (such as those for tilt), using equations of the form

$$\Delta r = k_1 r^1 + k_2 r^3 + k_3 r^5 + k_4 r^7 \quad (\text{Eq. 2-1})$$

where Δr is the radial displacement, $k(i)$ are the lens distortion coefficients, and r is the radial distance from the principal point.

Other displacements that are found in photographs include those attributable to earth curvature, atmospheric refraction and relief (Slama *et al.*, 1980). The displacements in image position due the effects of earth curvature and atmospheric refraction increase with increasing flying height and under many situations must be accommodated in a numerical solution. For most mapping applications involving large-scale aerial photographs, the combined effects are minor and may be masked at scanning resolutions of 20 to 42 μm (Figure 2-4). For example, at a radial distance of 120 mm, vertical photographs exposed at a height of 2000 m AGL will exhibit displacements of $-11.4 \mu\text{m}$ due to earth curvature and $+4.7 \mu\text{m}$ due to atmospheric refraction (Table 2-1). With a combined displacement of $-6.7 \mu\text{m}$ inward toward the principal point, the effects are well contained within a single scanned pixel and can be safely ignored. Relief displacement as well as the effects of tilt, however, can have a major affect on the geometry of the photographs and cannot be ignored (Moffitt and Mikhail, 1980; Bolstad, 1992).

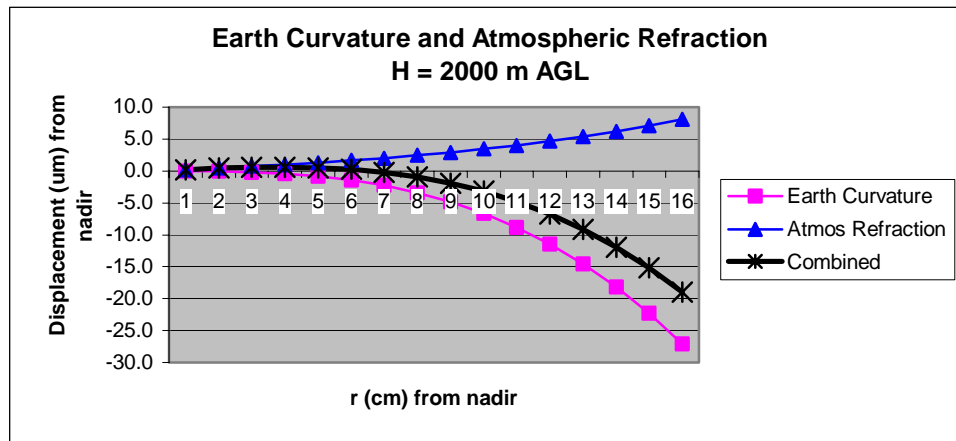


Figure 2-4. The combined effects of earth curvature and atmospheric refraction.

Table 2-1. Displacements due to earth curvature and atmospheric refraction for aerial photographs at 2000 m AGL.

Radial distance (mm)	Displacements (μm)		
	Earth Curvature	Atmospheric Refraction	Combined Effect
10	0.0	0.2	0.2
20	-0.1	0.5	0.4
30	-0.2	0.8	0.6
40	-0.4	1.0	0.6
50	-0.8	1.3	0.5
60	-1.4	1.7	0.3
70	-2.3	2.0	-0.3
80	-3.4	2.5	-0.9
90	-4.8	2.9	-1.9
100	-6.6	3.5	-3.1
110	-8.8	4.0	-4.8
120	-11.4	4.7	-6.7
130	-14.5	5.4	-9.1
140	-18.1	6.2	-11.9
150	-22.3	7.1	-15.2
160	-27.1	8.1	-19.0

Relief Displacement

Relief displacement is the shift in the position of an object on an aerial photograph caused by the height of the object above or below a specific datum. This displacement is radially outward from the principal point for objects above the datum and inward for objects below the datum (Figure 2-5). In areas of low relief (less than 0.5 % of the flying height), terrain effects due to relief may not require corrections for many mapping applications (Welch and Jordan, 1996a). As the terrain relief increases relative to flying height, however, relief displacements must be corrected to insure the correct positions of features extracted from the air photos. Relief displacement is computed using the standard equation:

$$de = rh/H \quad (\text{Eq. 2-2})$$

where de is the relief displacement (in millimetres), r is the radial distance from the principal point to the image of the top of the displaced object (in millimetres), h is the height of the object relative to the datum (in metres) and H is the flying height (FH) above mean terrain (in metres) (Figure 2-6).

Table 2-2 lists the effect of relief displacement for three concentric locations ($r = 50, 100$ and 150 mm) on an aerial photograph exposed from 2000 m AGL. It can be seen that when relief is greater than 0.5 percent of the flying height, displacements due to relief must be corrected in order to meet map accuracy requirements. This correction is normally accomplished through the use of a differential or orthorectification process where a DEM provides the data required to remove relief displacements in the image.

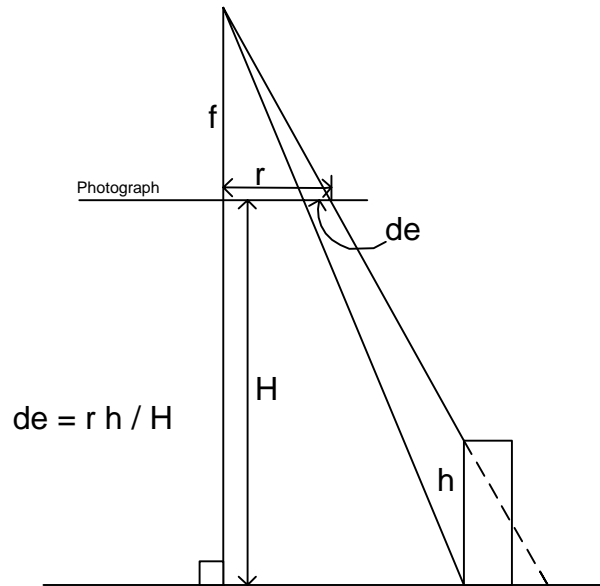


Figure 2-5. Image displacement (de) due to relief in a vertical photograph for an object above a horizontal datum.

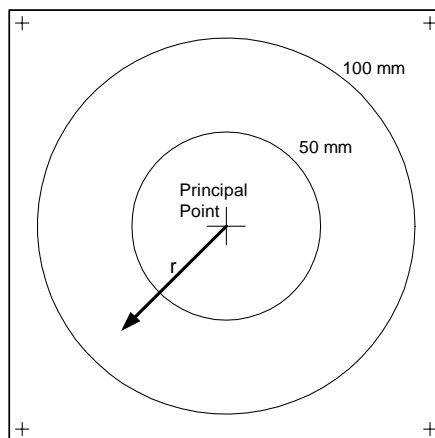


Figure 2-6. Relief displacement is radial from the center of a vertical photograph. As distance, r , from the center of the photograph increases, the displacement due to relief (de) also increases as noted in Table 2-2.

Table 2-2. Relief displacement calculated for a photograph exposed with a standard mapping camera (f=152.4 mm) from a flying height (FH) of 2000 m above mean terrain (AMT). Values in the shaded rows are typical in the Great Smoky Mountains.

		Relief Displacement (mm)					
		r = 50mm		r = 100mm		r=150 mm	
Relief (m)	% FH	de (mm)	de (m)	de (mm)	de (m)	de (mm)	de (m)
7	0.3	0.2	2.3	0.4	4.6	0.5	6.9
10	0.5	0.3	3.3	0.5	6.6	0.7	9.8
20	1.0	0.5	6.6	1.0	13.1	1.5	19.7
40	2.0	1.0	13.1	2.0	26.3	3.0	39.4
60	3.0	1.5	19.7	3.0	39.4	4.5	59.1
100	5.0	2.5	32.8	5.0	65.6	7.5	98.4
150	7.5	3.7	49.2	7.5	98.4	11.3	147.6
200	10	5.0	65.6	10.0	131.2	15.0	196.8
400	20	10.0	131.2	20.0	262.5	30.0	393.7
600	30	15.0	196.8	30.0	393.7	45.0	590.5
800	40	20.0	262.5	40.0	524.9	60.0	787.4
1000	50	25.0	328.1	50.0	656.2	75.0	984.2
1200	60	30.0	393.7	60.0	787.4	90.0	1181.1
1400	70	35.0	459.3	70.0	918.6	105.0	1377.9
1600	80	40.00	524.92	80.00	1049.84	120.00	1574.76

Tilt Effects

The final major component of the geometry of an aerial photograph has to do with the tilt of the camera at the time of exposure. The pilot of an aerial survey aircraft is tasked with flying straight and level along a flight path so as to acquire the best photographs possible along a preplanned flight line. Along the way navigation errors are corrected and the aircraft is buffeted by winds. Consequently, the aircraft (and camera) is rarely perfectly level or flying exactly in a straight line. The resulting tilts are defined in three directions: omega (ω) for tilt about the X-axis, phi (ϕ) for tilt about the Y-axis, and kappa (κ) for the rotation of the camera about the Z-axis. These three tilt parameters, along with the exact coordinates of the camera in space at the instant of exposure (X_L , Y_L , Z_L), are known as the elements of exterior orientation (Figure 2-7).

Normal specifications for aerial photograph state that tilt must be less than three degrees, and this specification is generally met. The effect of tilt in an aerial photograph is to create displacements across the photo (Figure 2-8). Tilt and relief displacement both can be corrected during image rectification using digital processing techniques as described below.

Rectification of an Aerial Photograph

The following general steps are required to rectify an aerial photograph (Welch and Jordan, 1996a).

1. The aerial photograph in film format is scanned and converted to an 8-bit (256 gray levels) or 24-bit (color) raster image.

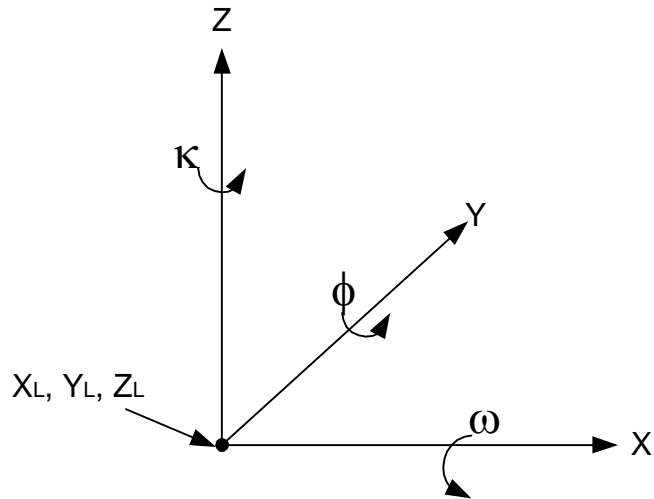


Figure 2-7. The elements of exterior orientation include three rotations angles omega (ω), phi (ϕ) and kappa (κ) about the X-, Y- and Z-axes, respectively, and the coordinates of the exposure center (X_L, Y_L, Z_L).

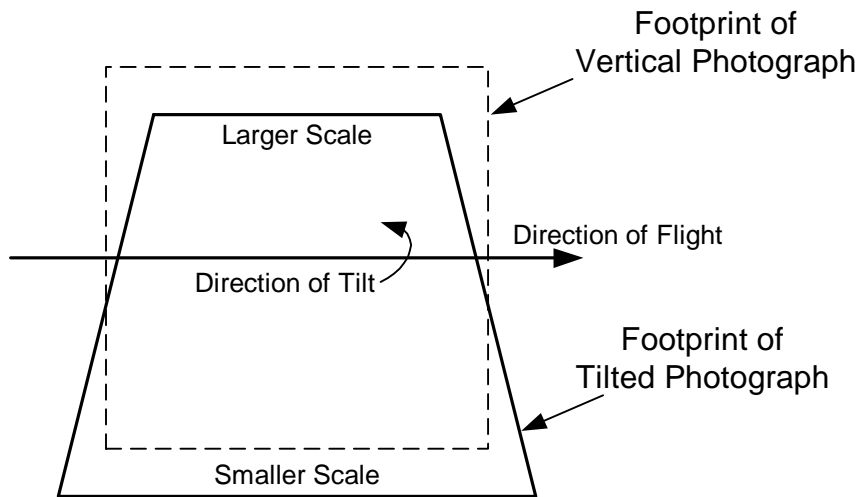


Figure 2-8. Tilt causes scale variations across the photograph. In this example, the tilt direction is perpendicular to the direction of flight.

2. A list of ground control points (GCPs) is created.
3. The image locations of the fiducial marks and GCPs are digitized to obtain x, y image coordinates.
4. The mathematical transformation parameters are computed to establish the relationship between the ground coordinate system (X, Y, Z) and the image (x, y).
5. Finally, the image is rectified to the ground coordinate system and resampled to a particular pixel (picture element) size or resolution. The resulting geocoded image is ready for use in a GIS or mapping application.

Conversion of the Photograph from Analog to Digital Format

A scanner is a device that is employed to convert an aerial photograph from an analog format (a continuous tone image) to digital format (an array of pixels with their gray levels quantified by numerical values) so that it may be used in a digital image processing/softcopy photogrammetry/GIS environment (Welch, 1993; Schenk, 1999). Scanners may be used to capture image data in reflection (paper prints) or transmission (film transparency) modes, in either color or black-and-white. Because film transparencies generally have higher spatial resolutions, greater dynamic range of gray values and are more stable than paper prints, they are the preferred source material when converting aerial photographs to digital images (ASPRS, 1980; Welch and Jordan, 1996b).

Two major classes of scanners are generally available for converting analog photos to digital format: desktop (flatbed) scanners, costing between \$100 and \$5000,

such as the Epson Expression 836XL and Hewlett Packard ScanJet series, and photogrammetric quality scanners costing \$50,000 to over \$150,000, such as the Zeiss PHODIS SC or the LH Systems DSW300 (Batsalvias, 1998; 1999). The desktop scanners are generally marketed for desktop publishing applications and offer resolutions as high as 32 to 21 μm (800 to 1200 dpi) with formats of 21 x 28 cm (8.5" x 11") to 28 x 43 cm (11" x 17") (Figure 2-9). The larger format has the advantage of being able to accommodate the entire 23 x 23 cm frame of the aerial photograph, including all eight fiducial marks, whereas a scan made with the smaller format scanner will only contain five fiducial marks at most. Desktop scanners are designed primarily to maximize image quality, rather than geometric fidelity.

While it is possible to calibrate a desktop scanner, this can be a time-consuming process that is not always completely successful (Baltsavias and Waegli, 1996). Boron (1996) found distortions of up to ± 5 pixels in the images scanned at 20 μm resolution with a low cost UMAX 1200 SE scanner. Although he was able to model the distortions to some extent, he concluded that some scanners should not even be used for mapping applications because of the poor geometric characteristics of the devices. Unfortunately, the selection of a scanner for use in photogrammetric applications can become a "hit-and-miss" operation (Baltsavias, 1999). Higher quality desktop scanners such as the Epson Expression 836XL may be employed with success for scanning aerial photographs for applications having less stringent accuracy specifications (Figure 2-10).

Scanners designed specifically for photogrammetric use will differ from desktop scanners in that they are engineered to maximize geometric stability and reduce errors in

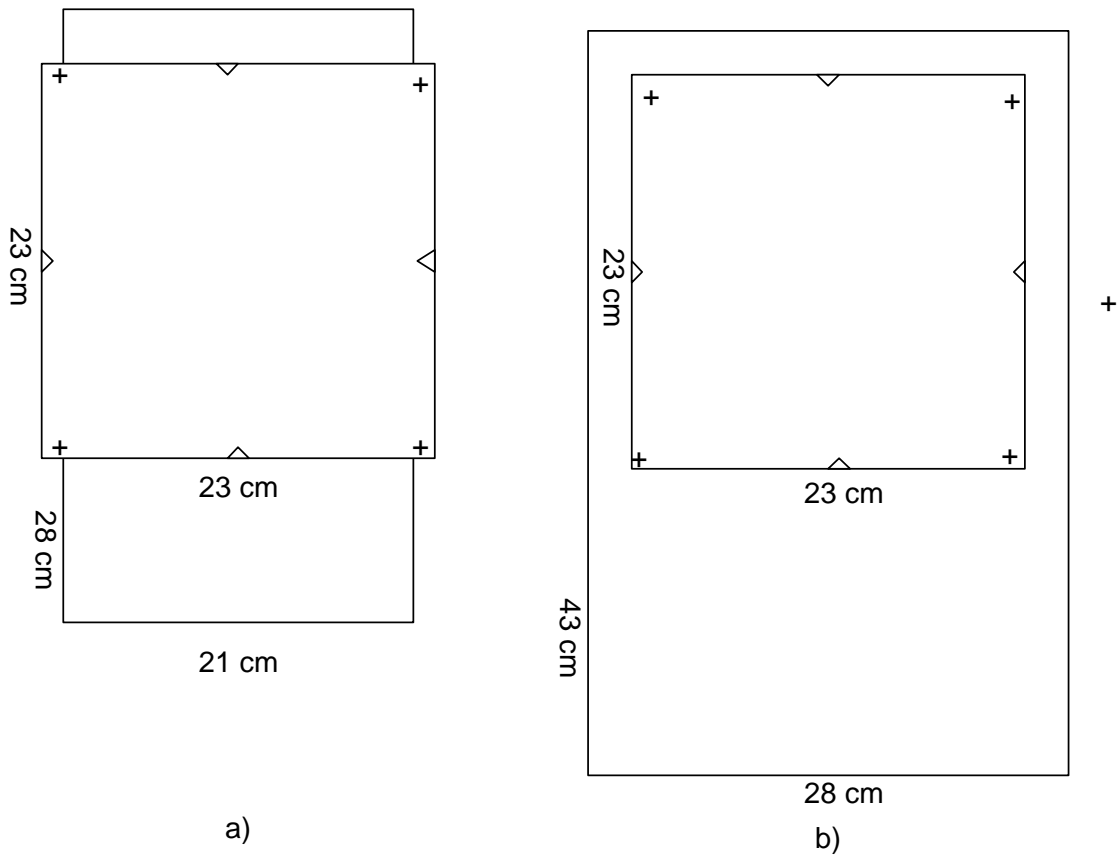


Figure 2-9. a) On standard 21 cm x 28 cm scanners, the full format of the aerial photograph, including all of the fiducial marks, cannot be scanned. This is not as suitable for photogrammetric applications as the larger 28 cm x 43 cm format scanner (b), which does accommodate the full frame of the photograph.



Figure 2-10. Epson Expression 836XL desktop scanner. Photos and documents up to 28 x 43 cm (11 x 17 inches) in size may be scanned at a resolution of 32 μm (800 dpi) in both reflective and transparency formats.

pixel positions to less than 5 μm . Scanning resolution can be set at fixed increments that vary according to manufacturer. Typical aperture settings are 7.5, 15, 22.5 and 30 μm (Kolbl, 1996). A useful feature found in some modern photogrammetric scanners is the ability to automatically scan roll film in unattended mode. The film is loaded into the device and the scanning process is begun. After each scan is complete, the film is advanced to the next frame. For high volume production environments, this is a valuable feature because it permits the operator to perform other tasks while the time-consuming (up to ten minutes per photo) scanning process proceeds without intervention. One does not have to purchase a photogrammetric scanner in order to obtain high quality scans as it

is possible to have scanning performed by commercial service groups such as Precision Photo, Inc. (Dayton, Ohio) or Hoffman and Company (Smyrna, Georgia).

The actual scanning aperture (resolution) one should employ to scan an aerial photograph depends on the original scale of the photograph and the desired output pixel size of the rectified photo. For example, scanning a 1:12,000 scale photograph at a resolution of 42 μm will produce a digital image having a pixel resolution of 0.5 m. Although this pixel dimension can be increased or decreased in the rectification/resampling process to achieve a desired output product scale, it is better to try to scan the photo with a pixel size close to the desired output pixel dimension so as to retain the optimum image quality. Generally speaking a scanning resolution of 25 to 35 μm will provide sufficient detail for most applications involving the use of large- to medium-scale aerial photographs (Welch and Jordan, 1996a).

A scanned image is structured as a matrix of pixels arrayed in columns and rows with values, or digital numbers (DNs), scaled according to the brightness of the original film transparency. Typically, an 8-bit scale is employed with DN's range from 0 to 255 to represent shades of gray from black to white (Figure 2-11). The size of the digital file stored on the computer can be quite large, depending on the scanning resolution employed. For example, a black-and-white 23 x 23 cm format aerial photograph scanned at 25 μm will produce a file containing 9200 x 9200 pixels, requiring about 85 Mb of storage space on disk. A color or color-infrared photo is scanned using filters to separate its red, green and blue (RGB) components. A color photo scanned at 25 μm will require 85 Mb for each layer, or 254 Mb for the complete photo (Welch, 1992).

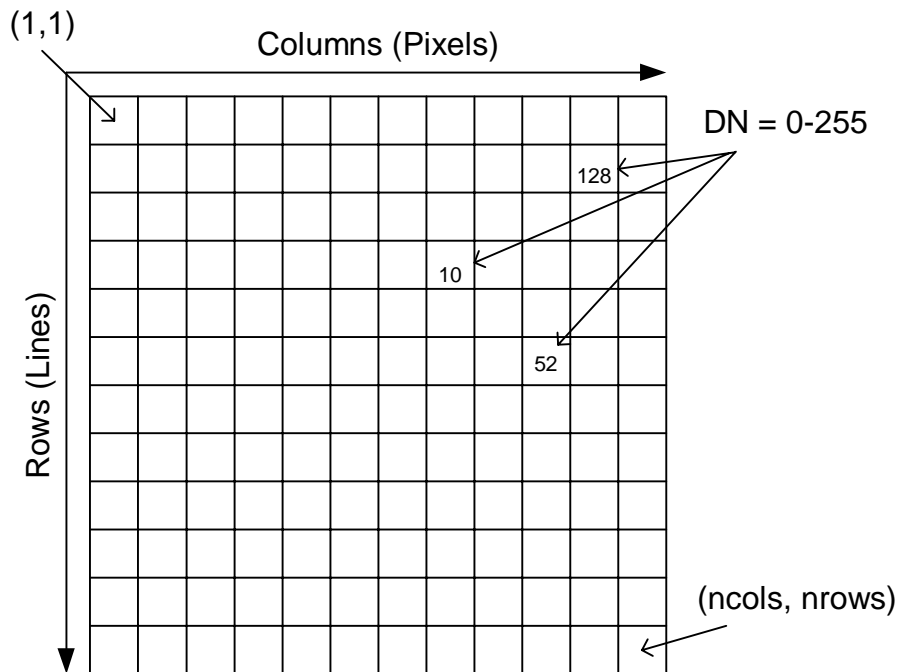


Figure 2-11: A digital image is structured as a matrix, or array, of digital numbers arranged in columns and rows. Values in an 8-bit images range from 0 to 255. Each position in the array can be addressed by its column and row (pixel and line) coordinates. Pixel and line coordinates are also typically notated as (x, y) .

Before a scanned aerial photograph may be employed for mapping purposes it must be rectified to match the geometry of a specific map coordinate system. In this process, a series of GCPs and image control points (CPs) are identified and a mathematical relationship between them is established. Photogrammetric software is required to correct for displacements due to tilt and relief in the rectification process (Welch, 1989).

Ground Control

Ground control points are markers or features visible on the aerial photographs for which the X, Y, and Z terrain coordinates are normally defined in rectangular plane coordinates in either the State Plane or the Universal Transverse Mercator (UTM) coordinate systems (Doyle, 1997). Of these, the UTM System is often employed for resource mapping applications. The UTM system divides the earth up into 60 zones of six degrees of longitude, each with its own central meridian (e.g., the central meridian of UTM Zone 17 is 81° W longitude). The central meridian is given the Easting (X) coordinate of 500,000 so as to prevent negative coordinate values. The origin of the Northing (Y) coordinates in the Northern Hemisphere is at the equator (Snyder, 1987).

Horizontal coordinates are referenced to a datum that is based on measurements of the shape of the earth called an ellipsoid. The North American Datum of 1927 (NAD 27), based on the Clarke 1866 ellipsoid, has been the standard datum for many years. A recent redefinition of the ellipsoid to the Geodetic Reference System of 1980 (GRS 80) resulted in the North American Datum of 1983 (NAD 83) and the closely related World

Geodetic System of 1984 (WGS 84) being adopted by U.S. mapping agencies (Schwarz, 1989; USGS, 1989; DMA, 1991). In general, NAD 83 has replaced NAD 27 in modern maps. Historically, however, all of the USGS topographic maps have been cast on NAD 27 (Welch and Homsey, 1996). Coordinates obtained from maps cast on NAD 27 can be readily converted to NAD 83 values using commercially obtainable software such as the Blue Marble Geographics Geographic Calculator (Blue Marble, 1994).

The coordinates of GCPs can be obtained by conventional ground or Global Positioning System (GPS) surveys, by measurements on digital orthophotos or published maps in hardcopy and digital formats, or by aerotriangulation. In general, accurate ground control is essential to virtually all photogrammetric operations: the accuracy of the GCPs determines the ultimate accuracy of the rectified image (Lillesand and Kiefer, 2000). For this reason, GCPs should be identified at well-defined locations (e.g., a road or sidewalk intersection that meets at a 90 degree angle is ideal), and the coordinates obtained from the highest accuracy source available. Finally, the GCPs must be well distributed throughout the photograph to insure an unbiased solution (Figure 2-12).

Obtaining GCP Coordinates by Ground Survey Techniques

The coordinates of a GCP may be measured directly on the ground using either traditional ground survey instruments (e.g., total station or theodolite) or GPS equipment. For a small area with very high accuracy requirements, the total station may be the instrument of choice for measuring GCP coordinates, especially when a local coordinate system is to be employed. If the photo is to be referenced to a standard coordinate system

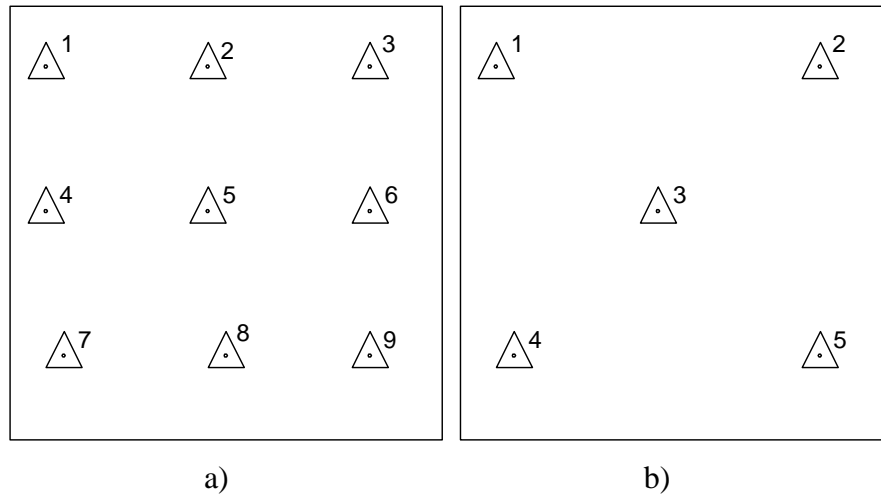


Figure 2-12. GCPs should be well distributed throughout the entire photograph. These diagrams illustrate two idealized plans for GCP locations. Mapping should be performed within the area of the photograph defined by the control network.

such as UTM, the coordinates must be referenced to an existing benchmark or other known point location. More often, however, modern ground surveys are undertaken with GPS satellite receivers. A GPS receiver uses signals transmitted from a number of satellites orbiting the earth to compute a triangulated coordinate of the precise position of the unit (Wells *et al.*, 1986; Hurn, 1989; Trimble, 2002). Without differential correction, this position will typically be accurate to approximately ± 5 m. This value can be improved to a sub-metre or even centimetre level through the use of differential correction techniques (Hurn, 1993; Cook and Pinder, 1996).

Obtaining GCP Coordinates from Published Maps

Ground control points for a project may be digitized from existing maps such as the USGS 1:24,000-scale topographic quadrangle series. A map is an appropriate source

for GCPs when there are enough cultural features visible on both the map and on the photograph to provide an adequate distribution. It is important to recognize that a map at 1:24,000 may not have the accuracy required to rectify a large-scale photograph. As previously stated, NMAS provide for points on a 1:24,000 scale map to be accurate to ± 7.2 m RMS. While this accuracy may be sufficient for natural resource applications, it is insufficient to support traditional high accuracy photogrammetric work.

Planimetric (X, Y) coordinates can be recovered from a printed map using a digitizing tablet. The map is placed on the digitizer and secured firmly with drafting tape. A number of known points, such as the corners of the map sheet, are digitized and used for registration purposes. Any number of points may be subsequently digitized and their coordinates and point identification numbers saved to a disk file. Elevations (Z) are read from existing spot heights plotted on the map or interpolated from contours and saved along with the point coordinates.

In recent years, the U.S. Geological Survey has produced a digital product known as a Digital Raster Graphic (DRG). A DRG is a standard USGS topographic quadrangle that has been scanned at a minimum resolution of 100 μm (250 dpi) and converted to a digital format (Figure 2-13). The area inside the neat line of the map is then rectified to the same projection and datum as the original map and is subject to the same accuracy standards as the original source map (USGS, 2001c)

Digital Raster Graphics at 1:24,000, 1:100,000 and 1:250,000 scales are available for the entire conterminous United States. In the Great Smoky Mountains National Park, the 1:24,000-scale topographic maps are cast on the UTM projection referenced to NAD

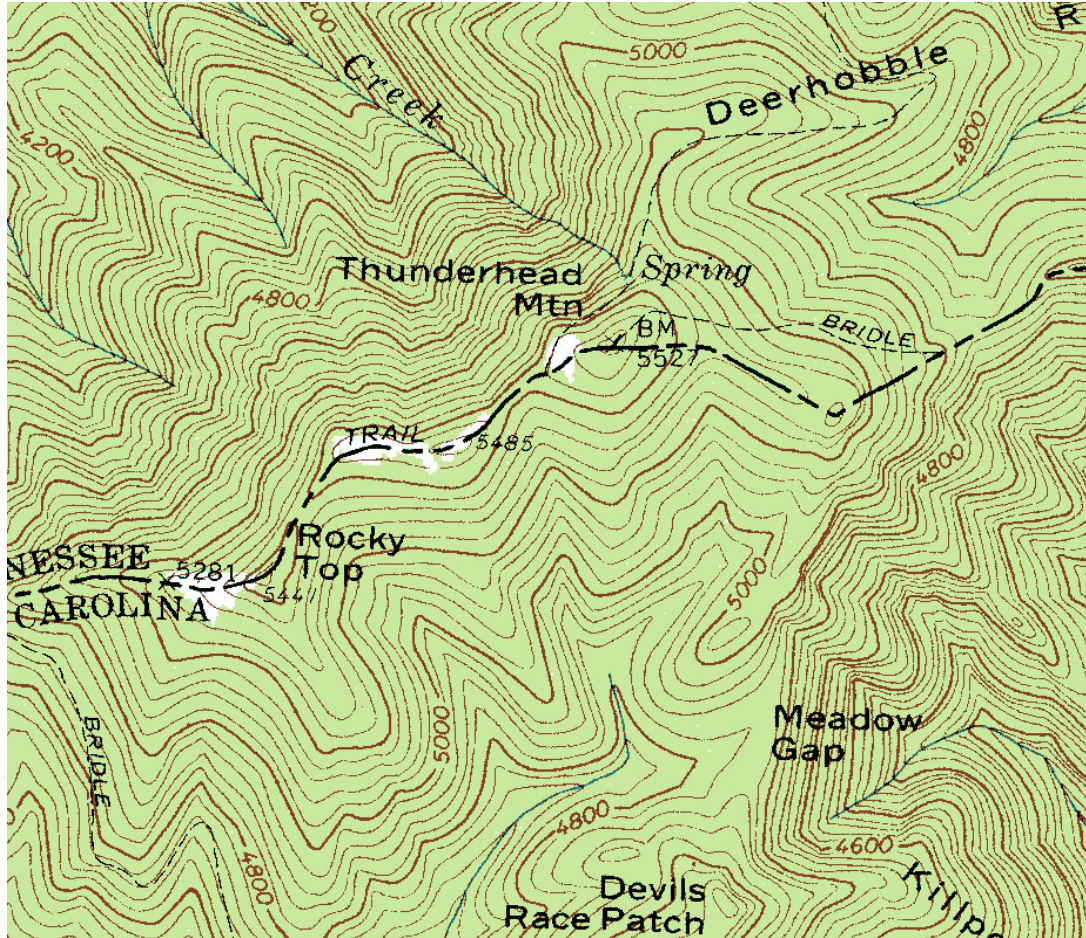


Figure 2-13: Detail of Thunderhead Mountain DRG file.

27. After scanning the maps at a resolution of 100 μm , the equivalent ground resolution of each pixel is 2.4 m.

In terms of accuracy, a DRG is designed to be equivalent to a printed map. Therefore, a 1:24,000-scale DRG should produce a RMSE_{XY} value of less than ± 7.2 m for well-defined points. In contrast to a paper map, when a DRG is employed in a GIS the image may be zoomed and panned to a specific location and the coordinates of the

point recorded directly from the image. In this application, the DRG is far superior to the printed map and much more versatile. When a study area encompasses a region covered by many map sheets, DRGs may be mosaicked together to form a continuous map of the area while retaining all of the detail, accuracy and ease of use of a single DRG file.

Obtaining GCP Coordinates from Digital Orthophoto Quarter-Quadrangles

A USGS Digital Orthophoto Quarter-Quadrangle (DOQQ) is a digital image product created from National Aerial Photography Program (NAPP) 1:40,000-scale black-and-white or color-infrared aerial photographs (USGS, 1991a; 1991b; 1994; 2001b). These photos are acquired from an altitude of 6000 m above ground level (AGL) using a standard aerial mapping camera with a nominal 152.4 mm focal length. With north-south flight lines, photograph exposure centers fall at standard locations within a quadrangle to provide both stereo coverage and single frame, quarter quad-centered photographs (Figure 2-14). This design provides for the widest range of uses for the photographs (Light, 1993).

The original photographs in film format are converted to digital format by scanning at 25 μ m resolution, which produces pixels with an equivalent 1-m ground dimension. A DOQQ is then created by differentially correcting the digital photographs using photogrammetric parameters and a DEM to remove the effects of tilt and relief displacement. The result is a digital image having an accuracy specification equivalent to a standard 1:12,000 map product. This equates to a RMSE value of ± 6.2 m at check

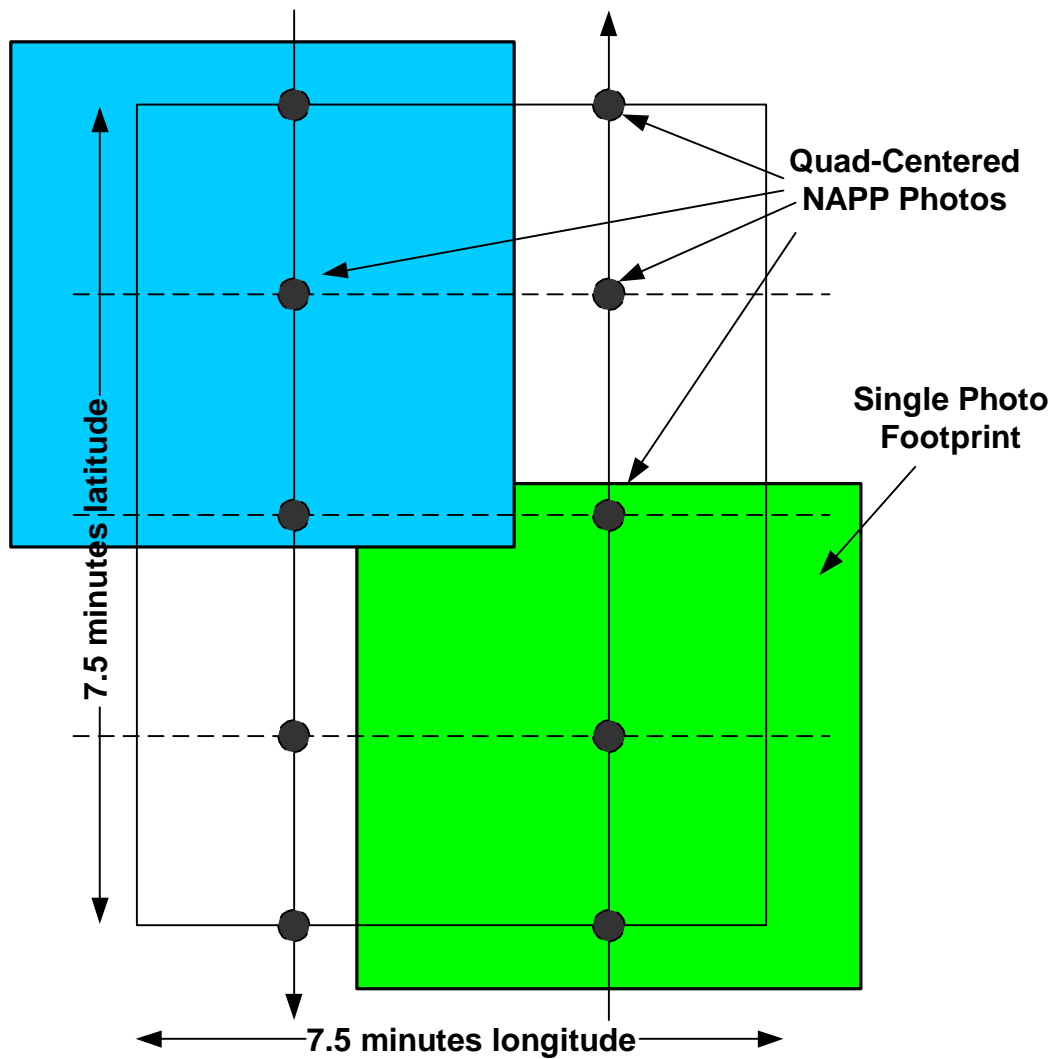


Figure 2-14. The layout of ten NAPP photographs as compared to a typical 1:24,000 USGS 7.5-minute topographic quadrangle (the photo centers falling within the quadrangle are marked by small black circles).

points. Each DOQQ is formatted to correspond to an area slightly larger than a quarter of a standard topographic quadrangle.

The DOQQs are rectified to the UTM projection, with information provided in the file header to permit registration to either the NAD 83 or NAD 27. The files generally have about 6400 pixels by 7700 lines of 8-bit gray scale data and require approximately 50 megabytes (MB) of storage space - or about 150 Mb for DOQQs produced from color photos. As with the DRG data, it is possible to recover planimetric (X, Y) coordinates from the DOQQs directly through measurements on the image. Elevations can be interpolated from DEMs.

Referring to the image structure illustrated in Figure 2-11, it is possible to obtain map coordinates (e.g., UTM) from direct measurements on the DOQQ using the formulas:

$$UTM_X = UL_X + (x * CellSize) \quad (\text{Eq. 2-3a})$$

$$UTM_Y = UL_Y - (y * CellSize) \quad (\text{Eq. 2-3b})$$

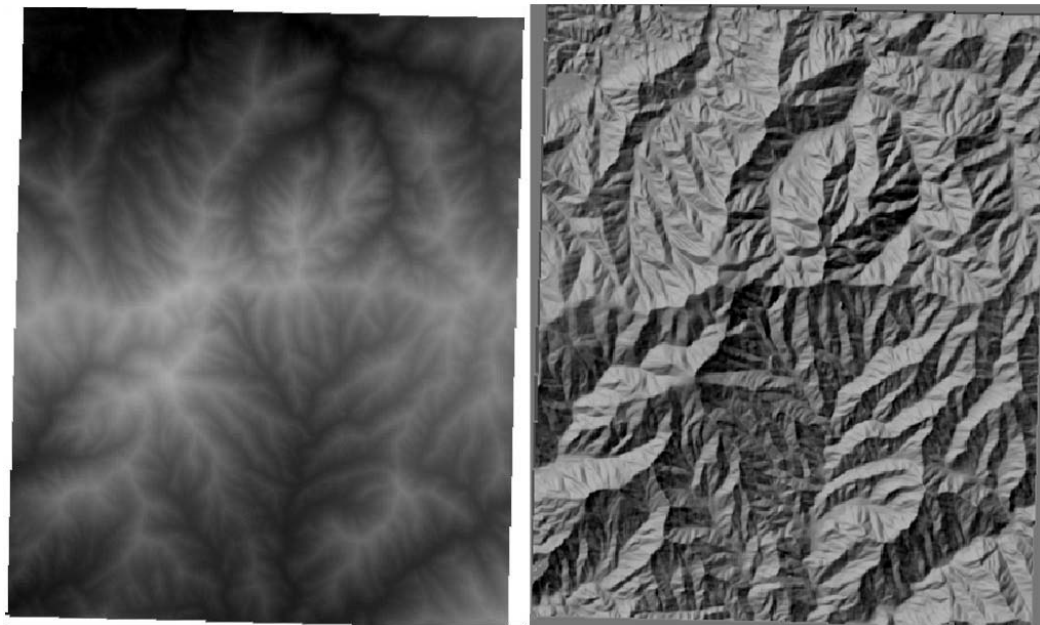
where UTM_X and UTM_Y are the map coordinates retrieved from the image, UL_X and UL_Y are the map coordinates of the upper left pixel in the image (known from metadata or header values), x and y are the pixel and line coordinates measured from the image, and $CellSize$ is the ground dimension of a pixel.

Digital Elevation Models

U.S. Geological Survey DEMs are grids of elevation values formatted to correspond to USGS 1:24,000 scale topographic quads and cast in the UTM coordinate

system on either NAD 27 or NAD 83 (Figure 2-15). Each DEM has approximately 390 pixels and 475 lines at 30 m spacing in X and Y with an elevation resolution of 1 m referenced to the National Geodetic Vertical Datum of 1929 (NGVD 29) (USGS, 1990). Elevation values for specific point locations may be extracted from the DEM by calculating the offset in pixels and lines from the upper left corner of the DEM and retrieving the value of the pixel (or cell) at that location.

The original Level 1 DEMs have a vertical accuracy of ± 7 to 15 m with no elevations having errors of greater than 50 m (Maune, 1996). These DEMs are generated from image correlation of NAPP (or equivalent) aerial photographs. Level 2 DEMs have been edited and smoothed to remove identifiable systematic errors. Data derived by



a)

b)

Figure 2-15. USGS 7.5-Minute DEM for the Thunderhead Mountain Quadrangle. a) Gray scale rendition where higher elevations are represented as lighter shades of gray. b) Hill shaded rendition of the same DEM.

digitizing existing contour maps may also fall into this category. Level 2 DEMs have improved accuracy over Level 1 data with elevation values meeting NMAS specifications of one-half of the contour interval and with no elevation errors exceeding the contour interval. A Level 3 DEM, with accuracy specifications of one-third of the contour interval, is a special product derived from contours, spot heights and break lines.

Image Control and Point Transfer

The locations on the photographs that correspond to the GCPs are called image control points or CPs. In the rectification process, the x, y coordinates of CPs are digitized from the image and employed in the mathematical transformation that results in the corrected image. The primary method for recovering CP coordinates in modern softcopy photogrammetry is to digitize the coordinates directly from the scanned image as it is displayed on the computer screen. This is accomplished by enlarging the image on the computer display so that the location of the point can be clearly seen and digitizing the pixel and line coordinates of the image control points to a fraction of a pixel (Figure 2-16). These image coordinates are saved to a disk file.

If a single photo is being rectified, a sufficient number of points must be identified on the image to solve the photogrammetric equations. This is sometimes difficult to accomplish, especially when the photos are of a natural area such as the Great Smoky Mountains and do not contain cultural detail. When multiple overlapping photos are employed, the CPs must be identified and measured on each photo using point transfer techniques. In this situation, it is possible to identify the locations of a limited

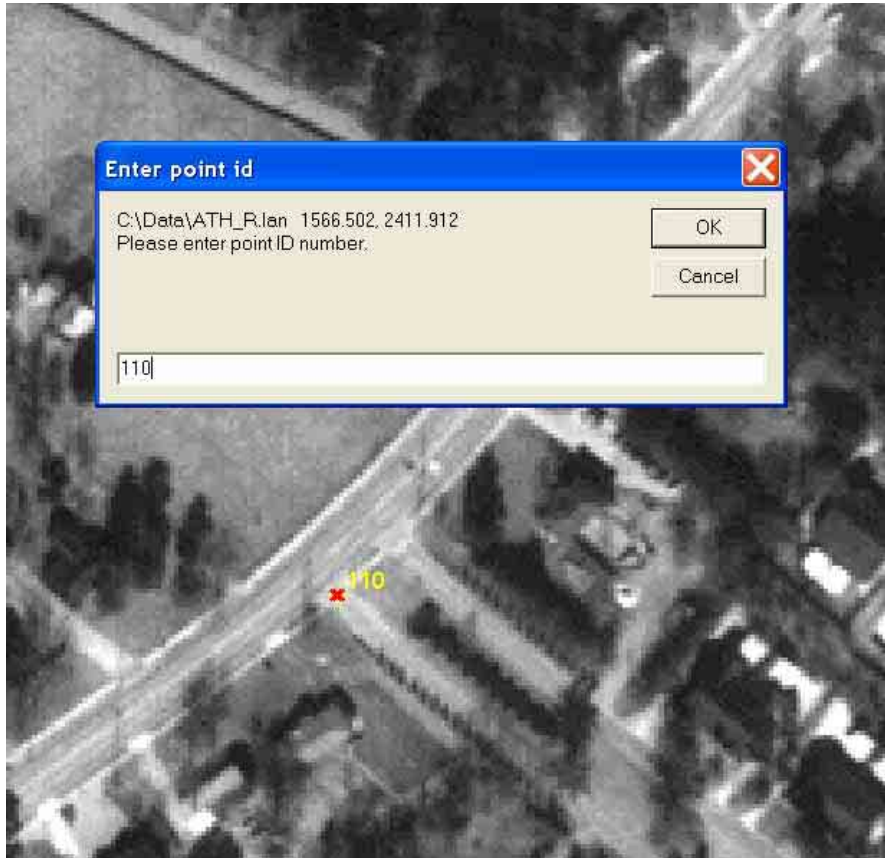


Figure 2-16. Image control points are digitized by zooming in on the image and clicking on the point location using the computer mouse. Unique ID numbers are assigned which correspond to the ID numbers of the associated GCP.

number of GCPs as well as the pass points which join adjacent photos together and use analytical aerotriangulation procedures to densify the control network to provide a sufficient number of GCPs to rectify the scanned photos (Wolf and DeWitt, 2000). Pass points are normally collected in standard positions in the image corresponding to those illustrated in Figure 2-12a. Although normally undertaken manually, it is possible to employ feature matching software such as OrthoBASE or DIME to automatically identify and digitize the coordinates of a large number of pass points in the standard locations (Erdas, 2001; Positive Systems, 2001).

Rectification Methods

The algorithmic approach to image rectification depends upon the situation and type of method to be used (i.e., polynomial, single photo photogrammetric or differential rectification). Regardless of the approach, more than the minimum number of GCPs should be employed to insure some redundancy in order to obtain an optimum solution and identify errors.

Polynomial Rectification

Polynomial rectification of a digital image employs a polynomial equation first, second, third or higher orders to establish the relationship between the image and map coordinate systems (Figure 2-17; Welch *et al.*, 1985). The most common form is the affine, or six-parameter, transformation, which accommodates differences in scale in the x and y directions, rotation and translation. In the affine transformation, parallel lines

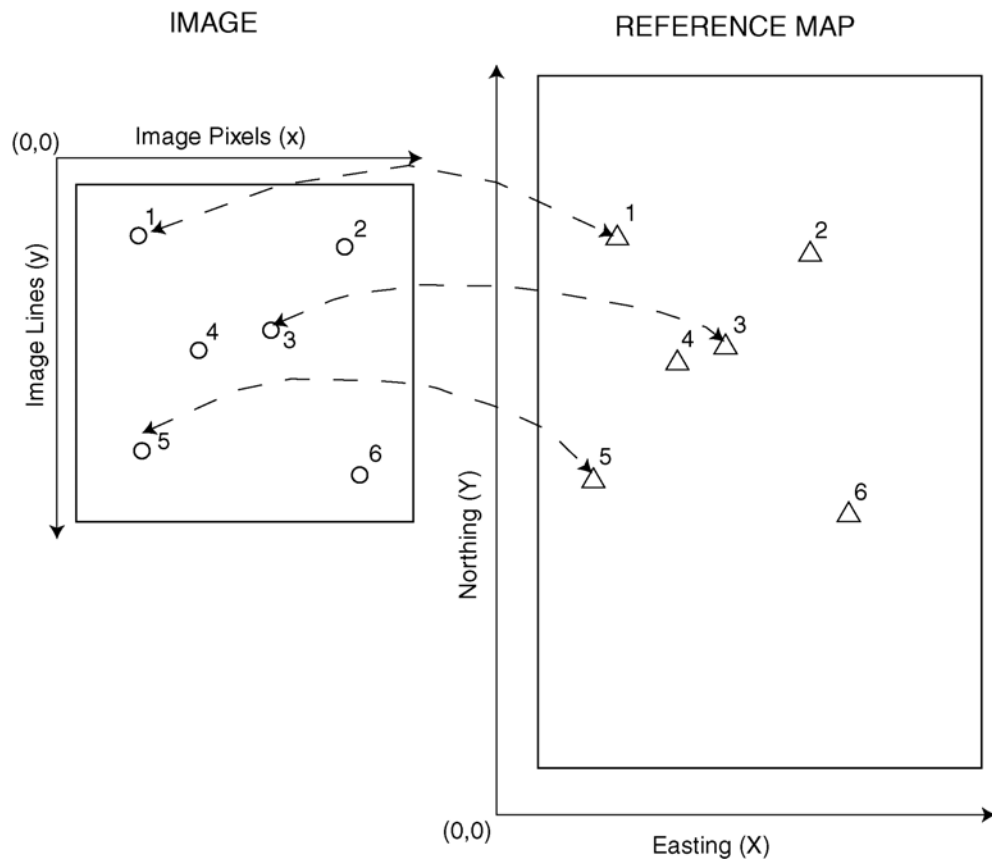


Figure 2-17. Ground control points identified on both the image (scanned aerial photograph) and reference map are used to rectify an aerial photograph.

remain parallel and the shapes of objects are retained making this particularly appropriate for mapping applications.

Using CPs and GCPs whose coordinates are known in both the image and map coordinate systems, a series of equations is developed of the form:

$$X = a_1x + b_1y + c_1 \quad (\text{Eq 2-4a})$$

$$Y = a_2x + b_2y + c_2 \quad (\text{Eq 2-4b})$$

$$x = a_3X + b_3Y + c_3 \quad (\text{Eq 2-4c})$$

$$y = a_4X + b_4Y + c_4 \quad (\text{Eq 2-4d})$$

where X and Y are the ground coordinates of the reference point; x and y are the image coordinates of the reference point; and a_i , b_i and c_i are the coefficients associated with the affine transformation. Equations 2-4a and 2-4b provide the transformation from image coordinate to ground coordinate, whereas equations 2-4c and 2-4d define the mechanism by which image coordinates may be obtained from ground coordinates.

The two affine transformation equations have a total of six unknowns and so require three two-dimensional (X, Y) control points for an exact solution. If additional points are included, the method of least squares is used to distribute the error among the points and find a best-fit solution. The benefit of using additional points is that the errors may be examined to identify and eliminate bad points from the solution. Height values for the GCPs are not required for this solution.

Once the equations defining the relationship between the photo and the object space coordinate system have been established, the original image is resampled to create a new rectified image. In practice, the physical parameters of the output image are

defined in terms of pixel size, upper left corner coordinates and number of pixels and lines. Each cell in the output image can then be associated with a discrete X, Y object space coordinate. For each cell in the output image, the pixel and line coordinates of the corresponding pixel in the input image are computed and the gray value of that pixel is retrieved from the input image and then placed in correct location in the output image. Generally, a resampling algorithm such as nearest neighbor, bilinear interpolation or cubic convolution is employed to compute an average gray value from pixels in the input image to place in the cell of the output image (Figure 2-18; Lillesand and Keifer, 2000).

Single-Photo Resection

Photogrammetric equations, known as the collinearity equations, can be employed to provide corrections for tilt and scale in the photograph. In the single photo resection method of rectification, full three-dimensional GCPs are required to compute the orientation parameters but a single ground elevation is assumed for the entire photo area for the actual rectification. This datum value is usually taken as the average of the GCP Z values (Combs and Bolstad, 1995). Relief displacements above and below the datum will remain in the rectified image as no differential correction is performed.

Collinearity is the condition that the exposure station, any object point and its photo image all lie along a straight line in three-dimensional space (Figure 2-19). The solution for the collinearity equations is nonlinear and includes six unknowns (X_L , Y_L , Z_L , ω , ϕ , κ) as follows (Harris *et al.*, 1962; Kraus, 1993):

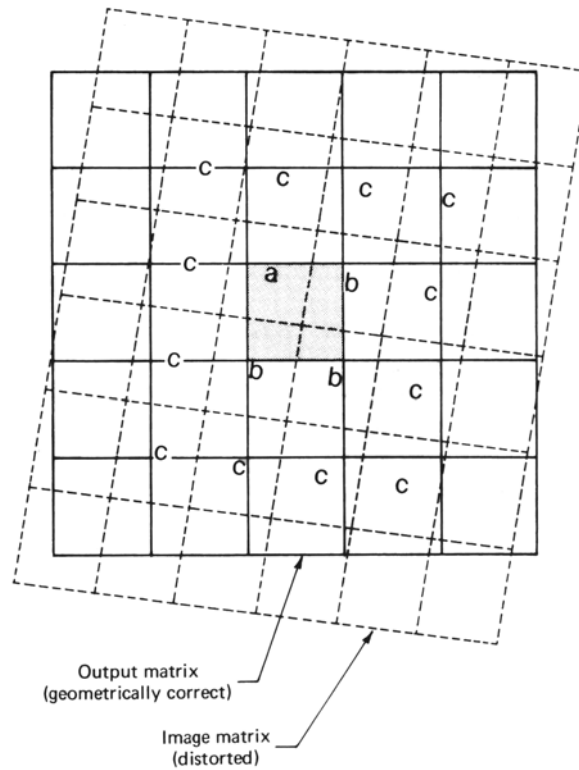


Figure 2-18. Matrix of geometrically correct output pixels imposed on matrix of original, distorted input pixels. Different resampling algorithms employ weighted averages of DN values from neighboring pixels to compute the new pixel value. a) Nearest neighbor assumes the value of the nearest pixel; b) bilinear interpolation averages four neighboring pixels; c) cubic convolution averages 16 neighboring pixels (Lillesand and Kiefer, 2000).

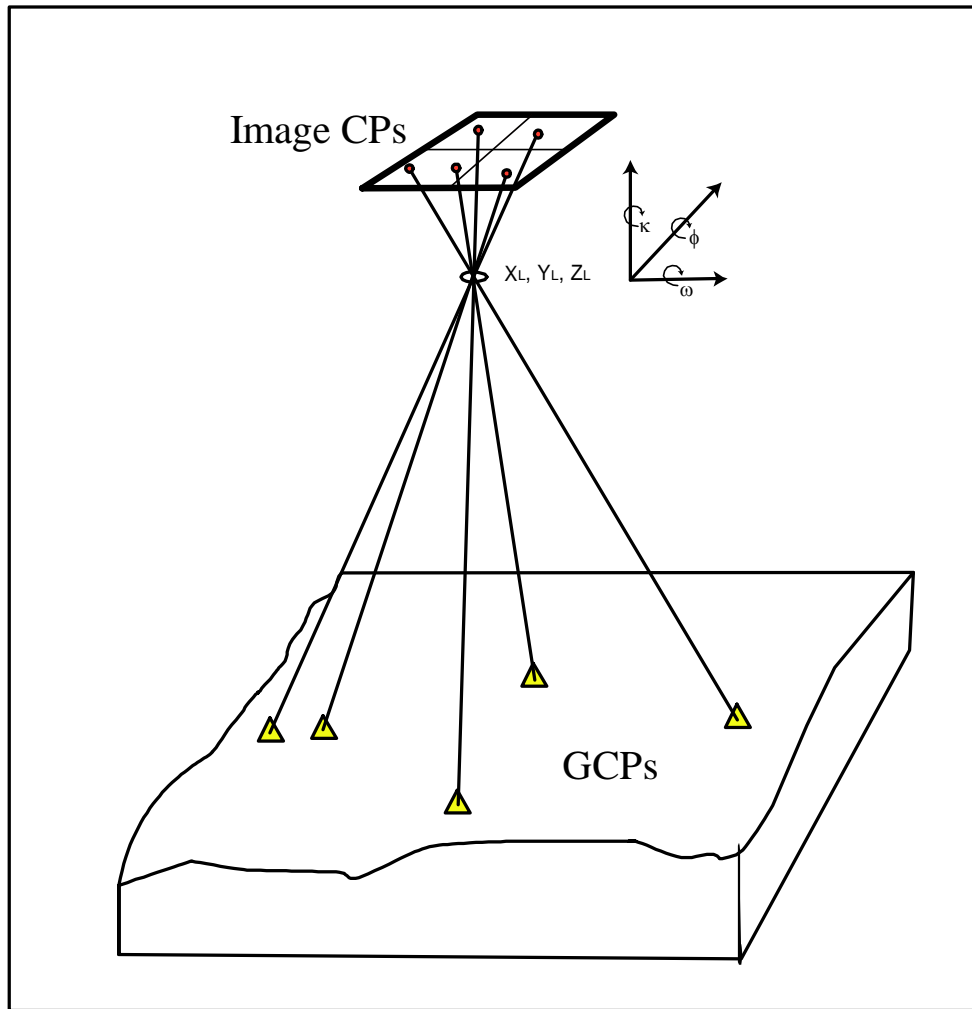


Figure 2-19. The collinearity condition and definition of six exterior orientation elements for a single photo. X_L , Y_L , and Z_L define the position of the camera lens in space and ω , ϕ , and κ are the rotation angles defining the attitude of the camera at the instant of exposure.

$$x_a = x_0 - f \frac{m_{11}(X_a - X_L) + m_{12}(Y_a - Y_L) + m_{13}(Z_a - Z_L)}{m_{31}(X_a - X_L) + m_{32}(Y_a - Y_L) + m_{33}(Z_a - Z_L)} \quad (\text{Eq. 2-5a})$$

$$y_a = y_0 - f \frac{m_{21}(X_a - X_L) + m_{22}(Y_a - Y_L) + m_{23}(Z_a - Z_L)}{m_{31}(X_a - X_L) + m_{32}(Y_a - Y_L) + m_{33}(Z_a - Z_L)} \quad (\text{Eq. 2-5b})$$

where x_a, y_a are the measured image coordinates of a point on the photograph, f is the camera focal length, X_L, Y_L, Z_L are the coordinates of the lens at the instant of exposure, m_{ij} are the nine terms of the three-dimensional rotation matrix defined by the rotation angles ω, ϕ, κ . In the above equations, the focal length (f), measured image coordinates of the point (x_a, y_a) and object space (map) coordinates of the point (X_a, Y_a, Z_a) are treated as knowns (constants). The remaining terms are unknowns.

A pair of equations of the form given above can be written for each control point. Thus, at least three GCPs, each with unique Z values, are required to solve for the six unknowns. Four or more GCPs permit the use of the method of least squares in the solution which adds redundancy and allows for the detection of errors. The collinearity equations are solved iteratively using initial approximations for the unknown exterior orientation elements. Corrections to the unknowns are computed and applied during each iteration, eventually converging on a solution when the corrections approach zero.

Orthorectification

Digital orthophotos increasingly are being used to form the baseline data set and foundation for GIS applications (Novak, 1992). Unlike normal aerial photographs, relief

displacements in orthophotos have been removed so that all ground features are displayed in their true ground position. They combine the characteristics of an aerial photograph with the geometric qualities of a map, and can be used to revise digital line graphs and topographic maps, or employed as the map base for earth science investigations (USGS, 1994; Corbley, 1996; Jensen, 1996).

Orthorectification employs the exterior orientation parameters computed using the single-photo resection method and a DEM to provide the actual Z value for each point in the output orthophoto. First, the DEM is resampled from its original resolution (e.g., 30 m) to the desired ground resolution of the orthophoto (e.g., 1 m) and cast in the same coordinate system as the GCPs. Then, on a scan line by scan line basis, an inverse transformation is established which computes the photo coordinates of each grid cell in the output orthophoto, taking into account the elevation of the point (from the DEM) and the photo orientation parameters. Since this image location is unlikely to fall at an exact pixel location, a gray scale value for the output image is obtained through resampling pixels in the input image. The result of this processing is an orthoimage at a given resolution that is a true image map where the ground coordinates for every pixel and line are known (or can be calculated) and accurate measurements may be obtained via direct measurement on the image.

Aerotriangulation

The great majority of maps created worldwide are produced from aerial photographs using photogrammetric techniques. To ensure accuracy, the photographs are referenced to a network of GCPs for which the horizontal and vertical (X, Y, and Z)

coordinates in a defined coordinate system are known to a high degree of precision. The coordinates of these points can be derived from existing maps, but more frequently they are the product of a ground survey using traditional survey or GPS techniques.

To achieve optimum results, it is desirable to have nine GCPs per photo. When a mapping project involving hundreds of aerial photographs, it is extremely difficult and expensive to collect adequate control using ground based surveys, including GPS. For this reason, aerial triangulation techniques were developed as a method of extending ground control (ASPRS, 1980). Aerotriangulation procedures permit coordinates for a very dense network of control points to be computed based on relatively few GCPs and the known geometry of the photographs. Under ideal conditions, the accuracy of aerotriangulation can be very high, with reported horizontal accuracies on the order of 0.01 to 0.02 percent of the flying height (ASPRS, 1980; Ayeni, 1982; Kletzu, 1996). In the Great Smoky Mountains, control extension is critical because of the lack of road intersections and other cultural features that are easily identified (and can serve as control points) and the near-continuous tree canopy that obscures the ground. Without aerotriangulation, therefore, it would be not be possible to map the Great Smoky Mountains National Park using the large-scale aerial photographs available for this project. The expected accuracy of the solution in this less than ideal area, however, is limited by the quality of the GCPs and CPs. Although manual and semi-analytical methods of aerotriangulation exist, they have been superseded in recent years by fully analytical methods (Ayeni, 1982). Therefore, the following discussion will focus entirely on the analytical methods.

Analytical Aerotriangulation Procedures

Typically, photographs are obtained by flying a pattern of parallel flight lines that cover the project area. The photos are spaced so that there is at least 60% forward overlap between photos in the same flight line and 20 to 60% sidelap between photos in adjacent flight lines. Together, the flight lines made up of individual photos form a “block” (Figure 2-20). Analytical aerotriangulation utilizes a process known as simultaneous bundle adjustment, in which the photogrammetric measurements on all photographs in the block are adjusted to ground control values in a single solution through the enforcement of the collinearity condition. The simultaneous bundle adjustment requires the estimated exterior orientation elements of each photo, the measured photo coordinates of GCP and pass point locations and the ground/map coordinates of all GCPs as initial inputs. Through iterative computations, the X, Y, Z ground coordinates for all of the pass points identified on the photos are derived, thus extending the network of existing GCPs (Figure 2-21).

The first step in the aerotriangulation process (data preparation) is to measure the image coordinates of the fiducial marks and pass points on each of the aerial photographs; and to identify and measure the GCPs on the DOQQs and aerial photographs. Each point must appear on at least two photographs but most can be observed on up to six photos. The locations of all pass points and GCPs are measured in each photograph that they appear in to ensure the maximum number of observations of each point. This, in turn, strengthens the solution and assists error detection by providing redundant observations (Edens, 1973; Ackerman, 1993).

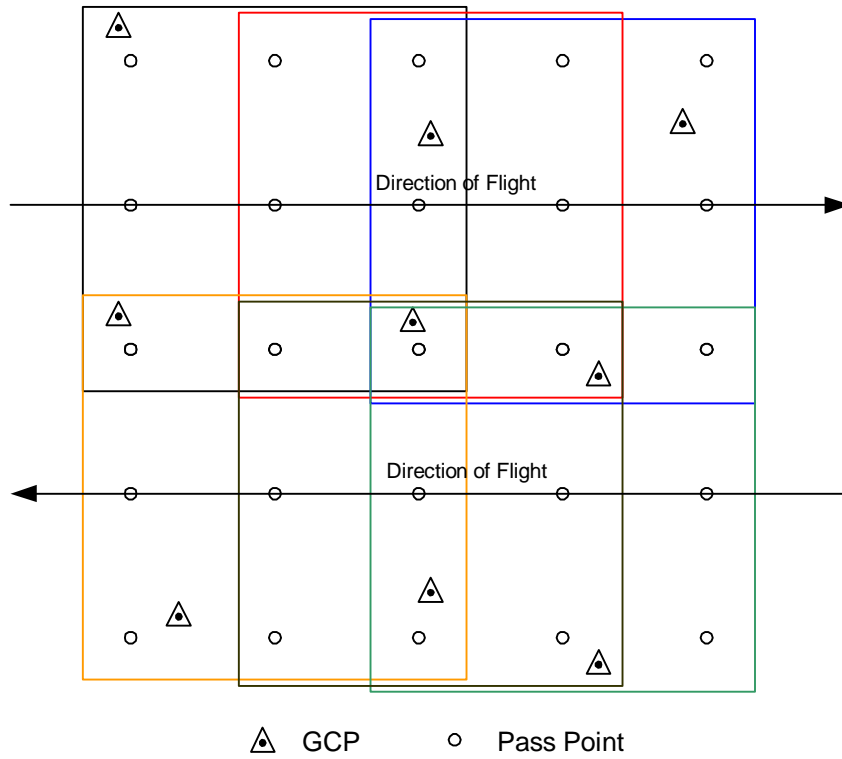


Figure 2-20. Schematic layout of a block of air photos showing nominal locations of GCPs (triangles) and pass points (circles).

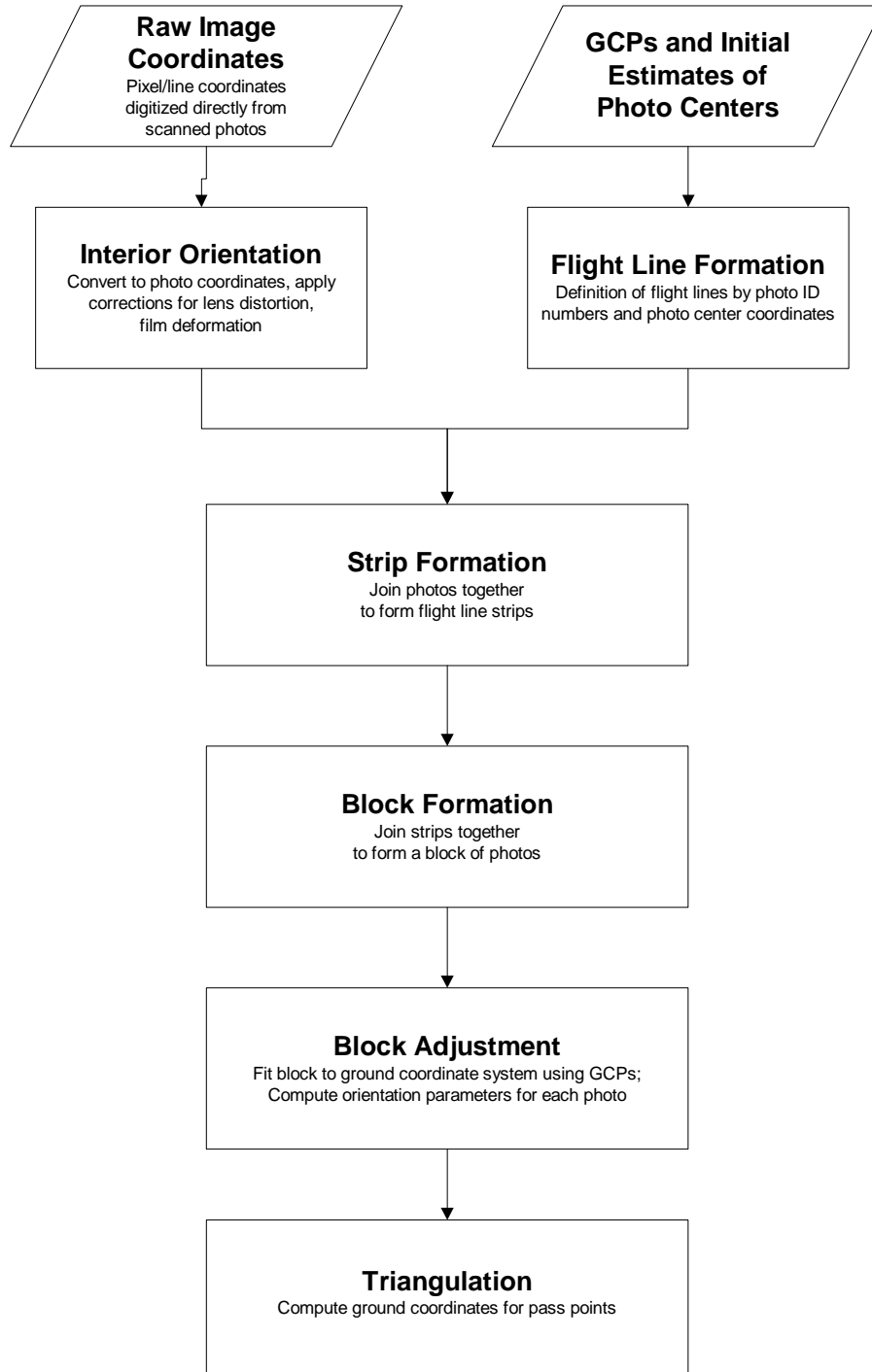


Figure 2-21. Aerotriangulation process flow.

The raw pixel and line (image) coordinates of pass points and GCPs locations are referenced to an origin of (0, 0) in the upper left corner of the image (Figure 2-22). These coordinates are converted to photo coordinates with the origin (0, 0) located at the center of the photograph as defined by the intersection of the fiducial marks. In this process the image coordinates are refined to eliminate the effects of lens distortion and film deformation.

A list of GCPs is compiled and their map coordinates listed along with their unique ID numbers. These provide the basis for the block adjustment step. Since the basic equations employed for aerotriangulation are non-linear, some initial approximations of the six unknown exterior orientation parameters (X_L , Y_L , Z_L , ω , ϕ , κ) for each photo in the block must be provided (Harris, 1962).

The exposure center can be estimated in several ways. One way is to use the coordinates of the starting and ending points of the flight line in addition to the forward overlap and flying height information to compute the individual photo centers. This method also reveals the orientation or direction of the flight line as an angle relative to north (0 degrees). Another method is to compile a database of photo centers and extract the coordinates for each photo in the block as needed. The angles omega (ω) and phi (ϕ) are estimated to be zero and kappa (κ) is estimated as the direction of the flight line relative to north. For example, for a flight line direction of east-to-west, the estimated kappa value would be 270 degrees. A standard deviation for each element is also required to set the limits for changes made to the exterior orientation values during the computations. Typically, these standard deviations are set to ± 1000 m in X, Y and Z.

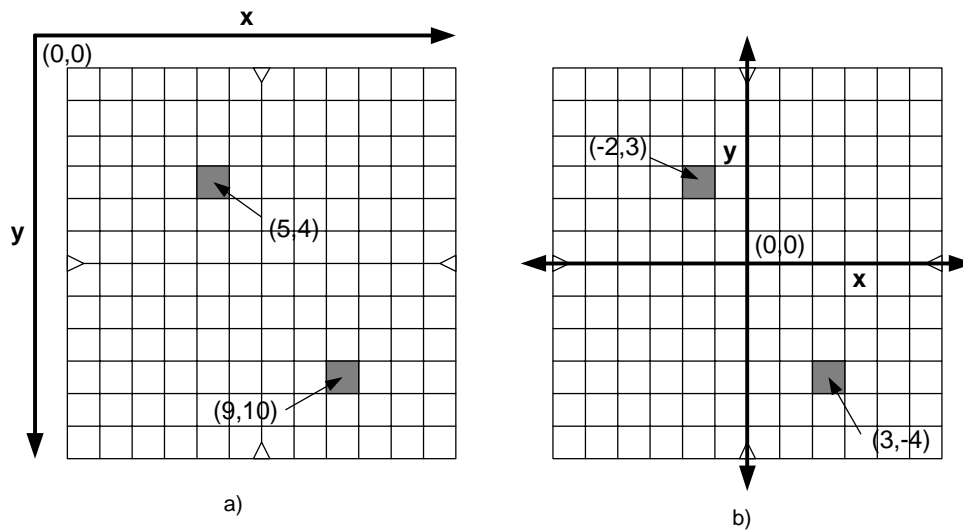


Figure 2-22. a) The raw image coordinate system has its origin (0,0) in the upper left corner of the image. The origin of the photo coordinate system (b) is at the center of the photo as defined by the intersection of the fiducial marks. for the photo center coordinates and 90 degrees for the ω , ϕ and κ angles (GPA Associates, 1994). Finally, each photo is assigned to a particular flight line and position within that flight line to facilitate strip formation.

In the strip formation process, adjacent photos forming independent stereopairs are relatively oriented to one another by means of pass points, beginning with the first pair of photos in the flight line (Keller and Tewinkel, 1967). Each succeeding photo in the flight line is then added to the solution one at a time until a continuous strip is formed using a local coordinate system for the strip defined by the first pair of photos. After a strip is complete, a two or three-dimensional polynomial adjustment transforms the photo coordinates to the ground coordinate system using whatever GCPs are available and the initial approximations for the exterior orientation parameters. At least two horizontal and three vertical control points must be available for each strip, although additional points add stability and redundancy to the solution. The result of this process is a set of very

good values for the exterior orientation elements of each photograph. With good approximations to work with, the simultaneous bundle adjustment attempts to enforce the collinearity condition on all photos in the block simultaneously. The iterative solution is repeatedly solved and adjusted until residual errors approach zero (Moffitt and Mikhail, 1980).

The final step is the triangulation of convergent rays to compute the ground coordinates of the pass points. Again using collinearity, the photos are fixed in space in position and attitude and multiple rays from observations of the same point from different photos are projected to the ground. The spatial intersection of these rays occurs at a specific X, Y, Z ground coordinate location (Figure 2-23). Where the intersection is not perfect, an error ellipse is defined that may be used to evaluate the quality of the point coordinate. In this manner, ground coordinates are computed for every pass point in the project.

The result of the aerotriangulation process is a list of GCPs of sufficient density to provide control for every aerial photograph in the project. This list is generated from data that includes a small number of conventional GCPs and up to nine pass points measured on each photo. In projects involving large numbers of photos or areas that are inhospitable to conventional ground surveys, analytical aerotriangulation provides a mechanism for generating the control required to complete the mapping project (Jordan, 1981; Welch and Jordan, 1983).

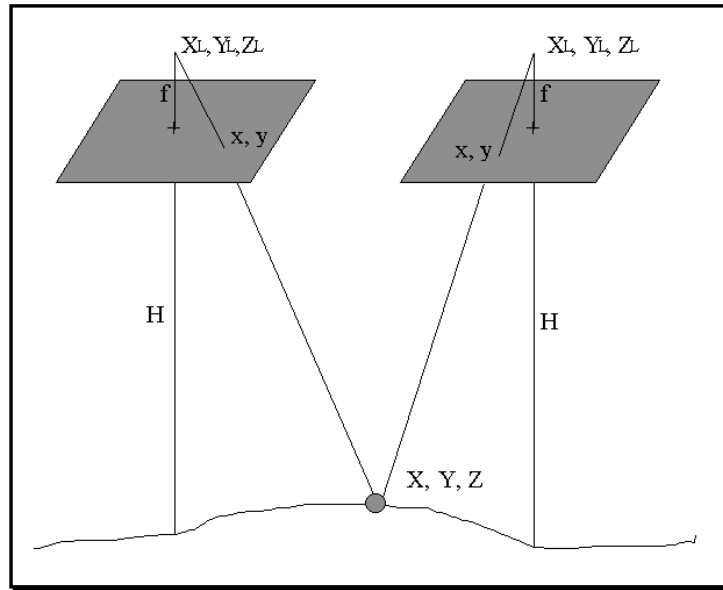


Figure 2-23. Spatial intersection enforces the collinearity condition to compute the X, Y, Z ground coordinates of pass points identified on two or more photographs.

GPS Photogrammetry

Recent developments in GPS and inertial navigation systems on-board aircraft have opened the possibilities for using these technologies in conjunction with aerial photography with the goal of reducing or entirely eliminating the need for GCPs. The idea was first introduced by James Lucas (1987) of the National Ocean Service, who proved that it was possible to solve the aerotriangulation mathematics without the use of independent GCPs. The coordinates of the exposure centers recorded by differential GPS provided a network of “virtual” control points that greatly enhanced the strength of the solution. These methods have been extended to include attitude measurements and are now operational (Ackerman, 1992; Mostafa and Hutton, 2001). Because of certain errors, it may be impractical to perform aerotriangulation without any GCPs at all. A reasonable alternative, therefore, is to minimize control rather than eliminate it. With

four GCPs in the corners of the block of photos, for example, all datum and systematic error sources can be resolved (Ackerman and Schade, 1993).

The basic mathematical solution for GPS photogrammetry is identical to that of normal aerotriangulation with the exception that the exposure centers are treated as known values instead of unknowns. The accuracies that can be obtained are comparable to standard procedures but with the advantage of requiring much less control. Typical results are on the order of 1.5 sigma for horizontal coordinates and 2.0 sigma for vertical, where sigma is the pass point photo coordinate measurement accuracy (Merchant, 1993; 1994).

Aerotriangulation Software

Two aerotriangulation programs were available for use in this study, PC Giant and AeroSys for Windows. Although PC Giant was used almost exclusively for the aerotriangulation work in this project, both programs were evaluated and will be described. PC Giant is a MS-DOS based program that is derived from the original program, General Integrated Analytical Triangulation (GIANT), which was developed at the USGS by Elassal (1976). PC Giant is versatile and robust and can be employed to solve very large blocks of aerial photos. It also can be used in close range or terrestrial photogrammetric applications. In this program, all input files must be built by hand using a text editor, using standard filenames (e.g., PREP.IN and OPT.DAT). Because the program was originally written in FORTRAN for use on mainframe computers and subsequently recompiled for use on a PC, the input formatting requirements are fairly

stringent and based on 80 column IBM punch cards. Two input files are required for use in PC Giant: 1) PREP.IN contains the camera calibration parameters and the raw (unrefined) image coordinates of all pass points and GCPs organized according to the photo number; and 2) OPT.DAT contains the aerotriangulation control parameters, estimated exposure centers and tilt parameters for each photo and the ground control point coordinates and weights (GPA Associates, 1994).

AeroSys for Windows performs the exact same function as PC Giant – it uses analytical aerotriangulation methods to convert photo coordinates to ground or map coordinates in order to densify a control network for a project (Stevens, 2000). The major difference between AeroSys and PC Giant is in the user interface: AeroSys operates in a Windows 95/98/NT environment vs. the MS-DOS environment of PC Giant. This difference simplifies many tasks, but also complicates matters somewhat. The point-and-click interface provided by Windows is more intuitive than the MS-DOS command line and file formats, and data structures are not as rigid as those imposed by PC Giant. The same input data are required for each program, however, and it must be prepared manually before running the program. AeroSys is not a single program but, rather, a series of programs, each of which performs a separate portion of the total operation. They are called in order by the AeroSys control program and use the results of the previous step in the sequence as input. The advantage of this method is that it is possible to detect errors at any stage in the process. The disadvantage is that you have a great many intermediate files to keep track of and possibly examine in an effort to detect and fix errors. Like PC Giant, output of the program includes files containing the final

ground coordinates of all pass and control points, and the final camera exposure station coordinates and orientation angles.

Both PC Giant and Aerosys provide accurate and virtually identical coordinate values given the same input data and will operate on large blocks of photos (up to 2,000 photographs in a single solution). Where they differ, however, is in the relative difficulty of identifying and correcting blunders and other errors. Although the runtime error messages in PC Giant are terse and often unrelated to the actual error, they generally indicate that there is an error somewhere in one of the two input files. With experience, it is possible to identify and correct data-related problems through examination of the different sections of the GIANT.OUT file and then editing the IMG.DAT and OPT.DAT files.

Similarly, AeroSys reports that errors have occurred but does not identify their sources. The user is left to examine a number of intermediate files with names like SIBA.REL, SIBA.CAM, and SIBA.PHC to locate and correct errors in the input data. Typically, the errors are a result of misnumbered points, photos out of order on a flight line or incorrect camera calibration data. In some cases, it actually is impossible to identify and correct the sources of error. In this respect, AeroSys is much more sensitive to errors in input data than PC Giant.

Vegetation Mapping Projects in National Park Lands

Vegetation mapping has traditionally focused on thematic concerns rather than the geometric components of the project. While this is not so much of a concern in flat areas,

it is obvious that geometry is a major issue in mountainous regions. Recent work has depended on the detail that can be interpreted from conventional aerial photographs, but a lack of understanding of the geometric correction procedures required to produce an accurate map continues. A few projects involving the use of both satellite imagery and aerial photographs to map vegetation in national parks are summarized in the following paragraphs.

Vegetation Mapping Using Automated Classification of Satellite Images

Satellite image data and automated classification methods have been used with some success in an attempt to produce vegetation maps of large areas. These efforts have been limited by the spatial resolution of the data and the limited number of classes that can be differentiated. In addition, a satellite image can only be rectified to about 0.25 to 0.5 pixel.

As part of the Gap Analysis Project, a land use classification consisting of 40 land-use/land-cover classes for the entire State of Florida was produced from Landsat Thematic Mapper (TM) image data at 30-m resolution (FBDP, 1996; Doren *et al.*, 1999). The aim of the project was to identify natural areas within Florida for use in regional-scale and statewide natural resource management and was not designed specifically for vegetation analysis. It was found that automated classification of satellite image data was not suitable for mapping Everglades vegetation because the results were incomplete and erroneous. For the level of detail and accuracy required, interpretation of conventional aerial photographs was preferred (Rutchev and Vilchek, 1994; 1999).

Classification of Landsat Thematic Mapper data was also used to develop vegetation and land use maps for Crater Lake, Mount Rainier, North Cascades and Olympic National Parks in northwestern United States. To assist in the construction of a comprehensive GIS system for the region, landform and vegetation maps were compiled by integrating TM satellite image data, aerial photography, digital topographic data and other existing GIS data layers (Campbell *et al.*, 1996).

Computer-based classification techniques were employed to identify vegetation information from the Landsat TM image data. In this case, the authors concluded that the satellite images would provide an advantage over conventional interpretation of aerial photographs. Although no classification information and accuracy figures were reported, it was felt that the resolution of the TM data permitted extremely detailed vegetation information where good spectral signatures were available.

The first comprehensive vegetation map of the Great Smoky Mountains National Park was created from Landsat Thematic Mapper image data using supervised classification techniques (MacKenzie, 1988; 1991; 1993). A total of 14 classes of vegetation were identified from the image data to create a vegetation map with a cell size of 90 x 90 m (0.81 ha). Georectification and accuracy assessment were hampered by a lack of high quality ground control in this project, but the map represented the best vegetation map available for the entire Great Smoky Mountains National Park prior to the vegetation maps being produced in the CRMS mapping project.

In general, the Landsat and Spot satellite image data used in these studies are of coarse resolution and small scale. Although useful for deriving general classes of

vegetation and land use corresponding to the USGS Land Use/Land Cover Classification System Levels I and II, they cannot provide the sort of detailed information on species and community required in recent vegetation mapping projects, which frequently require detail comparable to Levels III and IV (Anderson *et al.*, 1976). For example, MacKenzie (1993) identified 14 classes of vegetation in the Smokies from satellite imagery when, in reality, over 100 classes can be identified from aerial photographs. The large scale and high resolution associated with aerial photographs are better suited for discriminating this type of information (Lillesand and Kieffer, 2000).

National Parks in South Florida

In 1994, the Center for Remote Sensing and Mapping Science at The University of Georgia, in conjunction with the National Park Service, undertook to produce a detailed vegetation database and associated map products for a 10,000 km² area in south Florida encompassing Everglades and Biscayne National Parks and Big Cypress National Preserve (Welch *et al.*, 1995; 1999). In all, 72 separate 1:15,000 scale map sheets were produced, corresponding to USGS 1:24,000 scale topographic quadrangles. More than 100 vegetation classes are depicted on the maps. The primary source materials for the vegetation information were approximately 200 NAPP 1:40,000-scale color-infrared aerial photographs. Trained vegetation specialists performed the interpretation of the complex Everglades vegetation using 4x paper print enlargements of 1:10,000 scale with a minimum mapping unit (MMU) of 1 ha.

There are few features in the Everglades that are suitable for use as GCPs. Consequently, GCPs for this project were provided by a mosaic of eight SPOT panchromatic satellite images of 10-m resolution that had been rectified to 23 control points surveyed using differential GPS techniques and supplemented with points (road intersections, etc.) identified on the existing USGS topographic maps (Figure 2-24). The rectification accuracy of each SPOT scene was approximately 5 to 9 m (Welch *et al.*, 2002).

Ground control points required to rectify each individual photo were identified on the SPOT satellite image mosaic viewed on the computer screen and the hardcopy photographs and then marked on the overlays. These points consisted primarily of features such as distinct points on islands, trees, bushes and small ponds that could be reliably identified on both the satellite image mosaic and the photo. Each point was assigned an ID number and its ground coordinates were digitized in heads-up mode from the SPOT mosaic. Rectification coefficients were developed for the overlays using second-degree polynomials and generally yielded RMSE values at independent check points of approximately ± 4 to 5 m per photo. Because of the lack of topographic relief in the region, differential rectification with a DEM was not required to meet accuracy specifications.

The overlays were scanned at 400 dpi and saved as TIFF files. The raster lines in the scanned overlays were then converted to vector format using the R2V software package, geocoded using the previously determined rectification coefficients and converted to ARC/INFO format for integration into the GIS (Able Software, 1999).

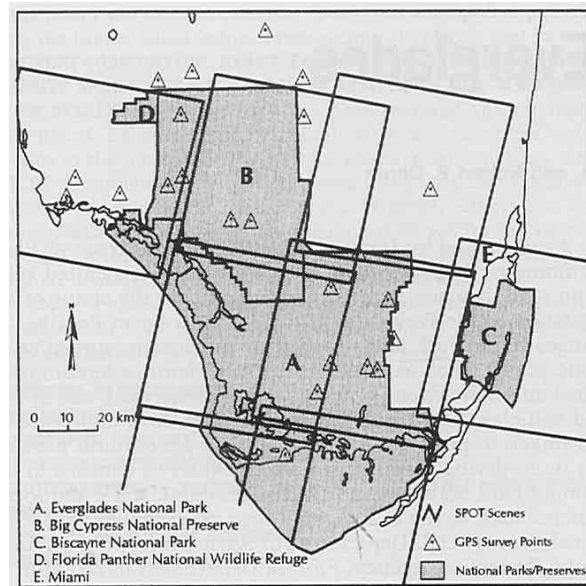


Figure 2-24. Location map of Everglades National Park, Big Cypress National Preserve, Biscayne National Park, and Florida Panther National Wildlife Refuge, along with the outline of eight SPOT scenes and the location of 23 GPS survey points employed to rectify the SPOT images (Welch *et al.*, 1999).

There, the vectors were converted to polygons, edited, edge-matched with neighboring photos and attributes assigned to create the final maps (Figure 2-25) (Welch *et al.*, 1999).

USGS - NPS Vegetation Mapping Project

In 1996, the National Park Service initiated a program to produce vegetation maps of all of the national park lands, including national historical sites, battlefields and military parks, monuments, seashores and preserves (USGS, 2001a). At the beginning of the project, the Environmental Systems Research Institute (ESRI) was hired to be the primary contractor for the production of a number of prototype maps. Environmental

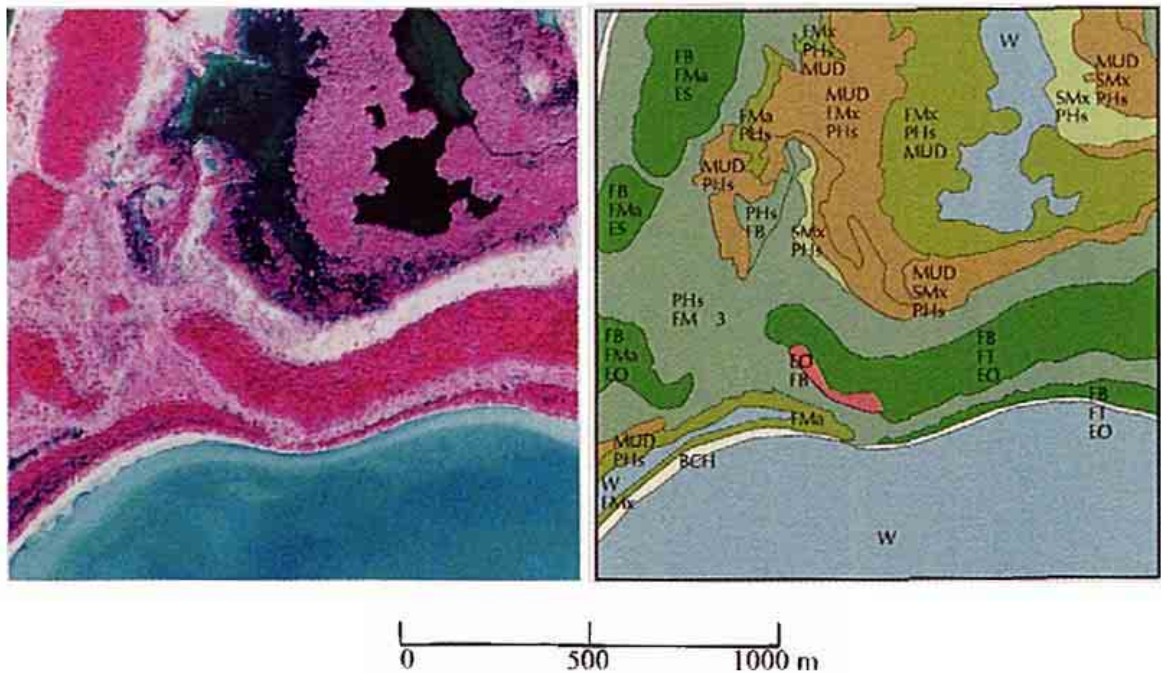


Figure 2-25. Portion of the Everglades vegetation map database and corresponding photo showing an area along the south coast of Everglades National Park. The map represents vegetation classes for halophytic herbaceous prairie (PHs), mixed mangrove scrub (SMx), and exotic lather leaf (EO) (Welch *et al.*, 1999).

Systems Research Institute then subcontracted with Aerial Interpretation Services (AIS) to perform the photointerpretation tasks. Additional parks are being mapped by the U.S. Bureau of Reclamation's Remote Sensing and Geographic Information Group (RSGIG). Both groups are cooperating with The Nature Conservancy (TNC) who are responsible for developing the vegetation classification system for the individual parks and for creating a National Vegetation Classification System (NVCS). The protocol for the mapping procedures was developed and refined as experience was gained in mapping the first several parks. This protocol included the development of a hierarchical vegetation

classification system based on field surveys and sample plots, acquisition of color infrared aerial photographs at a standard 1:12,000 scale, interpretation of the photographs, transfer of the interpreted data from analog to digital format, development of the digital GIS database, and accuracy checking. The standard MMU was 0.5 ha although a smaller MMU (0.25 ha) was employed in several of the smaller parks.

These parks range in size from 17 to 62,000 ha and required between three and over 200 photos of various scales to achieve full coverage (Table 2-3). Depending on the quality of the photos provided, either color infrared or true color aerial photographs were employed for photo interpretation. In general, the same procedure for mapping the vegetation was followed for each park. Photo interpretation was performed by viewing the aerial photographs in stereo under 3x magnification. Polygons were then delineated directly on polyester overlays registered to the photos. Edge matching between polygons on adjacent photos was performed as a final step (ESRI/AIS, 1998).

Transfer of the vegetation polygons from analog to digital format was done using a manual rectification method. The USGS DOQQs were printed on frosted polyester at a scale that approximated the photo scale – nominally, 1:12,000. The photos and overlays were then placed on the hardcopy of the DOQQ and the vegetation polygons transferred manually to a separate overlay registered to the DOQQ. This painstaking task involved the visual matching of detail between the air photo, overlay and DOQQ to make the best fit of the polygon data to the DOQQ. Where relief displacement or scale variations caused misalignment between the materials, the photos were shifted relative to the DOQQ until a small area of the photo was brought into alignment and the detail

Table 2-3. NPS Vegetation Mapping Project. Completed and partially completed National Monuments (NM), Seashores (NS), Historical Sites (NHS) and Parks (NP).

Park Name	Contractor	Area (ha)	Completed
Agate Fossil Beds NM	ESRI / AIS ¹	1,166	May 1998
Assateague Island NS	TNC ²	19,433	N/A
Congaree Swamp NM	ESRI / AIS	8,907	Oct 1998
Devils Tower NM	CDS / BOR ³	2,330	Feb 1998
Fort Laramie NHS	ESRI / AIS	337	Sept 1998
Glacier NP	USGS ⁴	4,104,280	N/A
Great Smoky Mountains NP ⁵	ESRI / AIS		June 2000
Isle Royale NP	ESRI / AIS	54,413	June 2000
Jewel Cave NM	CDS / BOR	542	July 1998
Mount Rushmore NHS	CDS / BOR	523	Feb 1998
Point Reyes NS	ESRI / AIS	62,753	N/A
Rock Creek NP	ESRI / AIS	709	Oct 1998
Scotts Bluff NM	ESRI / AIS	1,215	Dec 1998
Tuzigoot NM	ESRI / AIS	17	July 1997
Wind Cave NP	USGS / BOR	11,455	July 1998
Yosemite NP	TNC	562,753	N/A

¹ Environmental Systems Research Institute and Aerial Interpretation Services

² The Nature Conservancy. TNC in the contractor column indicates that the vegetation classification is complete or underway and that mapping has not yet begun.

³ Computer Data Systems and U.S. Bureau of Reclamation RSGIG

⁴ U.S. Geological Survey

⁵ The ESRI/AIS effort in Great Smoky Mountains National Park was a pilot project and limited in scope to the Mount LeConte and Cades Cove Quadrangles.

transferred to the polyester base. In this manner, all polygons from each of the interpreted photos were transferred to the DOQQ base.

The polyester overlay containing data from photos corresponding to a single DOQQ was then scanned and converted to ARC/INFO vector format, edited and attributed to create a final map coverage. The final step was to georeference the coverage by transforming the database from “digitizer inches” coordinates to UTM coordinates by identifying four to six registration points per coverage that could be identified on the polygon coverage and on the underlying orthophoto. The coverages were then transformed to real world coordinates. The accuracy of the transformed polygons was assessed by comparing the delineations to the orthophoto. Where discrepancies were identified, the coverages were edited and corrected to better fit the orthophoto. Again, these methods are satisfactory for use in regions of low relief but become difficult to implement and of uncertain accuracy in areas of rugged terrain.

Glacier National Park

The USGS Environmental Management and Technical Center is using procedures similar to those employed by the ESRI/AIS team on the prototype parks to map vegetation in Glacier National Park (Figure 2-26). One difference in the approach is that the transfer of the polygon data from the overlays to the DOQQ base is performed using a Zoom Transfer Scope rather than by manually adjusting the overlays to the DOQQ on a light table and redrawing the polygons (Hop, 2002, Personal Communication). The base maps are then converted to vector format and ARC/INFO coverages built, edited and

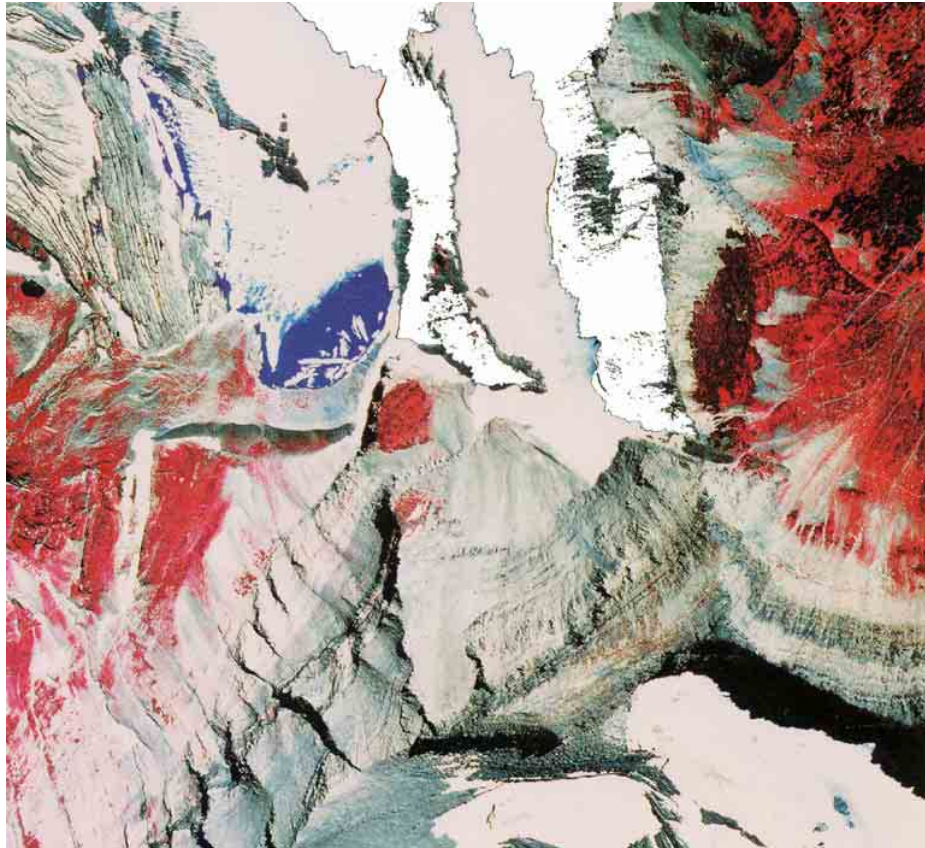


Figure 2-26. 1:12,000 scale color-infrared aerial photograph of Glacier National Park recorded as part of the vegetation mapping project (HJW, 1998).

attributed according to the protocol. Although work is still on-going, it is evident that this method is not well-suited to the extremely rough mountainous terrain of Glacier National Park. Thus, the mapping team is exploring other options including orthorectification of the photos and the associated overlays before scanning and conversion to digital format. This latter approach is similar to that developed by the CRMS for mapping the Great Smoky Mountains National Park, and is the focus of this dissertation.

Great Smoky Mountains National Park

In 1996, the ESRI/AIS team began mapping the Cades Cove and Mount LeConte Quadrangles in the Great Smoky Mountains National Park. Using standard 1:12,000-scale color-infrared aerial photographs recorded in the autumn to best differentiate tree species and communities, AIS interpreted every photograph on each quadrangle – about 120 photos on both quadrangles. Using the procedures described above, polygon outlines were drawn onto photo overlays and edge-matched with polygons on adjacent photographs. The polygons were then converted to digital format using heads-up digitizing methods directly onto the DOQQ base displayed on-screen within ArcView (ESRI/AIS, 2000). Finally, the polygons were edited and attributed within ARC/INFO to create the final GIS coverages. The total effort required five years to complete the two quadrangles – largely because of the difficulty in transferring the vegetation polygons manually from the aerial photographs to the DOQQ and GIS database. The Great Smoky Mountains National Park is the most diverse area of those mapped in the initial pilot study. This is evidenced by the fact that the classification system developed by TNC for the area has over 150 vegetation and land use classes.

It is evident from these discussions that in order to derive detailed community or species-level vegetation information, it is necessary to employ aerial photographs as the primary data source and that manual interpretation methods be employed. Further, although there are a number of techniques for transferring the detail from the aerial photographs to a map base, it is essential to accommodate relief displacements found in photographs in mountainous areas to insure the highest level of positional accuracy.

The Center for Remote Sensing and Mapping Science is producing vegetation maps of the remaining 24 quadrangles in Great Smoky Mountains National Park using the same large-scale aerial photographs and a similar vegetation classification system as that described above. The softcopy photogrammetric methods and procedures that have been adapted to the task of transferring detail from the aerial photographs to the GIS database will be described in the following chapter.

CHAPTER 3

CONTROL EXTENSION TECHNIQUES AND RECTIFICATION PROCEDURES REQUIRED FOR GIS DATABASE DEVELOPMENT

Mapping vegetation communities in the Great Smoky Mountains National Park for the purpose of building a detailed and accurate GIS database required the integration of photo interpretation, photogrammetry and GIS technologies (Figure 3-1). The photogrammetric problems that are the focus of this discussion are related to the location of ground control, extension of control through the use of aerotriangulation techniques, rectification of photographic overlays and positioning of polygons that form the vegetation layers. Methods and procedures developed to solve these problems are discussed in this chapter.

Data Sets

The foundation data sets for this project were developed by the USGS and provided by the GIS Lab at the Great Smoky Mountains National Park Twin Creeks Research Center. These included DOQQs, Level 2 DEMs, DRGs and DLGs, all referenced to the UTM coordinate system, Zone 17, and cast on NAD 27 (Table 3-1).

Digital Orthophoto Quadrangles (DOQs) and Quarter Quadrangles (DOQQs)

Black-and-white Digital Orthophoto Quarter Quadrangles (DOQQs) were derived from NAPP 1:40,000 aerial photographs recorded in the winter of 1993. The

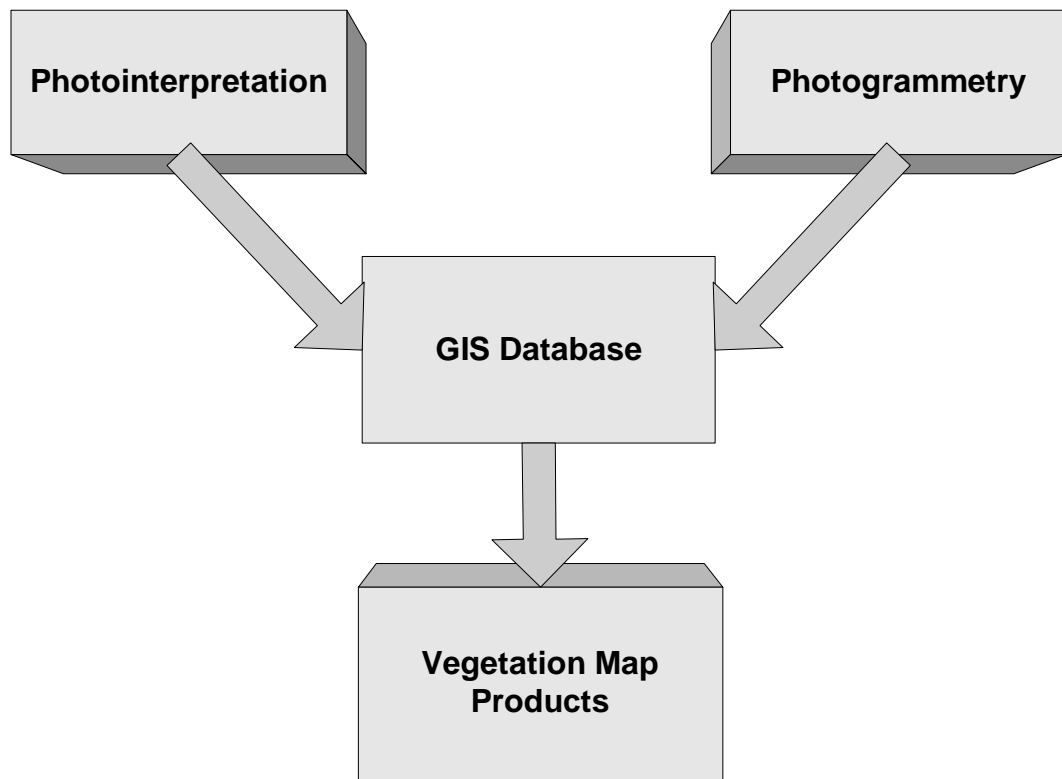


Figure 3-1 – The Great Smoky Mountains vegetation mapping project requires the integration of mapping technologies to create a GIS database.

Table 3-1. Data sources used in the map/database development for Great Smoky Mountains National Park

Data Source	Format and Type of Data	Flying Height (FH) and/or Scale	Resolution	No. Required to Cover the Park	Comments and/or Problems
CIR Air Photos October 1997 May 1998 October 1998	23 x 23 cm Analog film transparencies	Nominal FH \approx 1,800 m AGL 1:12,000	\sim 0.4 m	\sim 1,000	Terrain relief in excess of 30% of flying height. A smaller scale could alleviate this problem. Fall leaf-on conditions are ideal for mapping overstory forest communities.
USGS Topographic Maps	Paper maps	1:24,000	-	25	Last updated 1960-1970's.
USGS DOQQs Pan and CIR	Digital	-	1 m	112	USGS DOQQs have a planimetric accuracy of approximately \pm 3 m RMS.
USGS Level 2 DEMs	Digital	1:24,000	30 m post spacing	25	USGS Level 2 DEMs have a vertical accuracy of approximately \pm 3 - 5 m RMS.
USGS DRGs	Digital	1:24,000	2.4 m	25	USGS topographic maps scanned at 100 μ m

geographic extent of a Digital Orthophoto Quadrangle (DOQ) is equivalent to that of the corresponding 7.5-minute 1:24,000-scale topographic quadrangle, plus 50-300 metres of overedge to permit mosaicking and the inclusion of tick marks indicating the corners of the standard quadrangle. There are four DOQQs per DOQ, corresponding to the north-west, northeast, southeast and southwest quadrants (Figure 3-2). The primary datum for both DOQs and DOQQs is NAD 83, with UTM coordinates in metres. Metadata are provided with each DOQ (or DOQQ) that indicates the UTM coordinate of the upper left pixel for each datum to permit placement of the DOQ/DOQQ on either NAD 83 or NAD 27 (USGS, 1991a; 1991b). The ground pixel size is 1 metre and the average size of a DOQQ image file is about 40 Mb.

Coordinates of features derived from DOQs and DOQQs must meet NMAS horizontal accuracy requirements for 1:24,000 and 1:12,000 scale map products, respectively. The accuracy standards for well-defined planimetric features require root-mean-square-errors (RMSE) of less than ± 7.2 m at 1:24,000 scale and ± 6.2 m at 1:12,000 scale. In actual practice, coordinates measured from DOQQs frequently exhibit planimetric errors of less than ± 3 m (Dalby and Rea, 2001; Dalby and Blaty, 2001).

For this project, 10 CD-ROMs containing 112 DOQQs were provided by the Great Smoky Mountains National Park library located at the Sugarland Visitor Center. These DOQQs represent all 25 USGS topographic quadrangles covering the Park and adjacent areas. The image data were provided in native USGS DOQ format, which is a simple band-interleaved-by-line (BIL) format with a header file and metadata providing georeferencing information for both NAD 27 and NAD 83. Because the native DOQQ

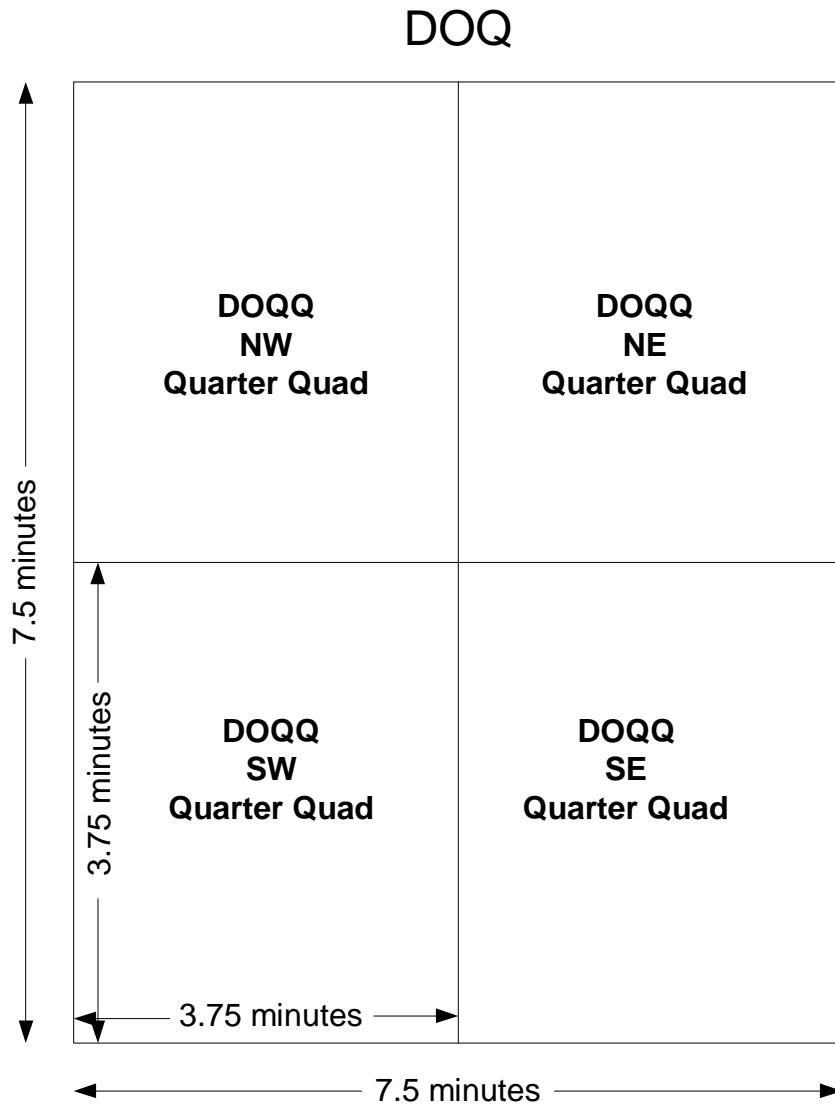


Figure 3-2. The organization of four DOQQs within a DOQ.

format is unique and designed primarily for data exchange rather than direct use in mapping software, a special computer program had to be written to import the files into the Desktop Mapping System (DMS) (R-WEL, Inc., 2000). This program offered the option of registering the file to either NAD 83 or NAD 27, with NAD 27 required for this project to maintain consistency with the existing ark GIS database. Subsequently, the DOQQs were imported into the DMS LAN image format, permitting their use in the DMS, ArcView and ARC/INFO software packages. The DOQQ images were used as a source for planimetric ground control and provided backdrops during the editing of vegetation coverages.

Digital Elevation Models (DEMs)

The USGS 7.5 minute DEMs feature a regularly spaced grid of elevations at 30-m intervals referenced to the UTM coordinate system (USGS, 1990). In this instance, the planimetric grid locations are referenced to NAD 27 and the elevations to NGVD 29. The DEM posts are arranged from south to north in profiles that are ordered from east to west and correspond in coverage to the 1:24,000 scale topographic quadrangles. The Level 2 DEMs used in this project have a stated vertical accuracy at the 90 percent level of confidence of ± 7 m (USGS, 1987). A single DEM covering the entire Park was created by mosaicking the Level 2 DEMs into a single file of 3148 pixels by 1741 lines. The original 16-bit integer elevation values were then scaled to 8-bit for use in the DMS.

When tested against 48 spot heights and bench marks identified on the Hartford and Clingmans Dome Quadrangles, the DEMs yielded a $RMSE_Z$ value of ± 3.75 m, which is well within the USGS vertical accuracy specification. Similar results also have

been found by other researchers in their tests of the vertical accuracy of DEMs (Atkins and Merry, 1994). The DEMs were used to derive elevation control and for the generation of terrain corrected orthophotos.

Digital Raster Graphics (DRGs) and Digital Line Graphs (DLGs)

The USGS DRG correspond to 1:24,000 scale topographic maps scanned at a resolution of 100 μm (250 dots per inch) and rectified in raster format to the UTM coordinate system. The resulting pixel resolution is equivalent to a ground pixel size of 2.4 m. The planimetric position accuracy and datum of the DRG matches the accuracy and datum of the source map (± 7.2 m RMSE and NAD 27 for this project area).

The USGS DLG data are vector data for transportation and hydrography collected from 1:100,000 scale maps. According to specifications, their planimetric accuracy is on the order of ± 30 m RMSE. However, the DLG vectors appear to fit reasonably well when overlaid on the DRG (Figure 3-3). Both the DRGs and the DLGs were used for reference in this project.

Aerial Photographs

Source photographs for the vegetation mapping included approximately 1900 color infrared transparencies with nominal photo scales of between 1:12,000 and 1:14,000 (Figure 3-4). Of these, about 1000 photos were used in the compilation of the vegetation database and map products for the quadrangles included in this study. The 23 x 23 cm format aerial photographs were recorded from a flying height of about 2800 metres AMSL or 2,100 m above ground level (AGL) on three different dates by EarthData, Inc

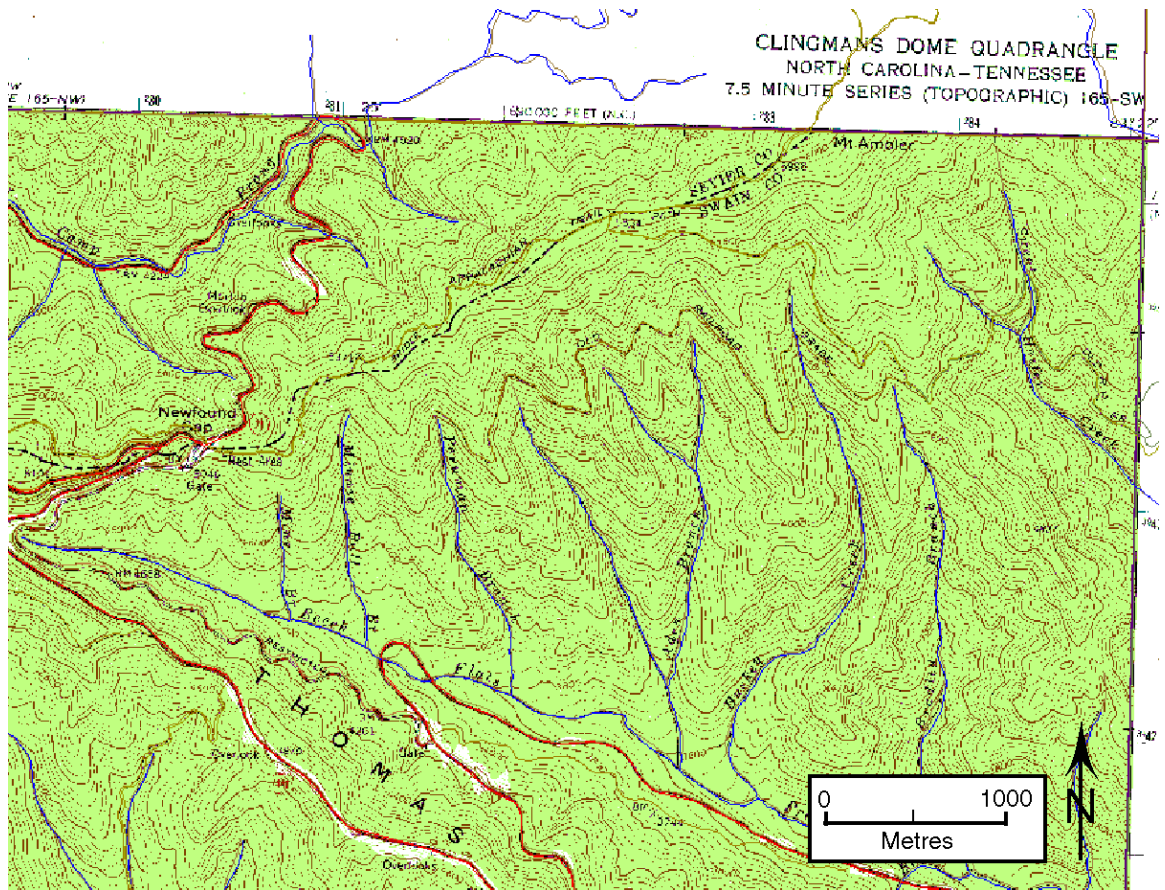


Figure 3-3. Portion of the Clingmans Dome DRG showing the DLG transportation (red) and hydrography layers (blue) as overlays.

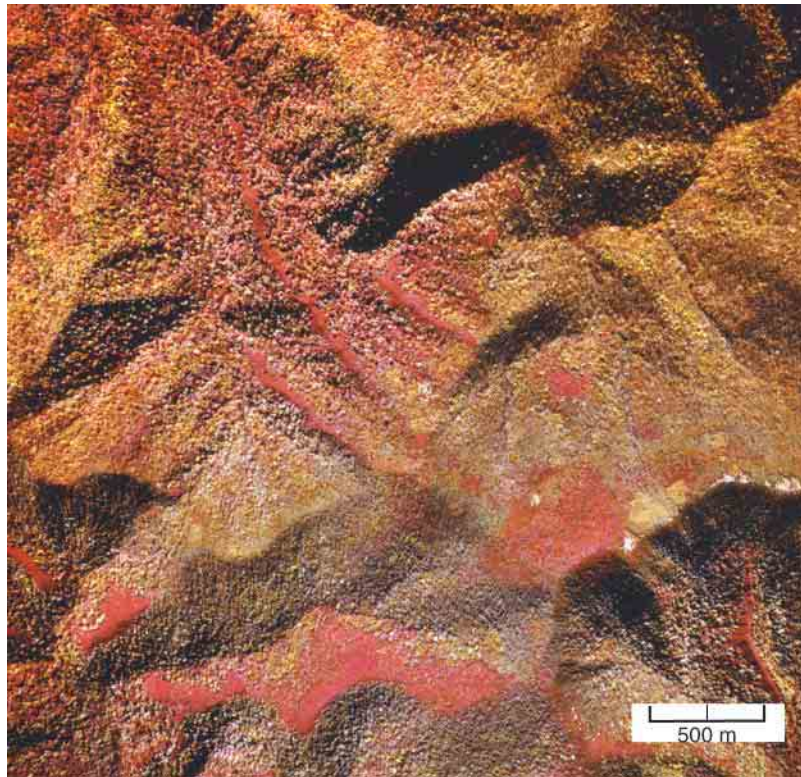


Figure 3-4. A representative large-scale color-infrared aerial photograph (# 10064) in the vicinity of Thunderhead Mountain. The Appalachian Trail crosses the area in the lower right corner of the photograph. The photo, recorded in October 1997, reveals the diversity of vegetation and the transition of species from low to high elevation. The terrain relief in this photo is approximately 570 m.

(Gaithersburg, Maryland) using a WILD RC 20 camera (S/N# 5132) with a calibrated focal length (CFL) of 153.482 mm and featuring forward motion compensation (FMC) (Table 3-2; Appendix A).

Flight lines were flown in the east-to-west or west-to-east direction with their starting and ending points and photo exposure centers controlled by GPS. Thus, all photo centers are basically structured as a grid (Figure 3-5). Regardless of the flight line direction, photo ID numbers begin with 1 on the eastern end of the flight line and increment by 1 until the end is reached. This creates a consistent and reliable numbering system as is illustrated for the Silers Bald Quadrangle in Figure 3-6.

Work in the project was organized according to U.S. Geological Survey (USGS) 1:24,000 scale topographic quadrangles, with each quadrangle representing a single unit. In a full quadrangle, there are approximately 11 photos along each of eight flight lines, for a total of 88 photos per quadrangle. Partial quadrangles contain fewer photos, ranging from nine in the Waterville Quadrangle to 55 in the Gatlinburg Quadrangle (Table 3-3).

Photointerpretation Overlays, Control Extension and Rectification Procedures Employed to Create the Database

The photointerpreters delineate vegetation communities by drawing detailed polygons directly on polyester overlays registered to aerial photographs by means of the photo fiducial marks. For identification purposes, the photo number is also written on the photo in the exact location shown on the photo. Because the photos are recorded with approximately 60 percent forward overlap, detail is delineated on every other photo in a

Table 3-2. Color-infrared photographs for the Great Smoky Mountains National Park vegetation mapping project.

Flight Line Number	Number of Photos	Date Acquired
1	41	10/28/1997
2	57	10/28/1997
3	63	10/28/1997
4	71	10/28/1997
5	78	10/28/1997
6	88	10/28/1997
7	93	10/27/1998
8	95	10/27/1998
9	96	10/27/1998
10	98	10/27/1998
11	98	10/27/1998
12	95	10/28/1997
13	96	10/28/1997
14	93	10/28/1997
15	91	10/28/1997
16	86	10/28/1997
17	83	10/28/1997
18	81	10/28/1997
19	79	05/22/1997
20	77	05/22/1997
21	65	05/22/1997
22	50	05/22/1997
23	37	05/22/1997
24	26	05/22/1997
25	16	05/22/1997
26	9	05/22/1997
27	5	05/22/1997

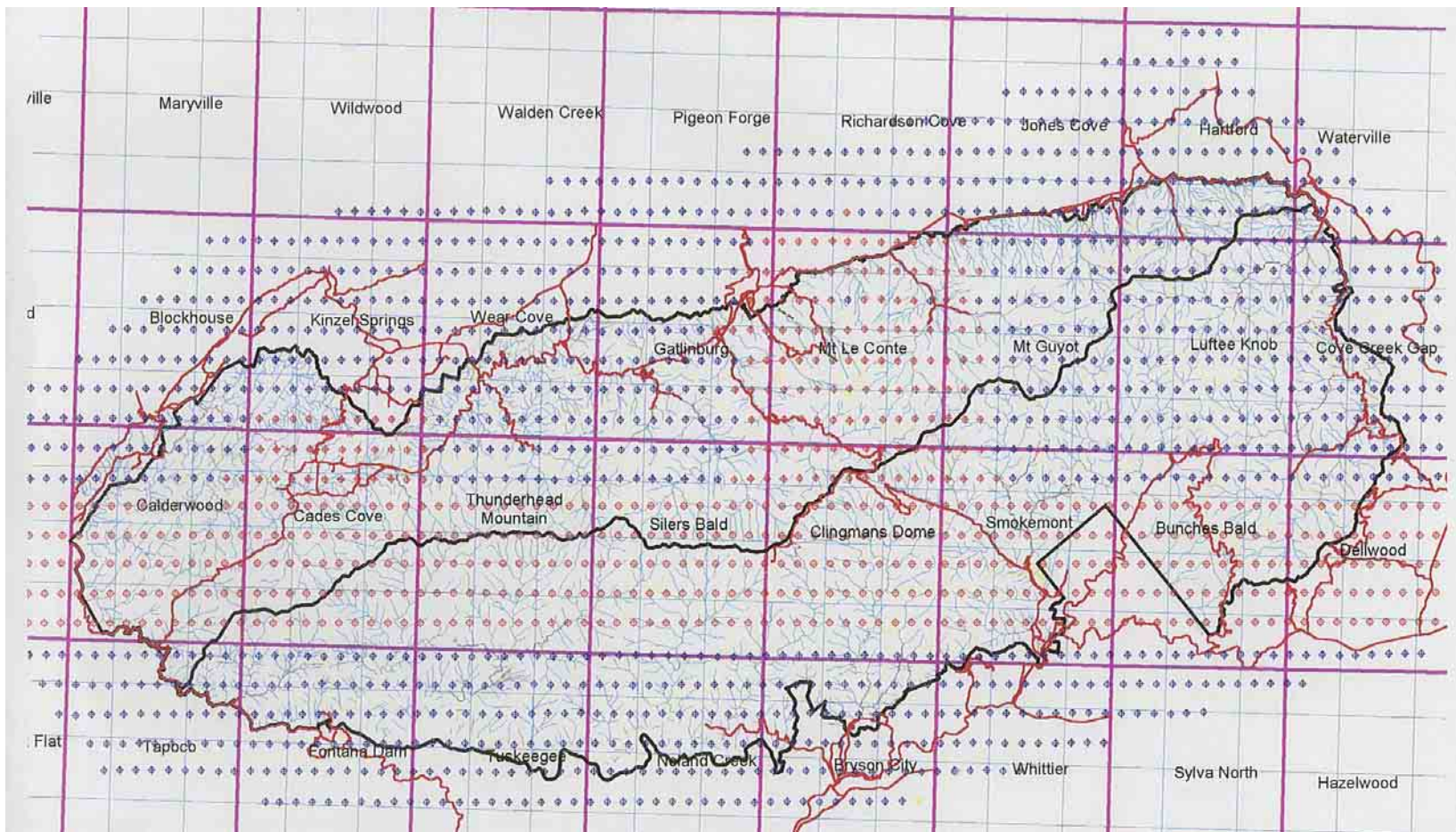


Figure 3-5. Map of Great Smoky Mountains National Park study area showing the USGS quadrangle boundaries, flight lines and photo centers. Flight line numbers are numbered from 1 in the south to 27 in the north.

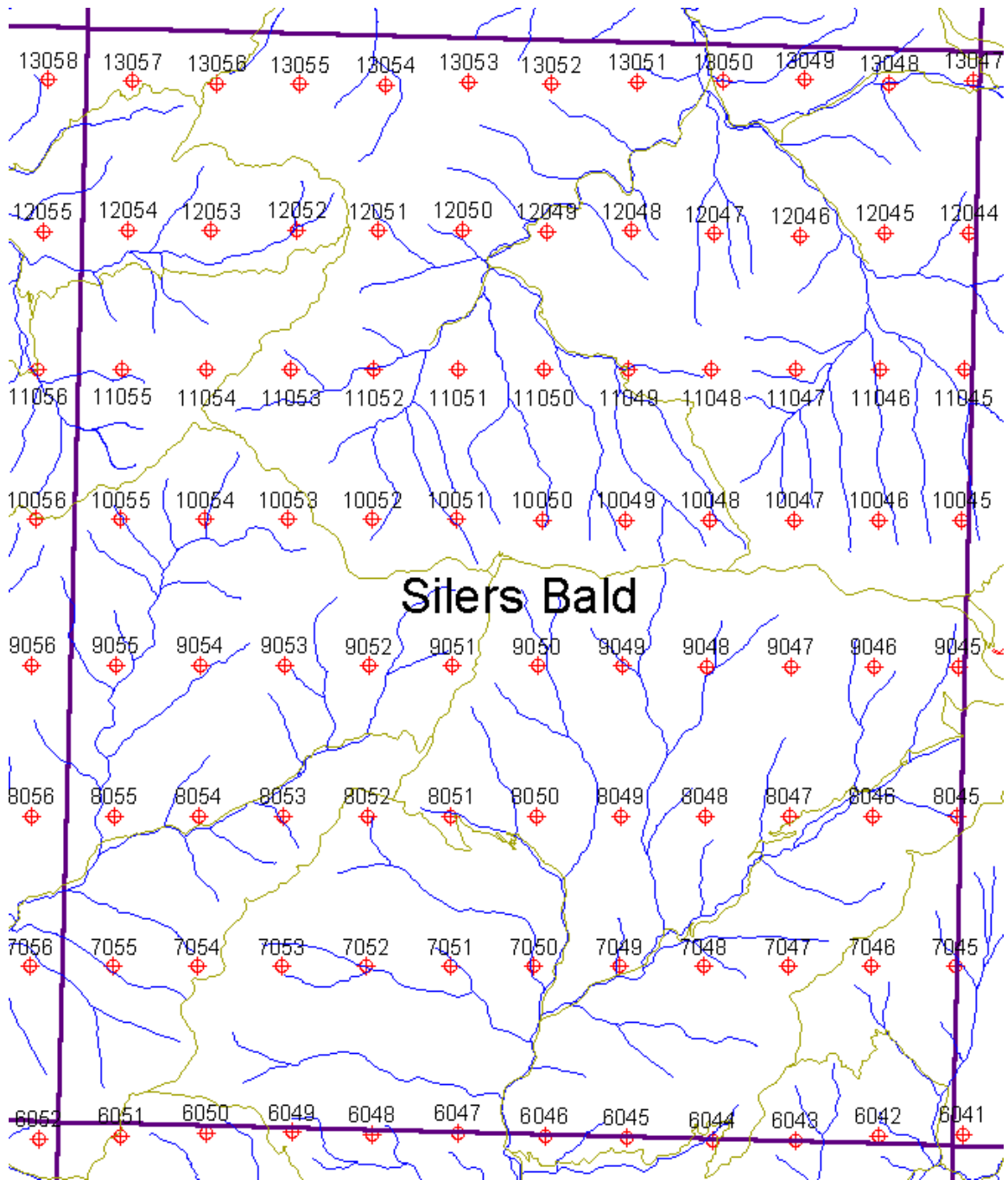


Figure 3-6. The photo index map for the Silers Bald Quadrangle shows the gridded pattern of photo exposure centers.

Table 3.3 – USGS topographic quadrangles in the Great Smoky Mountains National Park and the number of photographs in each. Data from 17 quadrangles were evaluated for this project.

Quad Name	NPS Abbreviation	Full or Partial	Included in Study*	Total photos
Blockhouse	BLOC	Partial	Yes	18
Kinzel Springs	KISP	Partial	Yes	33
Wear Cove	WECO	Partial	Yes	44
Gatlinburg	GATL	Partial	Yes	55
Mt. Guyot	MOGU	Full	Yes	88
Luftee Knob	LUKN	Full	Yes	88
Jones Cove	JOCO	Partial	Yes	15
Hartford	HART	Partial	Yes	22
Waterville	WATE	Partial	Yes	9
Calderwood	CALD	Full	Yes	88
Thunderhead Mountain	THMO	Full	Yes	88
Silers Bald	SIBA	Full	Yes	88
Tapoco	TAPO	Partial	Yes	15
Fontana Dam	FODA	Partial	Yes	44
Tuskegee	TUSK	Partial	Yes	55
Noland Creek	NOCR	Partial	Yes	55
Bryson City	BRCI	Partial	Yes	48
Cove Creek Gap	COCR	Partial	No	56
Clingman's Dome	CLDO	Full	No	88
Smokemont	SMOK	Full	No	88
Bunches Bald	BUBA	Partial	No	77
Dellwood	DELL	Partial	No	44
Mt. LeConte	MOLE	Partial	N/A	77
Cades Cove	CACO	Full	N/A	88
Total Photos				1371
* Quads evaluated for this dissertation. All quads except those noted as 'N/A' are included in the CRMS Great Smoky Mountains National Park Mapping Project. Quads marked "N/A" were mapped by ESRI/AIS (2000).				

strip. To accommodate relief displacements, extra care is taken to edge match the polygons on adjacent photographs by closing each polygon along a distinct topographic feature such as a river, valley or ridgeline. As a rule, interpretation was confined to the central portion of the photograph to avoid the most extreme displacements.

After all photographs in the quadrangle have been interpreted and the edges between them matched as best as possible, the overlays are passed to the photogrammetric process. In this process, the overlays are scanned and control points transferred from the aerial photographs by means of a mathematical transformation based on the photo and overlay fiducial mark coordinates. The overlays are then corrected for relief displacements using a differential rectification method so as to ensure a close match between vectors extending across adjacent photographs. Finally, the corrected overlays are converted to the UTM coordinate system in a format suitable for input to the GIS database.

The photogrammetric processes employed in this project required several complex, interrelated steps to remove displacements in the photographs and corresponding overlays caused by camera tilt and terrain relief (Figure 3-7). These are discussed in the following sections.

Scanning Procedures

An Epson Expression 836XL scanner was employed to scan the film transparencies and overlays (LaserSoft Imaging, 1999). The 836XL is well suited for softcopy photogrammetric applications because it has a 28 x 43 cm (11 x 17 inch) format

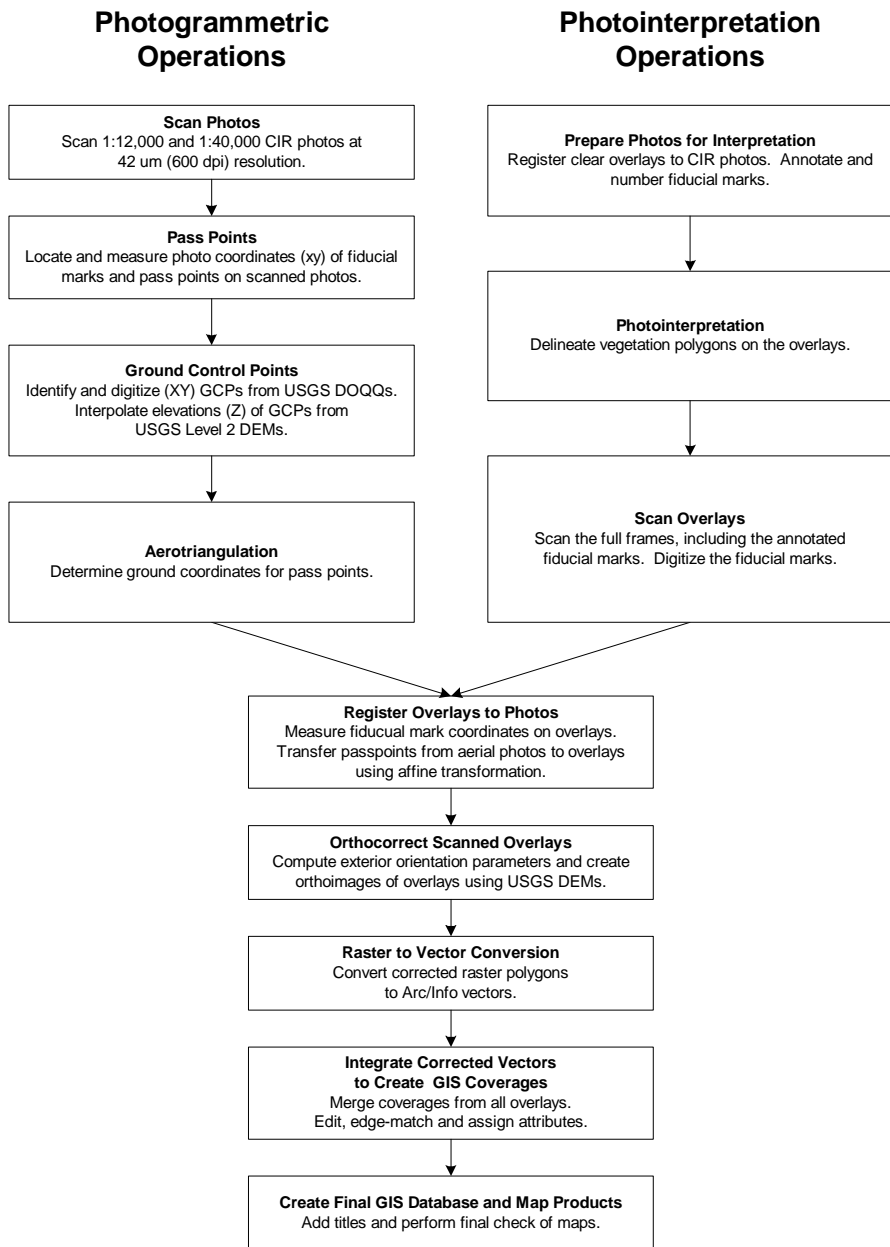


Figure 3-7. Diagram showing the relationships between photogrammetric, photointerpretation and GIS operations.

and can accommodate the entire frame of the 23 x 23 cm aerial photograph/overlay. This allows the fiducial marks needed to determine the interior orientation parameters of the photos to be captured, as well as the photo detail. Within the scanning software, photographs are captured as either 32-bit color or 12-bit gray scale (black-and-white) images to insure that the full dynamic range is recorded. Because of computer storage and representation standards, however, the dynamic ranges are necessarily rescaled to 24-bit color or either 8 or 16-bit gray scale before the scanned images are saved to disk. In the software, the scanning resolution can be set to within a range of 254 to 4 μm (100 to 6200 dots per inch (dpi)). The actual optical resolution of the Epson 836XL scanner is 32 μm (800 dpi), with the higher and lower resolutions provided through interpolation. Best results in photogrammetric applications, however, are achieved when the optical resolution of the scanner is not exceeded. This reduces the possibility of undesirable geometric distortions being introduced into the scanned photo (Welch and Jordan, 1996b).

The color-infrared transparencies are placed on the bed of the scanner and aligned so that the top of the scanned photo is oriented to the north (Figure 3-8). Maintaining this orientation results in a consistent point of view when examining the photos on the computer screen (north is always “up”) and permits pass points and control points to be located much more readily both along and between flight lines. In this study, color was not required for the aerotriangulation tasks. Consequently, the photos were scanned and saved as 8-bit gray scale TIFF images. It was also observed that scanning the photos at 32 μm (800 dpi) resulted in a 52 MB file, whereas scanning at 42 μm (600 dpi) created a



Figure 3-8. The photograph is placed on the bed of the scanner in preparation for scanning. A back-lighted transparency unit is required for scanning aerial photographs and overlays in film format.

smaller 32 MB file with no significant loss of information. Thus, all photos were scanned at 42 μm resolution. At a nominal photo scale of approximately 1:12,000, the ground pixel size is about 0.72 m.

The imaging software, Adobe Photoshop 5.0 (Adobe Systems, Inc., 1998), was employed to control the scanner and record and enhance the images. Scanners typically communicate with control software such as Photoshop using a TWAIN driver which is provided by the scanner manufacturer (note: "TWAIN" is not an acronym (<http://www.twain.org>)). This software driver is called using the "File-Acquire" command within Photoshop and provides an interface that permits the photograph on the

scanner bed to be previewed, cropped, enhanced and saved to provide the best possible image. The scanning resolution, color depth and transparent vs. reflective options are also set within the TWAIN driver interface. In operation, the “Acquire Image” option is selected from the Photoshop menu and the preview image is displayed in a window.

While viewing the display, it is possible to define the exact area of the photo to scan and to enhance the contrast of the image. An area corresponding to the exact outline of the photo, including all fiducial marks, is selected and the scan is initiated. The actual scanning operation takes about 5-8 minutes per photo, depending on the resolution and desired bit-depth. The image is then transferred (in the software) from the TWAIN window to a standard Photoshop window. Further enhancement or cropping may be undertaken within the Photoshop environment before the image is saved but, typically, no further modification of the image is necessary. Instead, the image is saved directly to hard disk as a TIFF file with a file name that is derived from the flight line number and photo number. For example, photo 52 on flight line 9 would be saved with the filename, 09052.tif.

A specific directory structure on the hard disk was employed to organize the many files associated with a project of this magnitude. The first level directory is the quadrangle abbreviation (e.g., SIBA; Table 3-2), followed by the flight line number and then the photo number. For example, the data associated with photo 52 of flight line 9 (to use the previous example) would be located in the GRSM directory on drive D in the D:\Grsm\Siba\FI9\052\ subdirectory. This strategy keeps all associated files grouped together and logically arranged. These data are stored on a network drive rather than a

local drive to facilitate use by various team members. The total data storage requirements for the unprocessed scanned image and overlay data and the DOQQs involved in this project is almost 50 Gigabytes (Gb).

Aerotriangulation Procedures

At least six ground control points are required to compute the photogrammetric orientation parameters for a given photograph (and the corresponding overlay).

Typically, these points include road intersections, driveways, building corners, streams and other well-defined features that can be both seen on the photograph and located on the ground. In the Great Smoky Mountains National Park, however, there are very few cultural features and, because of the near-continuous forest canopy, there are very few areas where the ground surface can be observed on the aerial photographs.

Consequently, it was necessary to employ aerotriangulation techniques to densify the control network required to rectify the individual aerial photographs and overlays.

Pass Point Identification

Aerotriangulation requires a relatively few points with known coordinates that can be identified on the photo. As described in Chapter 2, pass points are identified and measured on all photos in which they appear both along and between flight lines. Each point has a unique identification numbers that links the photos together. The aerotriangulation process then creates X, Y, Z coordinates for the pass points.

Image coordinates of pass points were measured in sequential pairs of photos using the Point Transfer program of the Desktop Mapping System (DMS), with the basic template shown in Figure 2-18 (Figure 3-9). The initial view in the program is of both photos zoomed all the way out so that the entire frames are visible (Figure 3-10). When a potential pass point location is identified, the images are zoomed to a 1x magnification (one pixel on the image is equivalent to one pixel on the display screen). At this zoom level, the individual trees and any ground details are visible and it is possible to identify the precise feature to be used as a pass point (Figure 3-11). Once the feature (e.g., a road intersection or a specific tree crown) is identified, the images are zoomed again to a 4x enlargement and the x, y image coordinates of the conjugate point locations are digitized. Unique point ID numbers are assigned as the points are digitized. The same point digitized on several different photos is assigned the same ID number.

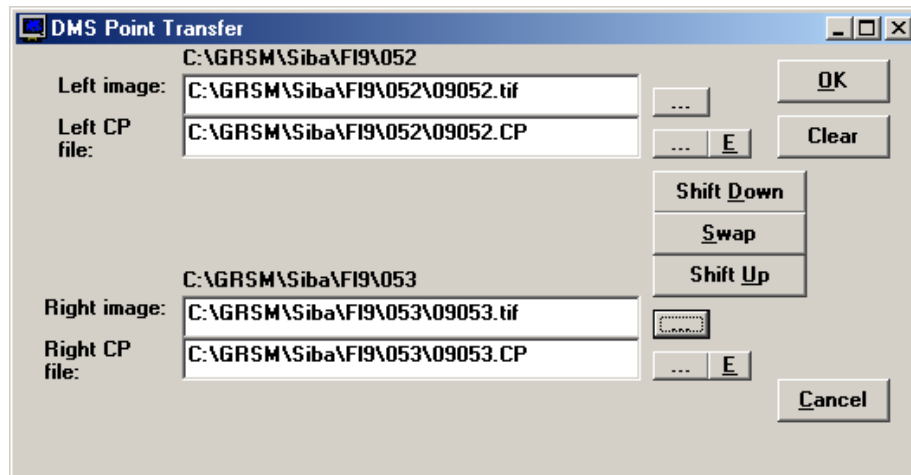
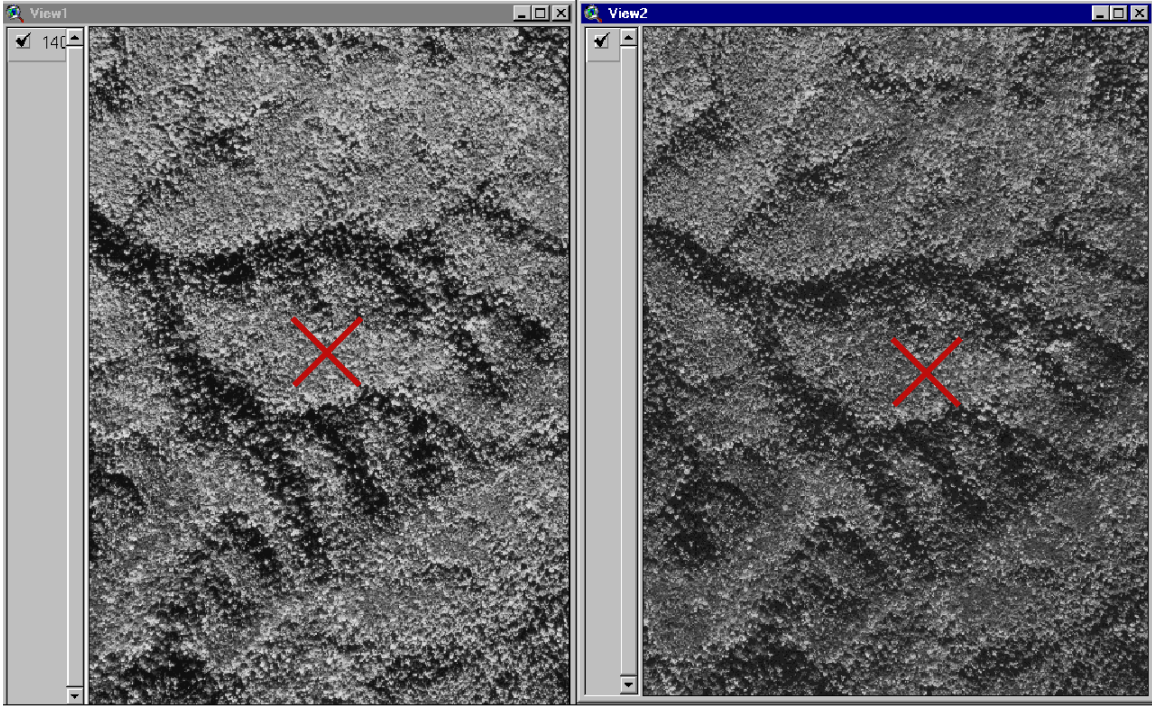


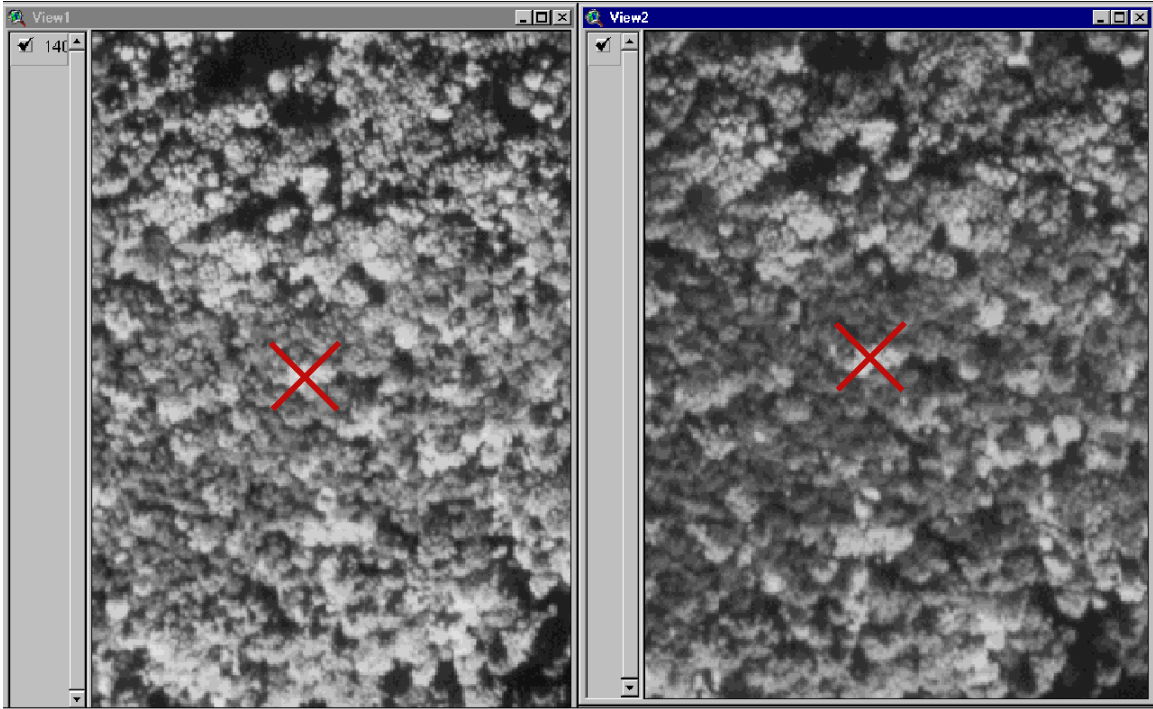
Figure 3-9 – DMS point transfer dialog.



Left

Right

Figure 3-10 – Point transfer graphics screen showing two images side by side. The “X” marker in the center of each image indicates a likely location for a pass point. In this example, the approximate point location is identified using topographic features as a guide. The left photo in the display is the master photo and points are transferred from the left to the right.



Left

Right

Figure 3-11 – A specific tree crown identified on 2 photos (indicated by the “X”) is selected as a pass point.

Pass point ID numbers are assigned according to the photo number and the position of the point on the photo itself (Figure 3-12). Points aligned with a vertical line through the center of the photo, defined by the top and bottom fiducials, are given an ID number in the format, XXXXXYY, where XXXXX is the photo number and YY is the position on the photo, with 01, 02 and 03 being near the top, middle and bottom of the photo, respectively. Additional points identified on photos are numbered similarly, starting with 04 and increasing by one with each point added. The leftmost column of points on Figure 3-12 represents points transferred from photo 09053 and the rightmost column corresponds to points transferred from photo 09051, thus providing nine pass points per photo. With this technique, it is possible to identify the precise photo and location within the photo of any point simply by knowing the point ID number. There will be at least six pass points common to adjacent photos on the same flight line. Of these, three will be transferred from the photo to the left and three will be new points measured on both photos. This process is repeated for all of the photos in the flight line (Figure 3-13).

When transferring and measuring the pass points it is critical that point locations be identified precisely at all times. This is not so difficult when a cultural feature such as road intersection or sidewalk corner is employed for a point location, and when present, these types of features were selected as pass points (Figure 3-14). Unfortunately, there frequently were no cultural features on a photo at all and tree crowns had to be used. In these cases, point locations were identified by the unique shape of tree crown and a specific feature of that shape (e.g., a distinct shadow). The difficulty of using this type

Photo 09052

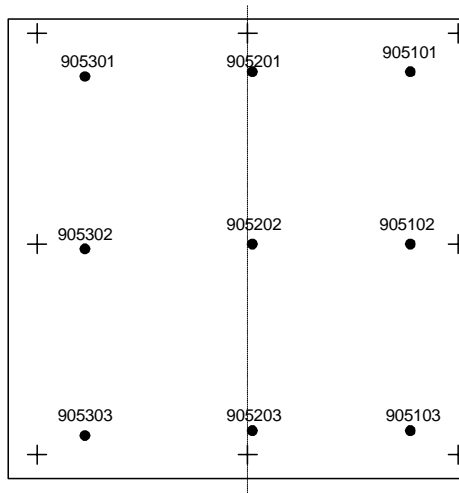


Figure 3-12 – Pass points are numbered according to the photo frame number and position on the photo (01, 02, 03).

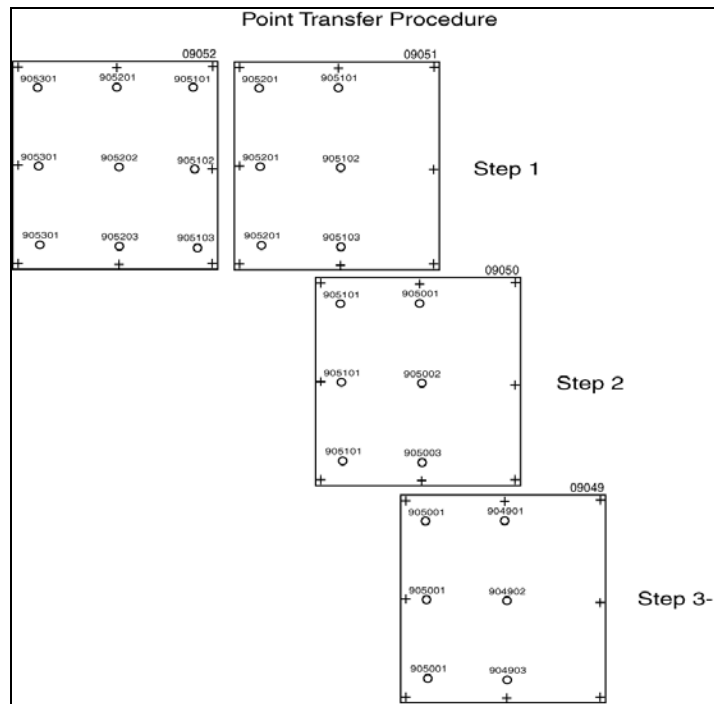


Figure 3-13. Point transfer procedure for measuring pass points along a flight line.

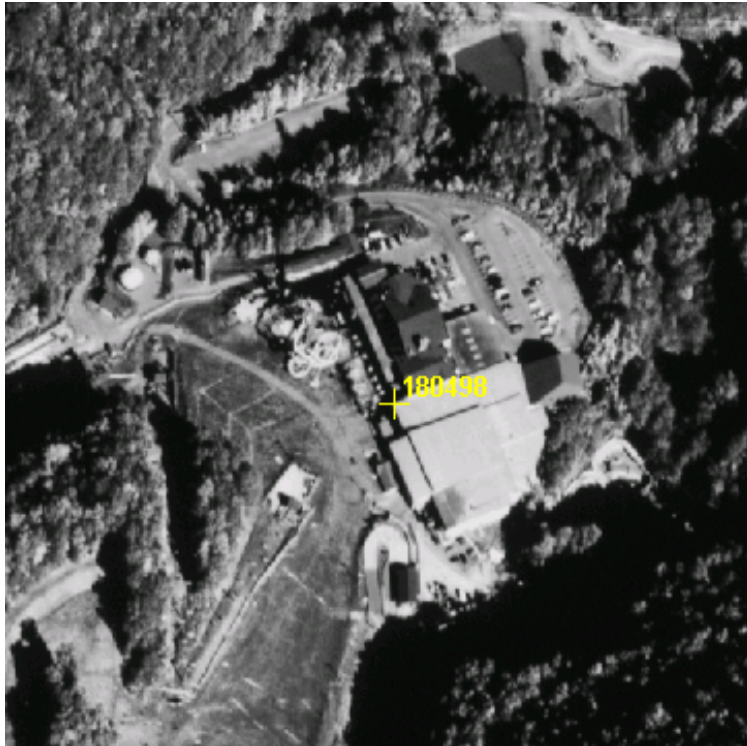


Figure 3-14. An ideal pass point is one that is a well-defined geometric feature.

of point is enhanced by the effects of relief displacement. When a tree is near the center of the photo, one sees the top of the crown and can easily identify a suitable spot on the tree to use as a pass point. In the adjacent photo, however, that same tree will appear to be leaning radially outward from the center of the photo. In this case, one can still see the top of the tree but it frequently is a different shape and may be distorted so that it looks like a different tree altogether (Figure 3-15).

When a new photo is loaded, all points from the previous photo (in the left screen position) are transferred to the new photo (in the right screen position) by first zooming the photos to 1x to identify the pass point. The exact point location on the right photo is

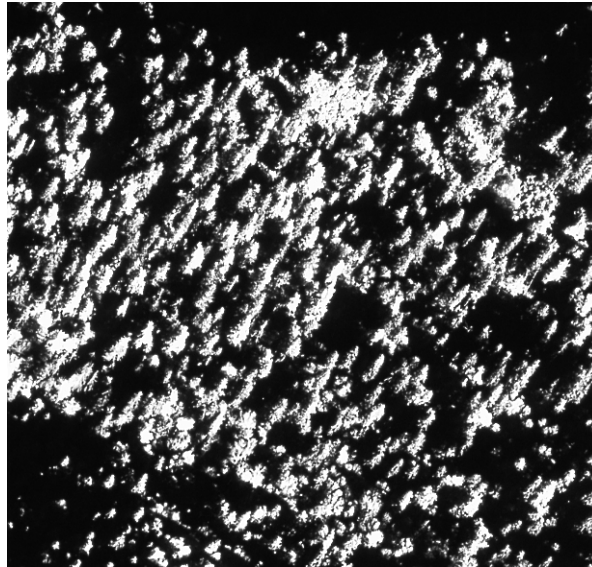


Figure 3-15. Tree crowns are frequently distorted by relief displacement when they are located near the edge of the photo.

marked at a 4x zoom and the point ID is assigned. The zoom level is then reset to view the full frame photos again and the procedure is repeated for the remainder of the pass points that are common to both photos. After all points are identified and digitized, the coordinates are saved. The left photo of the pair is then removed from the display, the right photo is moved to the left position and the next photo in the flight line is displayed as the right photo on the screen. In this manner, pass point coordinates are sequentially selected and measured on all photos in the flight line.

Ground Control Points

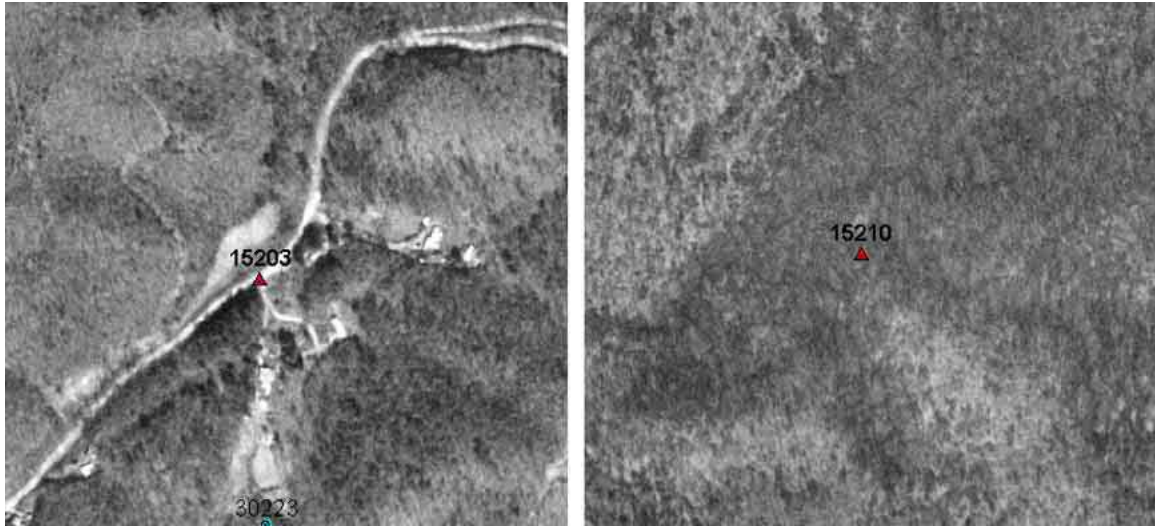
Finding GCPs in the Great Smoky Mountains is an extremely difficult task because the near-complete canopy cover obscures most of the ground surface in the photographs. Except for a few roads, there are not very many cultural features within the Park boundaries that can be used as control points. Furthermore, the Park is very large

and access to the remote areas is limited to foot trails. Consequently, it was not possible to employ traditional or GPS surveyed and targeted ground control in this project. This fact, coupled with the sheer volume of points required to reconstitute the approximately 1000 photos in the project, made it necessary to use aerotriangulation techniques and to develop alternative methods of identifying GCPs.

Planimetric Control. The source for planimetric (X, Y) control point coordinates was USGS DOQQs. Using the DMS Point Transfer program, the DOQQ for a particular area was displayed in the left panel while an aerial photograph was displayed on the right side. After careful examination of each photo, point locations suitable for use as GCPs were identified and their X, Y UTM map coordinates recorded. At the same time, the image pixel and line coordinates of the point were measured from the scanned aerial photograph and recorded.

Ideally, GCPs used in this project were identified at locations at road intersections, distinct curves or identifiable points along a road or in a parking lot, or at a distinct location in an open area. Often, however, these types of distinct features were not available in areas where GCPs were required – especially in the interior areas of the Park. In these situations, it was necessary to use any feature that could be recognized on the two photos. Typically, these points were distinctive points at curves in a stream or even unique topographic features (Figure 3-16).

Elevation Control. Ground control points measured from DOQQs have only planimetric coordinates. In photogrammetry, however, all GCPs must have both planimetric and elevation coordinate values. Conveniently, the USGS DEMs in raster format were



a)

b)

Figure 3-16. Typical examples of GCP locations. a) A good quality GCP is located at a road intersection, driveway or some other distinct location. b) Indistinct points identifiable only by shape or implication make poor GCPs. Unfortunately, circumstances dictate that these points sometimes must be employed in the aerotriangulation procedure.

available for the entire Great Smoky Mountains National Park and provided a ready source for elevation values for the GCPs. Elevations were extracted from the DEM using a program that read the elevation from the DEM file for each X, Y ground coordinate. Because the DEM has a ground resolution of 30 m and the DOQQ has a ground resolution of 1 m, a bilinear interpolation algorithm was employed to calculate the elevation at a specific coordinate based on four surrounding elevation points (Figure 3-17).

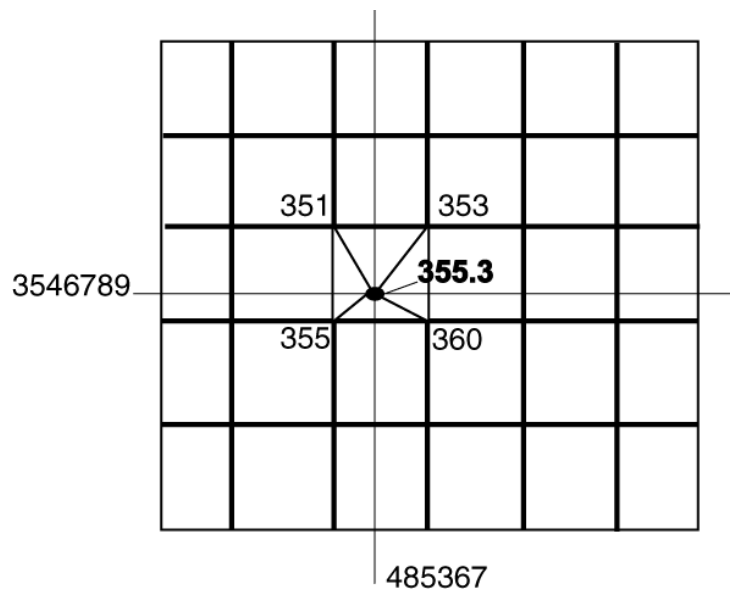


Figure 3-17. Elevations of GCPs are extracted from USGS DEMs using a bilinear interpolation algorithm.

In the program, the pixel and line coordinates in the DEM file corresponding to the X, Y UTM coordinates of the GCP measured from the DOQQ are computed using Equation 2-3. The elevation values for the four surrounding pixels are extracted from the DEM and the bilinear interpolation algorithm employed to compute the elevation for the GCP, as follows:

$$Z = (z1*d1 + z2*d2 + z3*d3 + z4*d4) / 4 \quad \text{Eq. 3-1)}$$

where $z1$, $z2$, $z3$, and $z4$ are the elevations of the four nearest neighboring cells, $d1$, $d2$, $d3$, and $d4$ are the distances from center of those cells to the target X, Y UTM coordinate of the GCP.

In operation, a GCP file containing only X, Y values and point ID numbers were read into the program along with the DEM filename. The points were then processed and their elevations extracted. The fully qualified X, Y, Z coordinates and point ID numbers were saved to a new file that was subsequently used in the aerotriangulation process.

Fall versus Spring Photographs

For this project, the photos for flight lines 1 - 18 were recorded in October of 1997 and 1998 so that the fall color changes in the foliage could assist in distinguishing the vegetation types (Figure 3-18). In contrast, flight lines 19 - 27 were recorded in May, 1997 when all of the trees were fairly uniform in appearance. The differences in appearance made identification of pass points linking flight lines 18 and 19 very difficult and uncertain (Figure 3-19). In fact, in most instances it was not possible to identify common points or features in the overlap regions between flight lines 18 and 19. For this reason, flight lines 19 - 27 were treated independently of the remainder of the Park in the aerotriangulation operations.

In the Mt Guyot Quadrangle, photos from flight lines 19 and 20 were included in the aerotriangulation solution for Jones Cove (see Figure 3-5). A second block included flight lines 19 and 20 from Luftee Knob and Cove Creek Gap as well as the entire

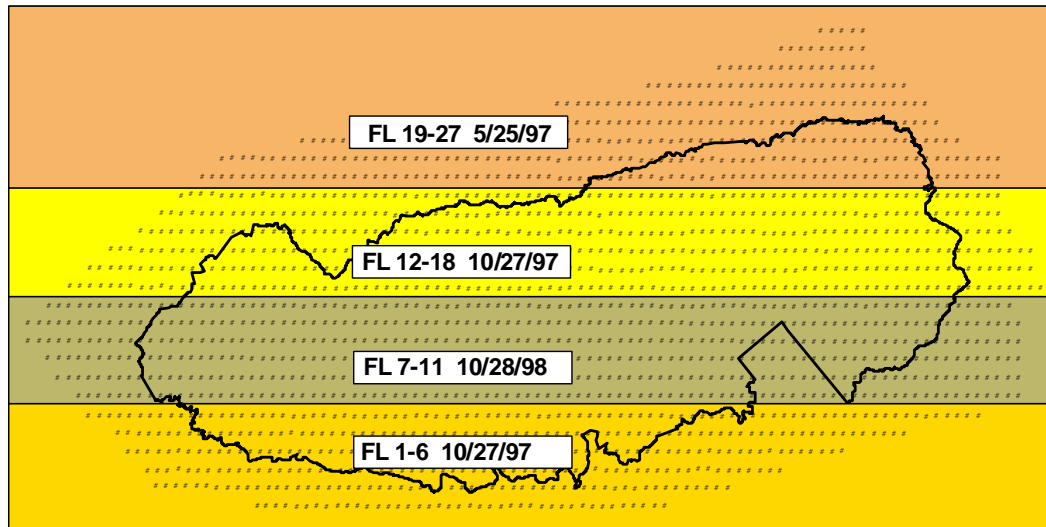
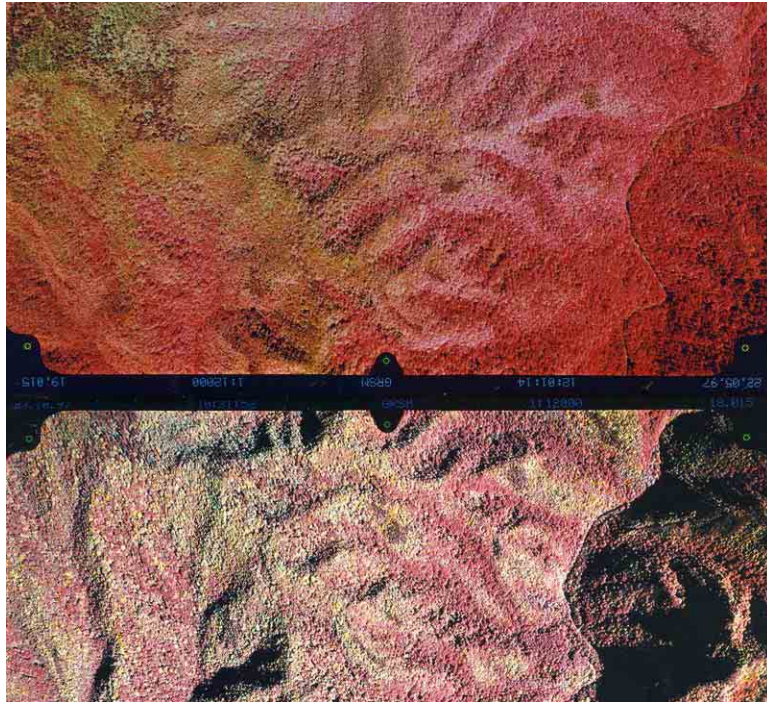


Figure 3-18. Flight lines and photo centers for Great Smoky Mountains National Park. Flight lines 1 through 6 and 12 through 18 were recorded in October 1997. Photographs located in the central area of the Park (flight lines 7-11) were recorded in October 1998. Photos for flight lines 19-27 (on the north side of the Park) were recorded in May 1997.



a) Photos 18015 (bottom) and 19015 (top)



b) Photos 18026 (bottom) and 19026 (top)

Figure 3-19. The significant difference in the appearance between fall and spring photography made identification of pass points between flight lines 18 and 19 very difficult. a) The overlap area between photographs 18015 and 19015 (Luttee Knob Quadrangle) contains a river to help orientation, whereas b) there are no visual cues in the 18026/19026 photo pair (Mt. Guyot Quadrangle) to help identify common features.

Hartford and Waterville Quadrangles. For the rest of the Park, aerotriangulation blocks included all of the photographs that fell within the boundaries of the individual quadrangles.

Aerotriangulation Adjustment

For each quadrangle in the study, CPs and GCPs were collected for all photos and then organized into a file called PREP.IN for input to the aerotriangulation program, PC GIANT (Figure 3-20). The program PREP.EXE was then used to read the PREP.IN file, apply refinements to the raw image coordinates and create the IMG.DAT file that contains refined coordinates in the photo coordinate system (with the (0,0) point located at the principal point of the photograph). Next, a program called CAMSTA.EXE was run to provide the initial estimates of the camera stations and orientation angles. Output from this program was a file called OPT.DAT. After creation of the file by CAMSTA, OPT.DAT was edited by hand to include data for additional flight lines and the ground control points. Using CAMSTA to build the OPT.DAT file was a very tedious and error-prone process. For this reason, an alternative program to CAMSTA was written specifically for this project to automatically build the OPT.DAT file based on user input specifications of photo numbers and flight lines. The photo centers, instead of being calculated, were drawn from a database of the photo center coordinates for all photos in the project. The final step of the aerotriangulation process was to run the program, GIANT.EXE. GIANT reads the refined photo coordinates from IMG.DAT and the

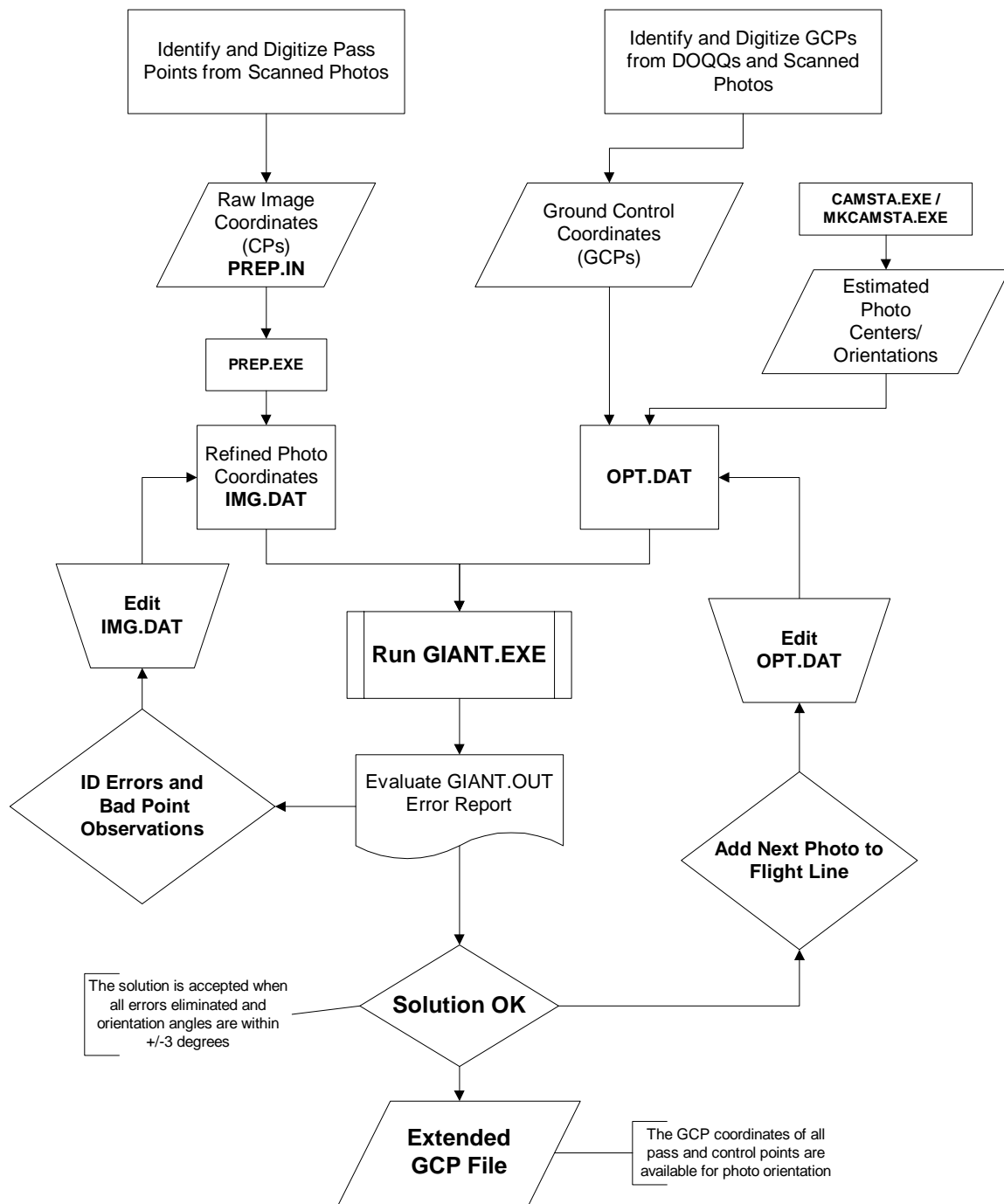


Figure 3-20. The aerotriangulation process flow using PC Giant.

exposure centers and control information from OPT.DAT and performs the aerotriangulation block adjustment.

When the input data are formatted properly so that PC GIANT successfully ingests the data without errors, the next task is to run GIANT identify and eliminate or correct errors in the point coordinates and ID numbers to arrive at the best solution. This is the most difficult part of the process. The single report file from PC GIANT, GIANT.OUT, usually contains enough information to identify errors in specific points (Table 3-4). Errors from these points are generally caused by: 1) misidentifying the point location on adjacent photos during the point transfer process; 2) misnumbering the point with a typographical error so there is apparently no conjugate point on adjacent photos; or 3) giving two different points the same ID number. The latter errors have the most disastrous consequences to the solution and also can be the most difficult to detect.

The results of the aerotriangulation are reported in five major sections in the file, GIANT.OUT. The first section contains the intermediate and final results of the initial block formation and corrections to the photo exposure centers and attitudes (See Table 3-4: Section 1). In the aerotriangulation solution, the photos are formed into a block, the exposure centers are given initial approximate values and a first iteration of the solution is performed. Based on the results of this first iteration, the exposure center coordinates and orientation angles are refined and the solution recomputed. The program continues to iterate the solution four or five times until the corrections are near zero. By examining the corrections to the exposure centers reported for each iteration, it is possible to assess

Table 3-4. Abbreviated PC GIANT report (GIANT.OUT). In this table, points identified with an asterisk (*0*; e.g., 15207*0*) beside the point number are control points.

SECTION 1 – Iterations Showing the Corrections to Camera Stations

	C A M E R A S T A T I O N S			C O R R E C T I O N S		
	----- P O S I T I O N -----			----- A T T I T U D E -----		
	X	Y	Z	Omega	Phi	Kappa
Iteration 1						
02022	-65.1268	-101.7490	-288.4798 m.	-0.007852	-0.026812	0.005961
02023	-50.8538	-74.4128	-289.7754 m.	-0.050240	-0.010517	-0.015020
02024	-51.6414	-66.6382	-286.5077 m.	-0.027666	-0.010597	-0.026987
02025	-55.2413	-57.1404	-287.6317 m.	-0.009441	-0.014304	-0.030658
Iteration 2						
02022	1.3872	1.8113	27.0989 m.	0.003118	-0.001552	0.001837
02023	8.2213	10.6264	25.4281 m.	-0.001794	0.002143	0.001211
02024	13.8148	7.6409	27.3697 m.	-0.000865	0.003664	0.000184
02025	12.2887	14.6749	30.6103 m.	-0.003918	0.002014	0.000095
Iteration 3						
02022	0.6723	0.2888	0.1139 m.	0.000071	0.000225	0.000113
02023	1.1811	-0.5089	0.6507 m.	0.000321	0.000426	0.000066
02024	1.2418	-0.3900	0.9309 m.	0.000261	0.000425	0.000043
02025	0.5234	-1.2011	1.2620 m.	0.000555	0.000011	-0.000023
Iteration 4						
02022	-0.4127	0.2440	-0.0589 m.	-0.000079	-0.000141	0.000004
02023	-0.3319	0.3891	-0.2266 m.	-0.000133	-0.000106	-0.000001
02024	-0.1922	0.3306	-0.2769 m.	-0.000110	-0.000048	-0.000005
02025	-0.0934	0.4274	-0.3172 m.	-0.000145	0.000009	-0.000013

SECTION 2 – Triangulation of Image Points and Residuals

Pt Num	T R I A N G U L A T E D I M A G E P O I N T S				R E S I D U A L S	
	Photo1	Photo2	Photo3	Photo4	Photo5	Photo6
20183	02019	02018	02017			
	16	-35	17			
	-15	-20	31			
15207*0*	02019	02018	03022	03023	02017	03024
	-350	-4	-341	83	129	390
	-194	-87	-571	-215	-175	-298
15206*0*	02019	02017	02018	03022		
	678	-423	-117	578		
	423	169	457	898		
20191	02020	02018	02019	03025		
	-44	-23	65	-7		
	147	-130	-4	11		
20231	02022	02023	02024	03027		
	-30	126	-58	48		
	54	-4	-52	-2		
60503	05043	05042	06049	06050	06051	
	229	34	193	330	-253	
	-97	-129	-210	-106	71	

Table 3-4 (Continued)

SECTION 3 – Summary Statistics for Final Camera Stations

		RMS For Standard Deviations			
	X =	267401.760 m.	+2.227D+02	+8.567D+01	+5.660D+01
02022	Y =	3923704.562 m.	+8.567D+01	+2.706D+02	-1.820D+01
	Z =	2538.619 m.	+5.660D+01	-1.820D+01	+5.831D+01
	Omega =-	00 16 16.5754	+6.108D-05	-1.745D-05	+3.544D-06
	Phi =-	01 37 30.5612	-1.745D-05	+4.551D-05	-5.183D-06
	Kappa =	180 26 48.5043	+3.544D-06	-5.183D-06	+4.739D-06
	X =	266351.967 m.	+2.347D+02	-2.968D+01	+1.836D+00
02023	Y =	3923739.214 m.	-2.968D+01	+3.170D+02	-1.109D+02
	Z =	2535.653 m.	+1.836D+00	-1.109D+02	+9.085D+01
	Omega =-	02 58 52.6846	+7.241D-05	+9.686D-06	-1.222D-06
	Phi =-	00 28 47.2037	+9.686D-06	+4.349D-05	-4.630D-06
	Kappa =	179 12 31.7185	-1.222D-06	-4.630D-06	+5.242D-06
	X =	265285.873 m.	+4.286D+02	+4.641D+01	+1.047D+02
02024	Y =	3923742.503 m.	+4.641D+01	+5.893D+02	-3.505D+01
	Z =	2540.862 m.	+1.047D+02	-3.505D+01	+1.337D+02
	Omega =-	01 38 04.8853	+1.142D-04	-1.852D-06	+4.584D-07
	Phi =-	00 23 50.0744	-1.852D-06	+9.105D-05	-1.041D-05
	Kappa =	178 27 51.5220	+4.584D-07	-1.041D-05	+8.622D-06
	X =	264209.847 m.	+4.773D+02	-2.242D+01	+1.640D+02
02025	Y =	3923757.535 m.	-2.242D+01	+6.081D+02	-8.666D+01
	Z =	2542.979 m.	+1.640D+02	-8.666D+01	+2.241D+02
	Omega =-	00 45 55.4335	+1.226D-04	+7.441D-06	-1.976D-06
	Phi =-	00 42 14.9420	+7.441D-06	+8.418D-05	-3.681D-06
	Kappa =	178 14 55.8457	-1.976D-06	-3.681D-06	+1.087D-05
	X =	263128.902 m.	+5.084D+02	+6.894D+00	+1.815D+02
02026	Y =	3923764.740 m.	+6.894D+00	+7.391D+02	-4.317D+01
	Z =	2544.186 m.	+1.815D+02	-4.317D+01	+3.476D+02
	Omega =-	01 52 04.7057	+1.529D-04	+3.184D-06	-8.447D-06
	Phi =-	00 14 07.3632	+3.184D-06	+9.462D-05	-5.878D-06
	Kappa =	179 29 46.8850	-8.447D-06	-5.878D-06	+1.163D-05

S U M M A R Y S T A T I S T I C S F O R C A M E R A S T A T I O N S
RMS For Standard Deviations

Count =	55	X =	21.6136 m.	Omega =	00 31 39.0116
		Y =	21.7066 m.	Phi =	00 31 31.0509
		Z =	12.8791 m.	Kappa =	00 10 42.7188

Table 3-4 (Continued)

Section 4 – Triangulated Object Points

Ident	Position (meters)	Covariance Matrix			Std Dev (m.)
15206 *0*	X = 271383.643	+4.344D+00	+1.306D-02	+3.950D-01	2.0843
	Y = 3924161.543	+1.306D-02	+4.242D+00	-2.623D-01	2.0596
	Z = 580.153	+3.950D-01	-2.623D-01	+1.222D+01	3.4954
15207 *0*	X = 271936.028	+3.803D+00	+6.738D-03	-1.106D-01	1.9501
	Y = 3924000.587	+6.738D-03	+3.902D+00	+4.824D-01	1.9753
	Z = 601.498	-1.106D-01	+4.824D-01	+1.046D+01	3.2344
20183	X = 271708.861	+1.934D+01	-8.599D-02	+1.575D+00	4.3979
	Y = 3922552.218	-8.599D-02	+5.292D+01	+5.826D+01	7.2746
	Z = 725.618	+1.575D+00	+5.826D+01	+1.190D+02	10.9064
20191	X = 270450.210	+1.917D+01	-5.321D-01	-2.687D+00	4.3779
	Y = 3924873.401	-5.321D-01	+2.513D+01	-1.367D+01	5.0135
	Z = 531.004	-2.687D+00	-1.367D+01	+9.162D+01	9.5718
20231	X = 266538.319	+3.136D+01	+2.071D+00	+1.737D+01	5.5998
	Y = 3924713.452	+2.071D+00	+3.669D+01	-2.615D+00	6.0576
	Z = 525.232	+1.737D+01	-2.615D+00	+2.164D+02	14.7112
60503	X = 263723.837	+1.447D+01	-1.776D-01	+3.483D+00	3.8040
	Y = 3930280.479	-1.776D-01	+1.509D+01	+6.883D-01	3.8851
	Z = 1081.748	+3.483D+00	+6.883D-01	+4.386D+01	6.6223
60504	X = 263802.645	+4.566D+01	-4.834D+00	+2.902D+01	6.7573
	Y = 3931612.733	-4.834D+00	+3.349D+01	-4.198D+01	5.7868
	Z = 1362.271	+2.902D+01	-4.198D+01	+1.828D+02	13.5221

S U M M A R Y S T A T I S T I C S F O R O B J E C T P O I N T S
RMS For Standard Deviations

Count = 207 X = 6.7564 meters
 Count = 207 Y = 8.4356 meters
 Count = 207 Z = 18.7203 meters

Section 5 – Corrections Applied to Object Control

C O R R E C T I O N S A P P L I E D T O O B J E C T C O N T R O L

15106	X = -1.8592 m.	15206	X = -0.8570 m.
	Y = 2.2031 m.		Y = 0.5426 m.
	Z = 0.4598 m.		Z = 8.2527 m.
15207	X = -0.4721 m.	15307	X = -0.2071 m.
	Y = 1.0872 m.		Y = -0.1812 m.
	Z = -6.8018 m.		Z = 0.3797 m.

X Number of Components = 50 RMS = 2.9969 meters
 Y Number of Components = 50 RMS = 1.9728 meters
 Z Number of Components = 50 RMS = 2.4040 meters

the initial quality of the solution and perhaps identify the specific photo where problems originate. For example, a photo center whose coordinates require corrections on the order of 500 m while the other photo centers in the flight line are only being corrected by 10 to 20 m is suspect. In this case, the pass point file for this photo likely contains an error in a point number or a point that has been severely misidentified. One must assume that most of the points are measured correctly during the point transfer process so that gross errors are most likely due to blunders of this type.

The second section reports the residual errors for each point on each photograph, sorted by point number (Table 3-4: Section 2). Residuals in x and y are given in micrometres and reflect the quality of the fit of the point in each photo in which it appears. All points with errors exceeding a three-sigma (3σ) threshold during the strip and block formation are identified with the note “ $>3\sigma$ ” in the report so that they may quickly be identified and examined in the GIANT.OUT file to determine the possible cause. Large errors indicate that a point is either misidentified or that the conjugate locations on adjacent photographs were not transferred as accurately as they should have been. In order to be included in the solution, a point must appear on at least two photos. Because of the forward overlap between photos on the same flight line and sidelap between flight lines, however, it is possible and geometrically advantageous for a point to appear on up to six different photos. Consequently, if one observation is a blunder, it is possible for a single measurement of one point on one photo to be in error and affect the quality of the entire solution. These are the points that need to be specifically identified and removed. When identified, the suspect points are flagged in the IMG.DAT file to

remove them from the solution. A subsequent run of GIANT demonstrates if this effort was successful or whether additional points must be examined.

The third section of the report lists the final exposure center coordinates (X, Y, Z) and attitude angles (Omega, Phi, Kappa) for each photo, as well as a three-dimensional covariance matrix for the position (Table 3-4: Section 3). Under good conditions, the omega and phi angles should be less than three degrees. Higher values indicate the presence of errors in point observations. Kappa is related to the flying direction and for this project is either near 0 or 180 degrees. The summary statistics for camera stations reports the number of camera stations (photos) in the solution and the RMS errors for their final positions.

The fourth section of GIANT.OUT provides the computed coordinates and intersection error values for the triangulated control and pass points (known collectively within GIANT as object points) (Table 3-4: Section 4). After the photos are oriented and fixed into place within the block, the UTM map coordinates of pass points and control points are computed using spatial intersection. The intersecting rays do not meet exactly and thus form a three-dimensional error “sphere” as defined by the X, Y, and Z error terms for each point. A summary for object point errors is provided with the number of object points and the RMS errors in X, Y, and Z. Experience in the Great Smoky Mountains has shown that errors at control points will be on the order of 5 to 20 metres with errors at pass points between one and three times higher. Although these values are high for normal aerotriangulation and mapping practices, they are considered to be acceptable for mapping natural resources where very few well-defined points exist and

boundaries between adjacent features are frequently uncertain. Points with errors in excess of these amounts, however, must be reviewed before accepting the results of the aerotriangulation. It is possible that a few points with very large errors can exert great influence on the overall error reported. Removing these points will increase the quality of the solution. The risk of removing too many points in an effort to eliminate all errors, unfortunately, is that there may not be enough points remaining in the photo for the photogrammetric solution. Where this situation is unavoidable, it is necessary to remeasure points from the images or identify new ones. The fifth section of GIANT.OUT reports the corrections applied to the object control (the GCPs only) in the final adjustment (Table 3-4: Section 5). The final adjusted object point coordinates are then computed and saved into file called OBJ.OUT.

Unfortunately, receiving a report that indicates no points have errors in excess of the three sigma (3σ) threshold does not always mean that the solution is good throughout the entire block. A final examination of the omega and phi angles for each photo in the GIANT.OUT file will reveal potentially bad photos. Since nominally vertical photos are supposed to have less than three degrees of tilt in omega and phi, values of these angles that fall significantly outside of this range indicate the presence of suspect points. Typically when this happens, angles of zero or one degree will be followed by increasing angles up to a maximum (e.g., eight or more degrees) and then the angle will decrease again to around zero. In this situation, the point is very difficult to identify since it has already passed the point matching, resection and intersection computations within PC

GIANT. Once identified and corrected (or eliminated), the block is rerun and the angles checked. If the run is successful, the angles will all be less than three degrees.

When the aerotriangulation is complete, the three-dimensional coordinates of all control and pass points are available for use in photo orientation (Figure 3-21). These point coordinates are provided in a GCP file called OBJ.OUT. Although the camera orientation parameters (X_L , Y_L , Z_L , ω , ϕ , κ) are also reported by GIANT, they are slightly different from the values used by the DMS and so must be recomputed within DMS using the original CP files and the GCP file resulting from aerotriangulation.

Quality Assurance

The quality of the overall aerotriangulation solution is checked by creating a large orthophoto mosaic from the scanned photographs. The DMS orientation parameters are computed for every photograph in the quadrangle and orthophotos are generated using the USGS DEM as elevation reference. Typically, a 2-metre pixel size is used for these quality control products. The orthophotos are then mosaicked using the DMS Manage – Mosaic Images option and the resulting composite image printed on a Hewlett Packard HP755cm large format inkjet plotter using the print functions available in ArcView (Figure 3-22). The edges of each photo in the mosaic are carefully inspected to insure that all features and topographic details line up correctly between photos. Discounting contrast differences, the mosaic should appear to be a continuous image with no major shifts in the detail between photos. Significant errors in the orientation (and hence, the GCPs) can be identified in this manner. If errors are detected, it is necessary to identify

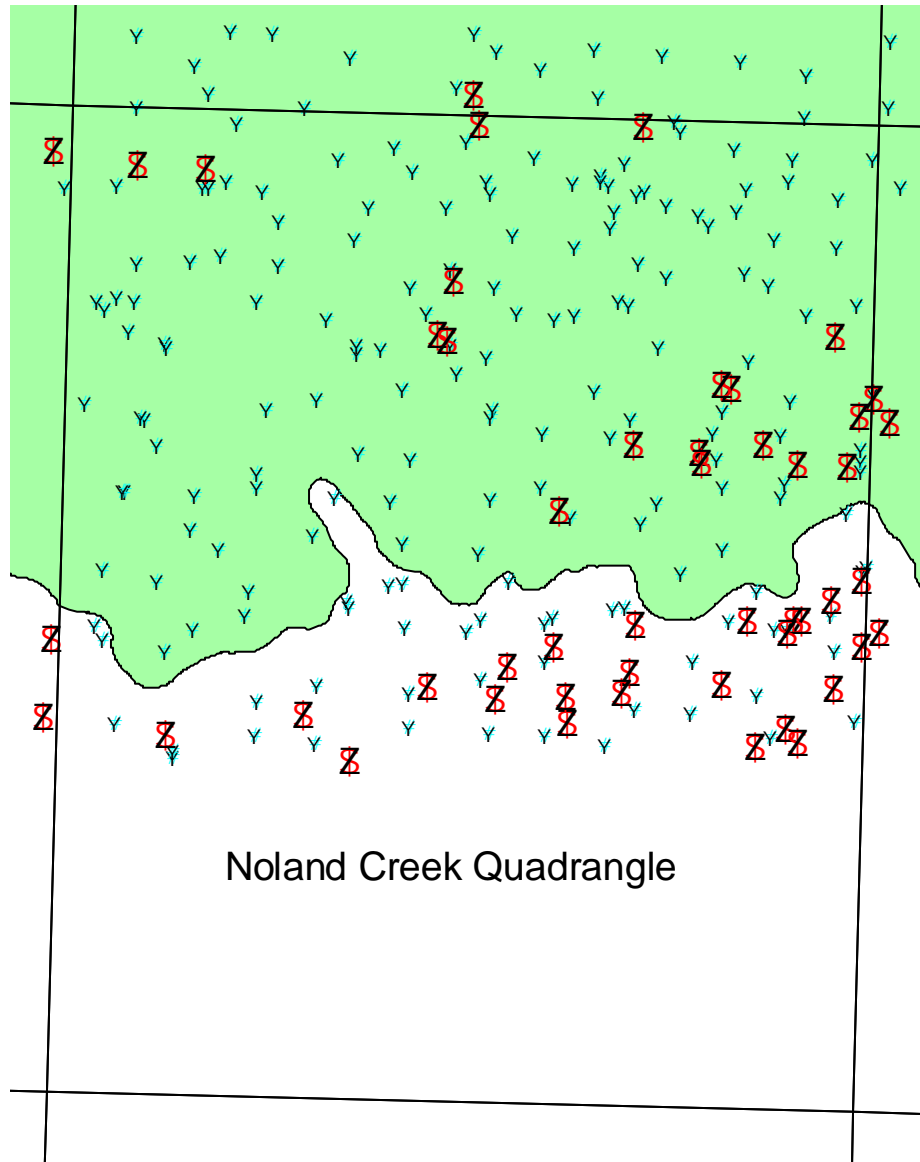


Figure 3-21. Distribution of control and pass points in the Noland Creek Quadrangle. Red triangles represent ground control points and blue circles denote the locations of pass points. The area within the National Park boundary is shaded.

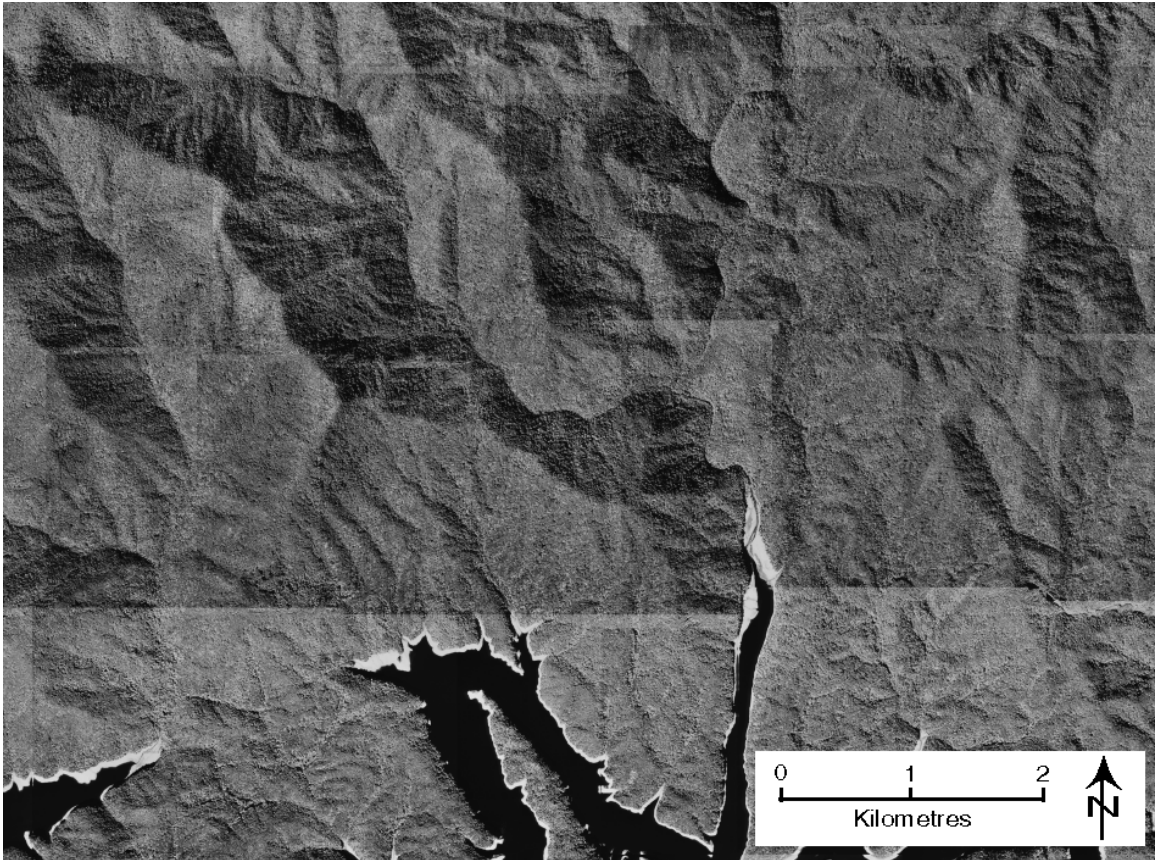


Figure 3-22. A portion of the Noland Creek digital orthophoto mosaic constructed from about 24 individual orthophotos. A close inspection of terrain features such as the lake shore, ridges and stream courses indicate good alignment and a satisfactory aerotriangulation solution.

additional control points or refine existing points in areas lacking suitable control and to repeat the aerotriangulation process. The questionable photos are then reprocessed into orthophotos. The quality of the individual reprocessed orthophotos is checked by inserting them into the mosaic. The fit is then assessed by displaying the image on-screen in either DMS or ArcView, zooming in and examining the detail as before.

Orthorectification of Overlays

The entire aerotriangulation process is performed to provide a mechanism for correcting displacements caused by tilt and relief and placing the detail from the vegetation coverage overlays produced by the photointerpreters into the UTM coordinate system. This rectification process is essential and must be conducted prior to attempting to mosaic the overlays together to create a vegetation coverage. Consequently, a program shell was developed from components of the DMS software package to permit the rectification of overlays in a series of steps. The push-button design of the program makes the process simple to execute (Figure 3-23).

The steps required to correct an overlay and create a vector coverage of the polygons are listed in Figure 3-24. First, the overlay is scanned at 42 μm using Adobe Photoshop and saved as an uncompressed, 8-bit gray scale TIFF image. The fiducial marks of the scanned overlay are then digitized using either the DMS Geocode – Image CPs or Point Transfer options. Point numbering is critical and fiducial mark ID numbers are ordered the same as on the original scanned photos. A six-parameter affine transformation is established between the original photo coordinates and the overlay

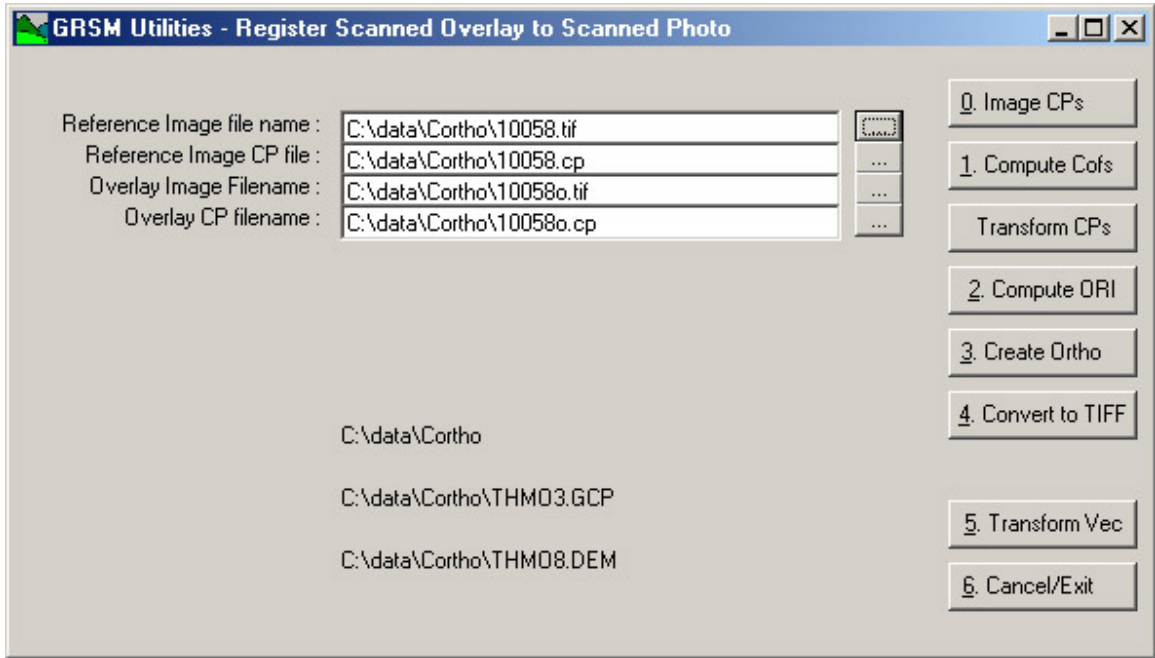


Figure 3-23. The user interface of the GRSM Utility program for orthorectification of vegetation overlays.

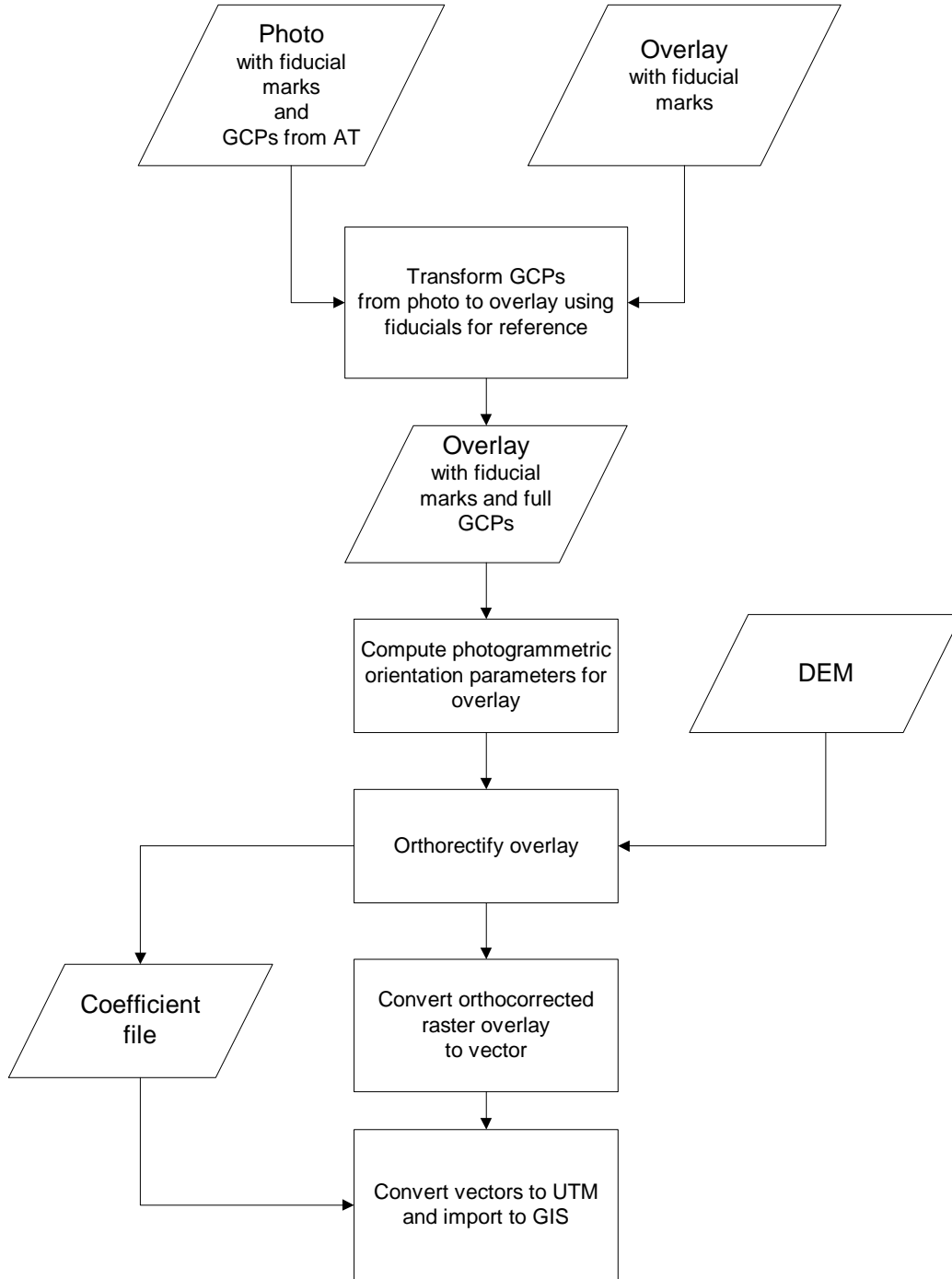


Figure 3-24. The procedure employed for orthorectification of vegetation overlays. After conversion to vector format, the vectors are transformed to the UTM coordinate system and imported to the GIS for editing, edge-matching and attributing.

the using the fiducial marks as reference points. Transformation coefficients from photo to overlay and from overlay to photo are then computed.

Using all eight fiducial marks, the error associated with the least squares fit is generally on the order of about 2 to 3 pixels (approximately 2 m). This is within the size of the inked symbols denoting the fiducial marks on the overlays. While it is possible to eliminate one or more “bad” points from the solution, it is generally not necessary to do so to satisfy the requirements. Thus transformed, the new CPs are now precisely registered with the overlay, creating, in effect, a set of photo coordinates for GCPs and pass points in the coordinate system of the scanned overlay. Exterior orientation parameters for the overlay are computed using the DMS Softcopy Orientation Option. Here it is generally necessary to identify and eliminate “bad” points from the solution. In this case, point observations removed from the aerotriangulation adjustment for a particular photograph will still be located in the original CP file used to compute the photogrammetric solution. There is no automatic mechanism for flagging such points. In the DMS implementation, however, this is not a major problem since one or more points can be removed and the solution recomputed very quickly to permit evaluation.

The most difficult problem to overcome in this process is when there are insufficient GCPs to permit the photogrammetric solution or when the distribution of GCPS is poor. More often than not this occurs at the end of a flight line or the edge of a quadrangle when the last photo in the line has only one stereomate. In this case, there can be as few as six points in the photograph, which is not enough to permit error checking. The solution to this problem is to extend the flight line into the adjacent

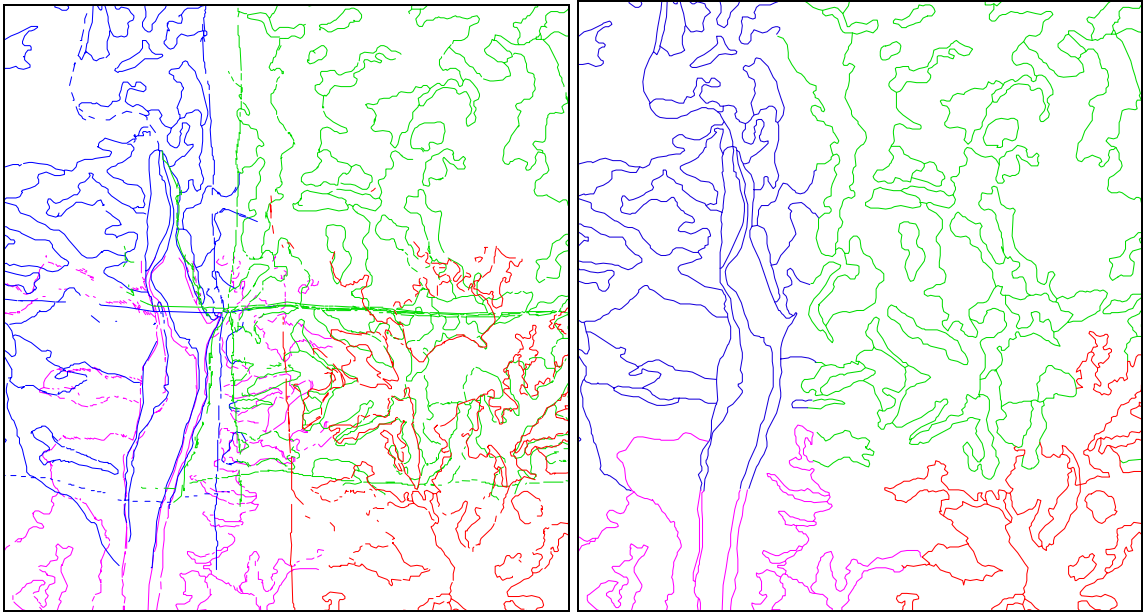
quadrangle by one or more photographs, identify additional pass points, regenerate the aerotriangulation solution and restart the orthorectification process for the photograph. This process can be quite time consuming, however, and efforts should be made to ensure that nine or more control points are available in each photograph in the quadrangle.

Finally, the overlay is orthorectified to a 2-meter output pixel size using the USGS DEM for the elevation reference information. In this step, displacements in the overlay due to tilt and relief in the original photos are removed. A coefficient file containing the image to ground transformation parameters is also created at the same time.

The LAN-format file generated when the overlay is orthorectified is converted to uncompressed 8-bit TIFF format for compatibility with the program, R2V (Able Software, 1999). The conversion of the orthorectified vegetation overlays from raster to vector format is easily accomplished using the R2V program and a standardized procedure that results in a set of vectors in ARC/INFO Generate format referenced to the image pixel and line coordinate system. This process converts all lines and vectors on the overlay, including text and smudge marks, into vectors. Sometimes, too, lines become broken or jagged in the orthocorrection process as a result of discontinuities or errors in the DEM. In these cases, some of the spurious marks are removed by smoothing and snapping functions in the R2V software, while others must be eliminated in the editing process in ARC/INFO. The coordinates of the vectors are converted to UTM coordinates with affine transformation coefficients created by the DMS software during the overlay orthorectification process.

Finally, the corrected vector files and associated orthorectified overlays are transferred via FTP to a Sun Microsystems Enterprise 450 Server for editing and attributing in ARC/INFO operating in the Sun Solaris environment. Because the overlays were first orthorectified before conversion to vector format, they fit together well when displayed in ArcView (Figure 3-25). After correction, there generally is a good correspondence between the same polygons delineated on adjacent photographs. Using tools available in ARC/INFO and custom routines created by CRMS staff members, the overlay is edited to close polygons and remove artifacts. During the editing process, questions about specific polygons or lines are resolved through examination of the rectified overlay, DOQQs or original aerial photographs viewed in stereo on a light table. It is frequently necessary to delete small “dangles” or entire lines and then to redraw the lines by tracing the rectified overlay in heads-up mode. A typical overlay may contain as many as 50 to 100 individual polygons. Where unresolved problems in the aerotriangulation persist, there are also associated problems with the fit of the overlay. In these cases, the DOQQ is used to position the vector data. This insures the accuracy of the plotted vectors in problem areas where the aerotriangulation results were not sufficient to permit a reliable fit at all points.

The next step is to edge-match the individual photo coverages with the data from adjacent photographs. Here, the coverages are displayed in the same editing screen in ARC/INFO (much like that depicted in Figure 3-25) and any discrepancies between polygons are resolved – again with reference to the rectified overlays, DOQQs and aerial photographs. When this process is finished, all overlapping lines and polygons will have



a)

b)

Figure 3-25 (a) Raw unedited vectors for a portion of the Noland Creek Quadrangle showing the correspondence of corrected polygons from adjacent overlays (shown in blue, green, magenta and red). (b) Vectors for the same area after editing and edge-matching in ARC/INFO.

been brought into agreement and converted to clean polygons. The coverages corresponding to individual photos are then merged into a single vegetation coverage. In a final operation, the dominant, secondary and tertiary vegetation classes for each polygon as annotated on the overlay by the photointerpreter are assigned as attributes in the GIS database. When the map is subsequently displayed, all three attributes are listed and the color is drawn from the dominant vegetation type (Figure 3-26). A completed map may have up to 6500 polygons with over 100 vegetation classes. The average number of polygons per quadrangle is about 2200 (Table 3-5).

The quality of the ground control determines how well a photo may be oriented and its overlay orthorectified, how well the vectors derived from the corrected overlay will fit together and how much editing will be needed to complete the map. In this respect, locating pass and control points and performing the aerotriangulation to generate an extended control network is a fundamental concern without which no subsequent step in the complicated process of building the vegetation map of the Great Smoky Mountains is possible. The ultimate result is a set of polygons that are correct in size and shape and positioned correctly within the UTM coordinate system to facilitate their integration in the GIS database. The success of these operations on the photos and overlays are discussed in Chapter 4.

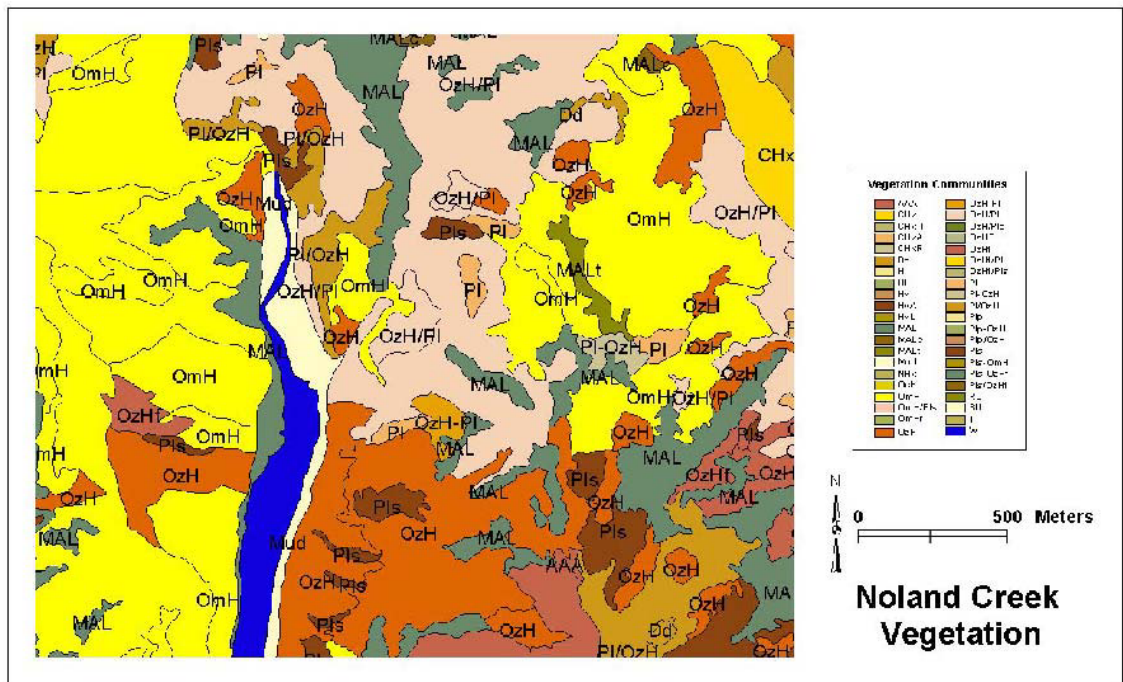


Figure 3-26. Final edited and attributed map coverage for the sample Noland Creek Quadrangle area. Attributes associated with the dominant vegetation type are indicated.

Table 3-5. Over 38,000 individual polygons have been mapped in 17 quadrangle areas in Great Smoky Mountains National Park.

Quadrangle Name	# Polygons
Blockhouse	625
Bryson City	1663
Calderwood	6478
Fontana Dam	1599
Gatlinburg	2690
Hartford	1786
Jones Cove	701
Kinzel Springs	1566
Luftee Knob	4774
Mount Guyot	3998
Noland Creek	1307
Silers Bald	3584
Tapoco	1072
Thunderhead Mountain	2811
Tuskegee	1349
Waterville	354
Wear Cove	1659
Total	38016
Average per quad	2236

CHAPTER 4

SOFTCOPY PHOTOGRAMMETRY AS THE FOUNDATION FOR GIS DATABASE DEVELOPMENT

Issues of major concern in developing a vegetation database and corresponding map products included the large number of aerial photographs associated with the project, extreme terrain relief, a near-continuous canopy cover and the difficulty in identifying potential ground control points in the forested terrain. In spite of these problems, softcopy photogrammetric techniques were successfully employed to provide the foundation for the database and maps. The results of these operations are described below.

Control Extension and Aerotriangulation

Aerotriangulation procedures were implemented in an effort to create a large enough number of GCPs to permit orthorectification of the aerial photographs. A total of 4301 points (1224 GCPs and 3077 pass points) were located on 882 photos, requiring 16256 discrete point measurements to accomplish (Figure 4-1). On average, each point was observed on four photos. The adjusted exterior orientation elements for all photographs and the final ground coordinates for all control and pass points were reported in the GIANT.OUT files described in Chapter 3 (see Table 3-4). The overall planimetric fit of the GCPs computed after the final aerotriangulation adjustment for the 17 quadrangles in this study was ± 16.5 m. This value was derived by computing the RMSE between the coordinates resulting from aerotriangulation and the coordinates for GCPs measured from

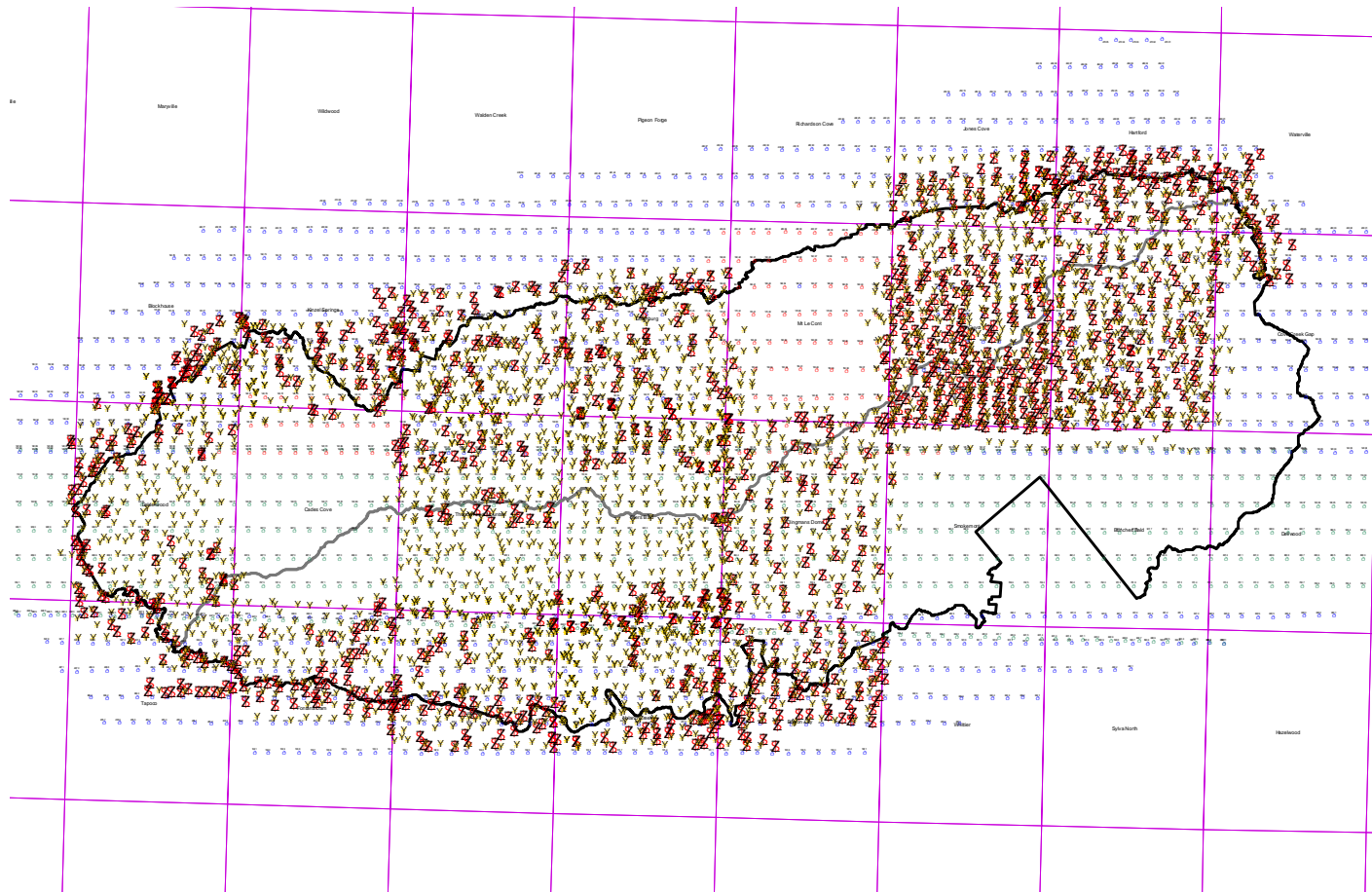


Figure 4-1. Distribution of control points (triangles) and pass points (circles) identified and computed using aerotriangulation procedures for the Great Smoky Mountains National Park.

the DOQQs (Table 4-1). Pass point errors in Table 4-1 correspond to intersection error as reported in the GIANT.OUT file and are determined by the intersection of rays from the photos in which they appear, with larger errors resulting from an inability to precisely identify the locations of the pass points on overlapping photos. The pass points in the 17-quadrangle area had an overall RMSE_{XY} of ± 24.2 m, which is about 1.6 times the error at the GCPs.

The residuals from the aerotriangulation adjustment take into account every GCP that passed the image matching and intersection tests in PC GIANT. A comparison of the computed GCP coordinates with the original GCP coordinates measured from the DOQQs, however, revealed X, Y vector errors as high as ± 125 m at a few individual points. These large errors were not even marginally acceptable and were not employed in the mapping process. After withholding all such points with vector errors greater than ± 50 m, the error for many quadrangles was reduced by as much as one third to one half (see the last two columns of Table 4-1). In all, 29 GCPs were withheld from the computation and the resulting RMSE_{XY} was reduced from ± 16.5 m to ± 12.6 m at the remaining 1195 GCPs. This value is well within the accuracy requirements for resource mapping and is equivalent to 0.8 mm on a 1:15,000-scale map.

A further examination of Table 4-1 reveals that quadrangles located in the northeastern portion of the Park generally have higher errors than those around the periphery in the western portion. (These quadrangles are shaded in the Table.) In addition, quadrangles along the central ridgeline of the mountain range also tend to have higher errors, although they are within an acceptable range. The map presented as Figure

Table 4-1. Summary of aerotriangulation results by quadrangle. GCP errors are reported in metres.

			GCP Errors		Pass Points		GCPs	Final GCP
Quadrangle	Nphotos	Nobs	Npts	RMSE_{XY}	Npts	RMSE_{XY}	Withheld	RMSE_{XY}
Tapoco	19	331	70	6.9	60	30.5	0	6.9
Tuskegee	61	906	113	12.2	180	12.2	2	9.39
Calderwood	84	1211	31	4.5	207	20.6	0	4.5
Gatlinburg	66	1069	45	8.3	208	13.0	1	6.3
Fontana Dam	42	682	18	32.4	120	23.6	1	14.6
Noland Creek	49	853	41	3.6	194	31.0	0	3.6
Silers Bald	88	1202	156	23.6	271	23.9	3	18.9
Thunderhead Mountain	83	1419	100	21.7	254	20.5	3	11.7
Blockhouse	19	379	33	15.8	76	29.0	1	12.4
Kinsel Springs	30	489	42	10.3	99.0	11.1	1	5.8
Wear Cove	58	1163	74	11.2	235	8.0	1	8.9
Bryson City	43	698	78	10.7	150	22.8	0	10.7
Mt Guyot	77	2255	140	19.0	365	16.1	2	17.6
Hartford - Waterville	61	1404	127	29.4	243	33.6	4	24.8
Jones Cove	41	859	48	23.9	151	37.3	1	23.0
Luftee Knob	61	1336	99	30.2	264	53.4	9	22.6
TOTAL	882	16256	1224	16.5	3077	24.2	29	12.6

4-2 shows aerotriangulation errors in two general classes: quadrangles with X, Y planimetric errors less than ± 20 m are shown in light green, while those with higher errors are shown in darker green. This map also shows the roads in and around Great Smoky Mountains National Park. It is interesting but not surprising to note that those quadrangles with lower errors also tend to have a more highly developed road network due to the presence of residential areas around the borders of the Park. Hence, more high quality well-defined GCPs are available for use in the aerotriangulation adjustment. The central quadrangles rely more heavily on the use of natural points or points transferred from adjacent quadrangles as GCPs since there are very few roads within the Park boundaries.

One of the difficulties encountered in the northeastern corner of the Park may be attributed to the appearance of vegetation and other features on the aerial photographs recorded in spring and fall. Because of the new leaf growth on the hardwood trees, the spring photographs had a uniform appearance. This made it very difficult to identify individual trees that could be used as pass points. This was not the situation with the fall photographs where the variations in tree appearance resulting from the seasonal color changes in the trees facilitated the task of finding pass points.

The Luftee Knob Quadrangle is an exception. The photographs were recorded in the fall but the aerotriangulation results had the highest errors of all of the quads in the study. While it is difficult to identify the exact reasons for this since the data passed the intersection and point matching tests in PC GIANT, an examination of the orientation angles resulting from aerotriangulation reveals that a disproportionate number of photos

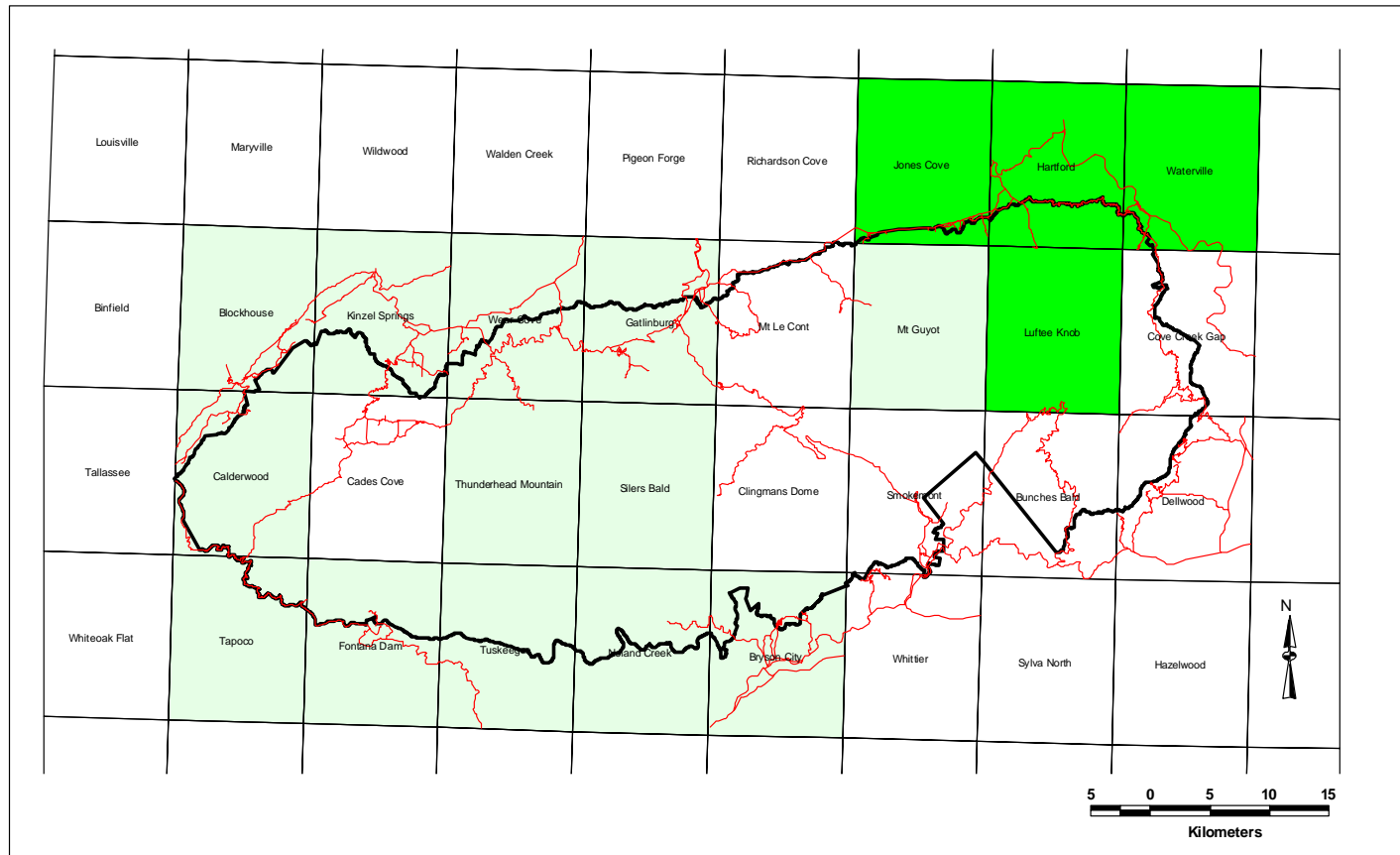


Figure 4-2. The accuracy of the aerotriangulation solution was higher in quadrangles containing roads and other cultural features that were for GCPs. Quadrangles with planimetric errors less than 20 m are shown in light green, while those with higher errors are shown in darker green on this map of Great Smoky Mountains National Park.

have angles exceeding the nominal three degree of tilt threshold. Figure 4-3 shows the photo center locations in the Luftee Knob Quadrangle as graduated circles, where the size of the circle corresponds to the magnitude of the combined Omega and Phi angles. In this Quadrangle, there are likely several individual points that are disrupting the aerotriangulation solution. Identification of the “bad” points was very difficult, however, and not very successful. As a result of this marginal solution, the corrected overlay vectors for Luftee Knob did not fit together as well as most of the other quadrangles and had to be edited very carefully to match the underlying DOQQ.

Figures 4-4 through 4-9 provide the distribution of GCPs and pass points for the Calderwood, Thunderhead Mountain and Gatlinburg Quadrangles superimposed on base maps and DOQQs, respectively. The GCP distribution maps for the remainder of the quadrangles are found in Appendix C. The Calderwood Quadrangle is on the western end of Great Smoky Mountains National Park and has a significant area of residential development in the northwestern portion of the Quadrangle. The southwest boundary is formed by Fontana Lake and a small two-lane highway (Figures 4-4 and 4-5). Due to the presence of the built-up areas around the periphery of the Park, many of the GCPs selected were road intersections with other roads or driveways. Additional points included agricultural field boundaries, fence lines and cultural detail (e.g., swimming pools) that were visible on the DOQQs and on the aerial photographs. One small road cuts through the interior area of the Quadrangle but is obscured by trees through most of its length. Thus, only one GCP in the entire Quadrangle was selected from the road. The majority of the remaining GCPs inside the Park boundary were chosen along streams. A

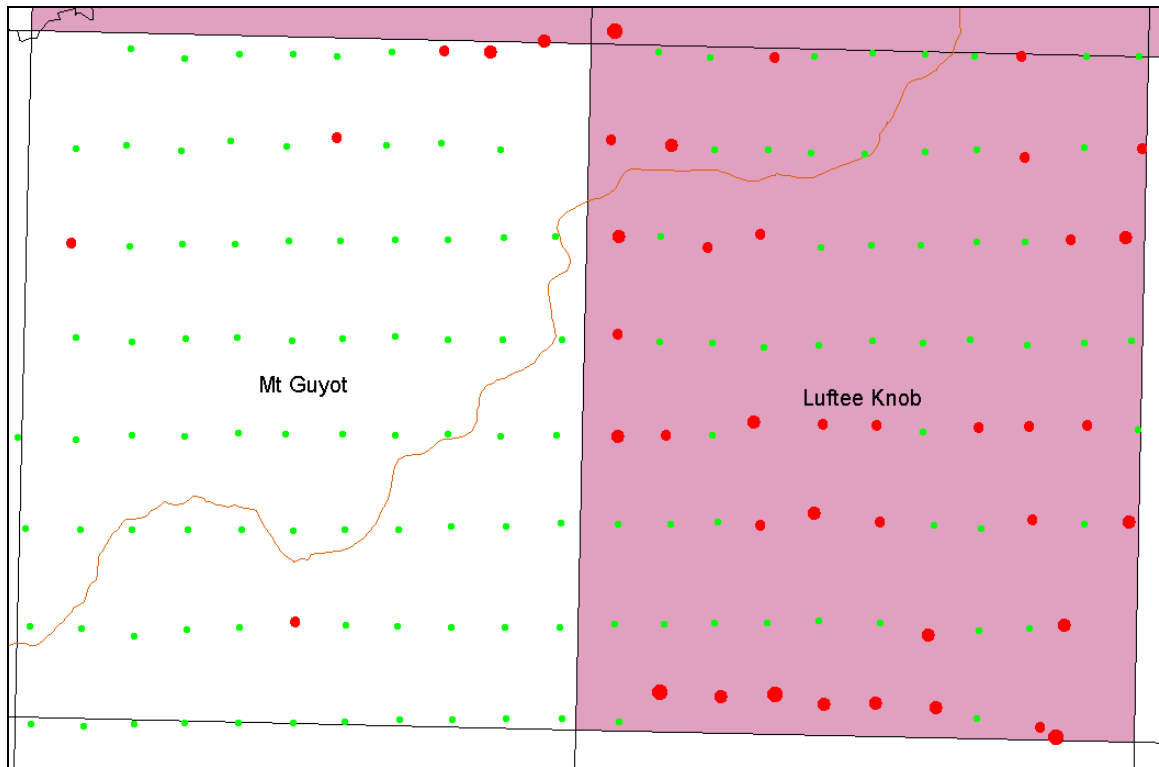


Figure 4-3. In contrast to the Mt Guyot Quadrangle, the photo centers in the Luftee Knob Quadrangle appear to be displaced from their correct locations. In addition, the orientation angles for many photos exceed the tolerance of ± 3 degrees tilt (as indicated by the graduated circles in red). Photo centers shown as green dots are within ± 3 degrees. The photos in the topmost flight line in each quadrangle were recorded in the spring.

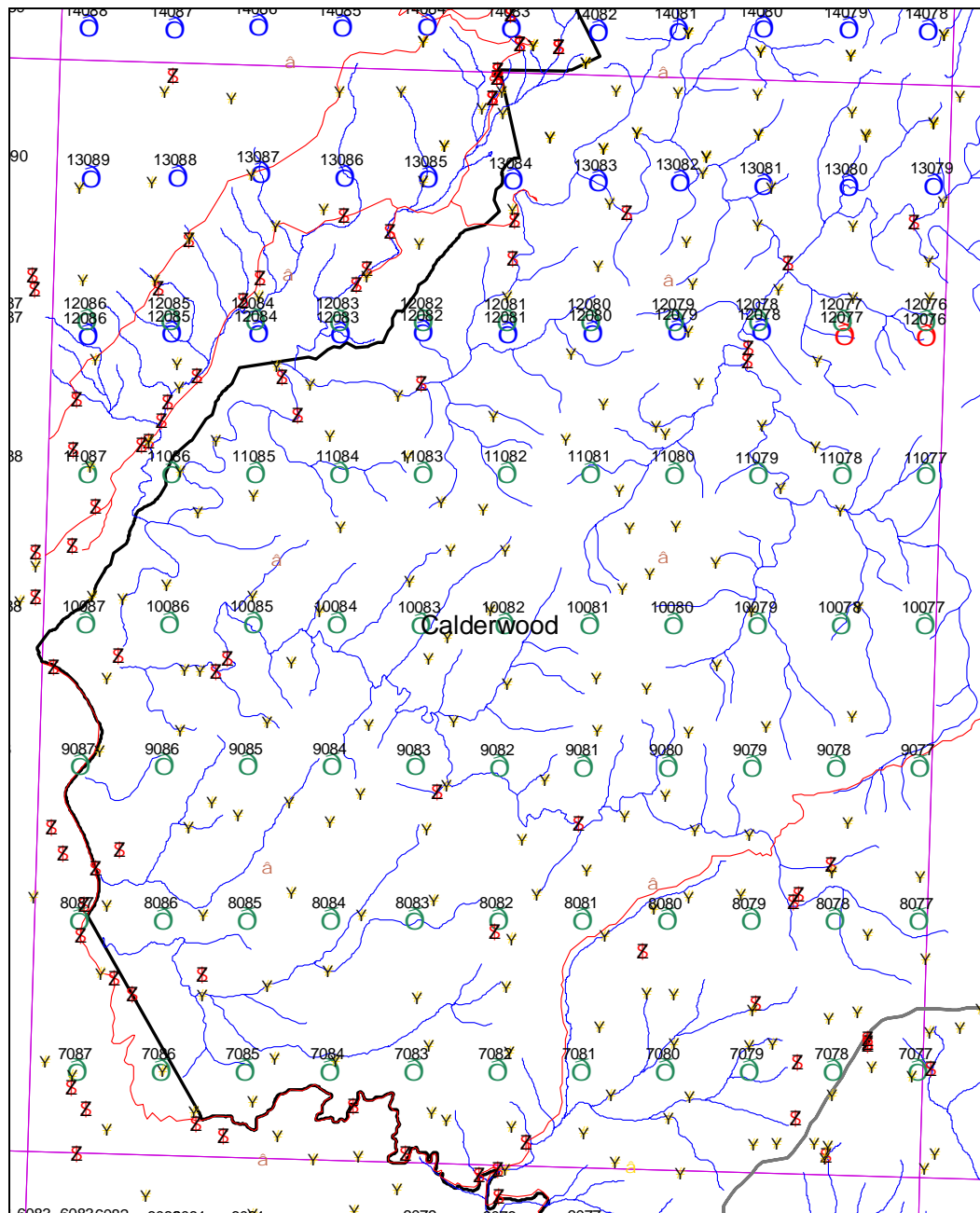


Figure 4-4. Distribution of photo centers, GCPs and pass points in the Calderwood Quadrangle. In this figure, aerial photo centers are marked with a circle and cross and identified by the photo number; GCP locations are marked with triangles and pass points with circles. In the Calderwood Quadrangle, there are 84 photos, 31 GCPs and 207 pass points. Planimetric error at GCPs was ± 4.5 m.

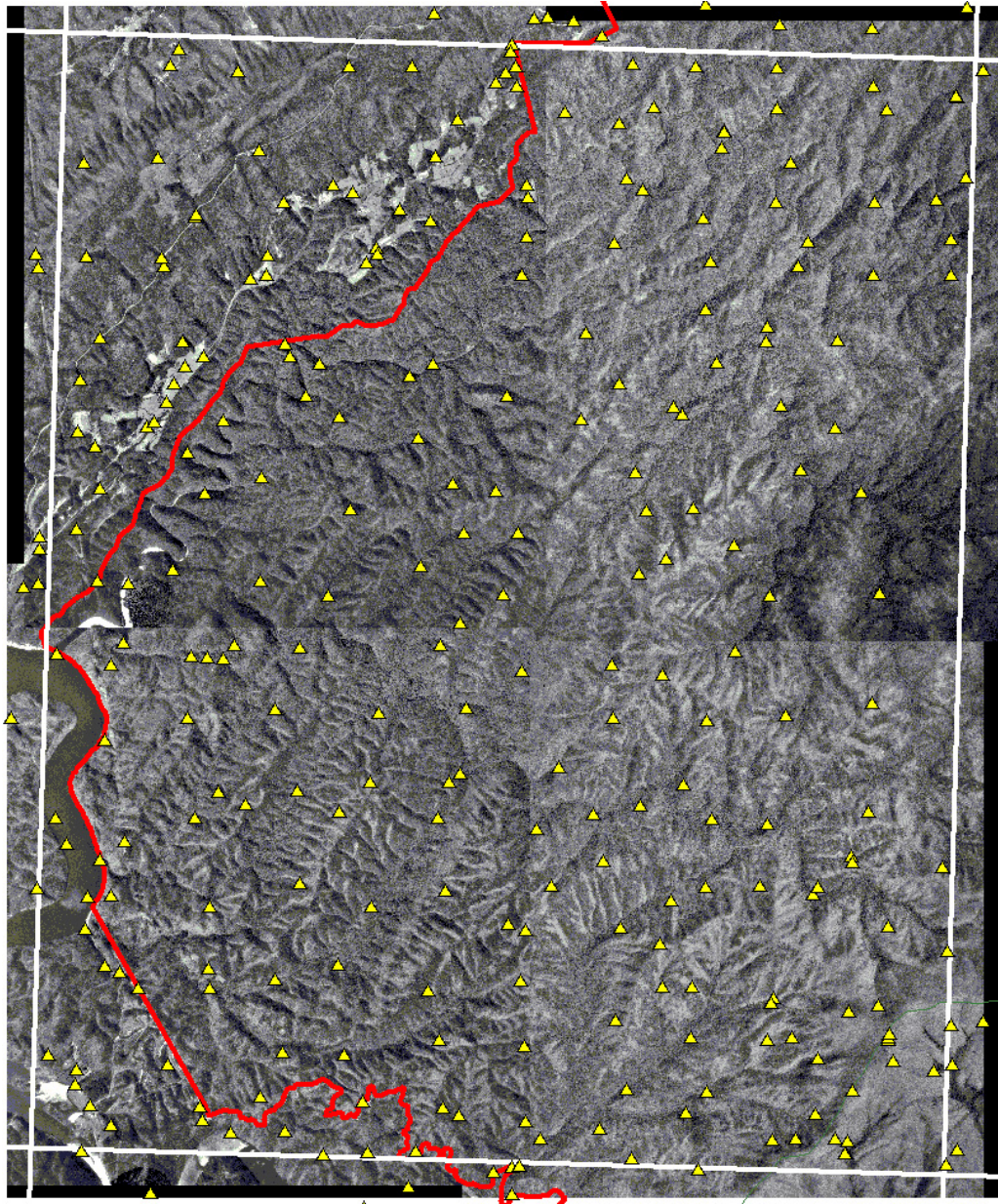


Figure 4-5. The Calderwood DOQQs have been mosaicked to create a single image covering the entire Quadrangle. GCPs are shown in yellow and the Park boundary in red.

total of 31 GCPs and 207 pass points were identified and digitized from 84 photographs in the Quadrangle. The X, Y vector error (RMSE) resulting from aerotriangulation was ± 4.5 m for the ground control points, reflecting the high quality of point locations available around the Park. The vector error at pass points was ± 20.6 m which is 3.7 times the error at the GCPs and is due, in part, to the lack of good quality GCPs in the interior region of the Quadrangle.

The Thunderhead Mountain Quadrangle is in the central portion of the Park along main Appalachian Mountain ridgeline. With a total relief of over 1200 m, some of the highest mountains in the Smokies are within this Quadrangle. A few short roads on the north edge of the Quadrangle provide some control points, but the majority of GCPs were found along streams, in open areas (“balds”) at the top of the mountain and at distinct topographic features such as the intersection of two ridges (Figures 4-6 and 4-7). A total of 100 GCPs and 254 pass points were identified and digitized from 83 photographs in the Quadrangle. The planimetric error resulting from aerotriangulation was ± 11.7 m for the ground control points while the error at pass points was ± 20.5 m. Both error values were about average for the Park as a whole and are surprisingly good considering the fact that GCPs of reasonable quality are very difficult to locate in this central portion of the Park.

The Gatlinburg Quadrangle at the north side of the Park encompasses a large portion of the Park as well as the town of Gatlinburg and surrounding area. In addition, U.S. Highway 441, the major highway through the Park, and a number of Park roads are within the Quadrangle area. The use of these features as GCPs, as well as a few points on

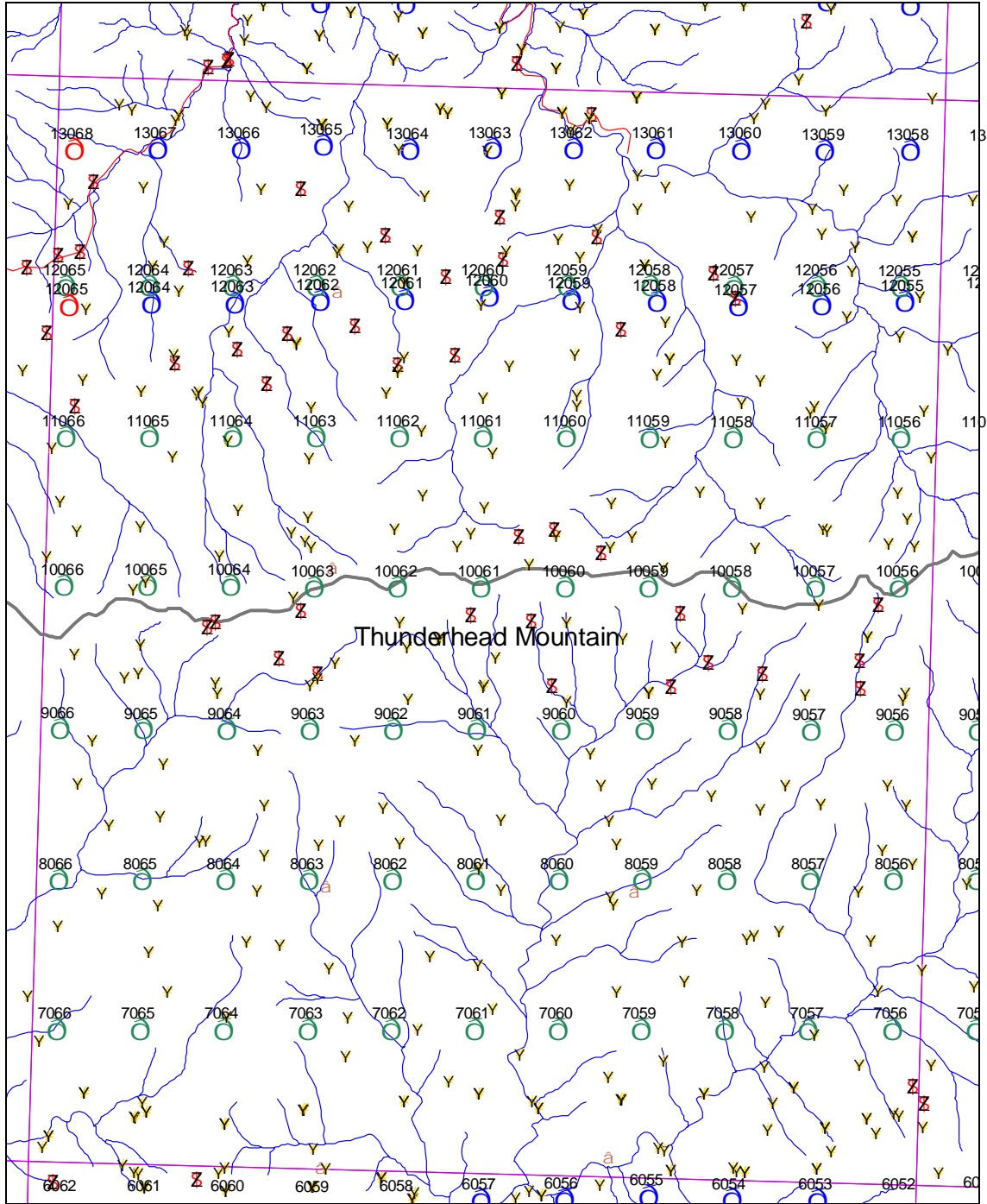


Figure 4-6. Distribution of photo centers, GCPs and pass points in the Thunderhead Mountain Quadrangle. There are 83 photos, 100 GCPs and 254 pass points in this Quadrangle. Planimetric error at GCPs was ± 11.7 m.

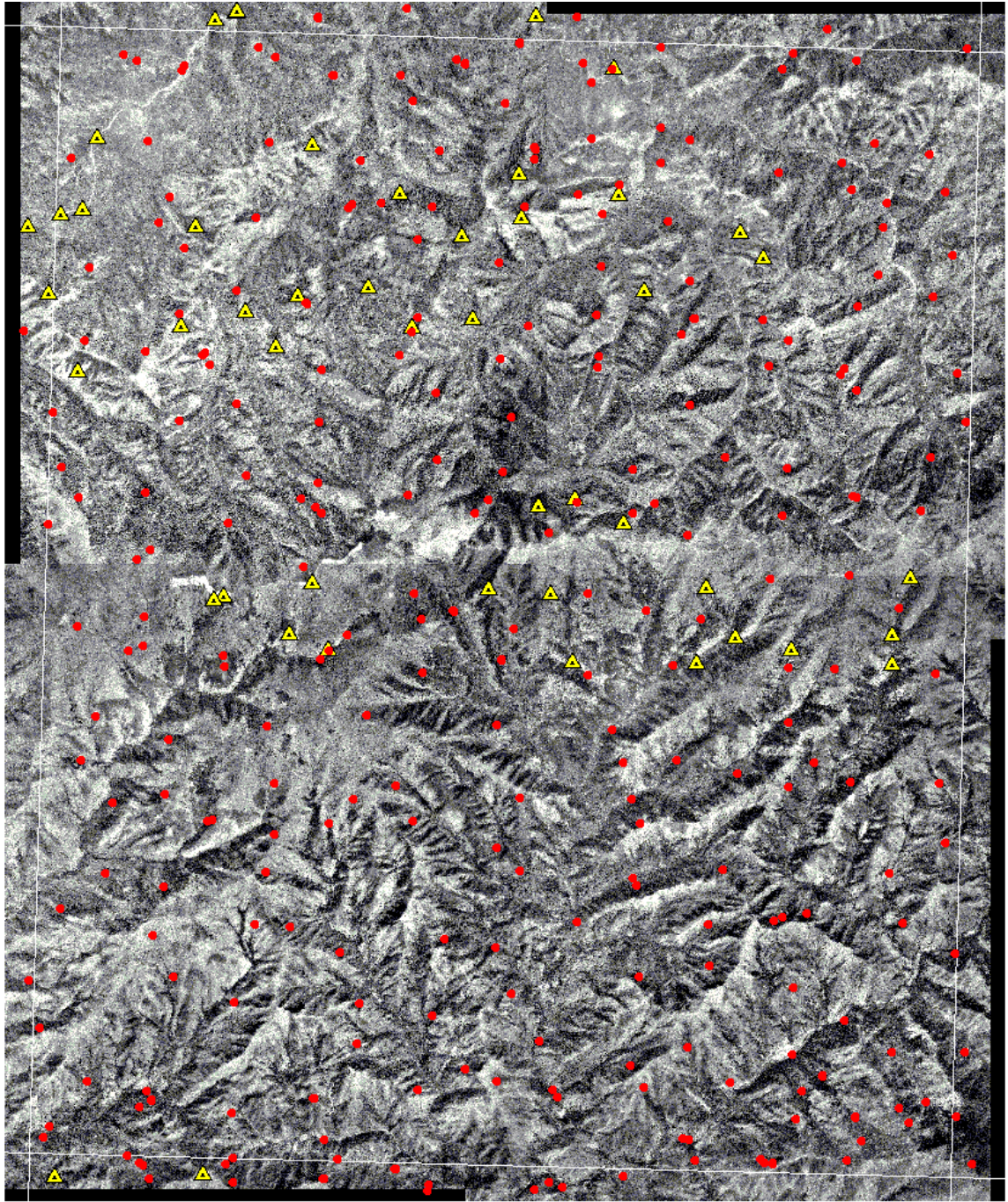


Figure 4-7. The Thunderhead Mountain DOQQ mosaic showing the locations of GCPs and pass points.

streams and topographic details resulted in an excellent aerotriangulation solution at the 45 GCPs of ± 6.3 m, with a pass point error of ± 13 m at 208 points. Sixty-six photos were included in the solution (Figure 4-8). Figure 4-9 shows the mosaic of approximately 30 of the large-scale aerial photographs for the area.

An alternative way to assess the quality of the photogrammetric solution is through an examination of a mosaic of orthorectified aerial photographs. Inspection of the ridges, valleys and stream courses in the rugged terrain at join lines between photos reveals the quality of the data. As the vegetation overlays are rectified using the same parameters, they are similar in quality. Figure 4-10 is a portion of the orthophoto mosaic of Kinsel Springs Quadrangle. The join line between the two photos that bisects this image horizontally is nearly invisible due to the high level of correspondence in the topographic detail between the two images resulting from a successful photogrammetric solution for each of the photos.

Development of the Vegetation Maps and GIS Database

The polygons making up vegetation maps produced for this project provide delineations for features that in reality have indistinct boundaries. In addition, there are very few well-defined features Park-wide with which to perform a quantitative accuracy assessment. Consequently, it is appropriate to evaluate the overall quality of the overlay rectification process in terms of the fit of the rectified overlays to the DOQQ base map. This can be achieved by displaying the raw (pre-edit) polygon vectors on top of the DOQQ and inspecting the details of the “fit”. In Figure 4-11, the raw vectors for

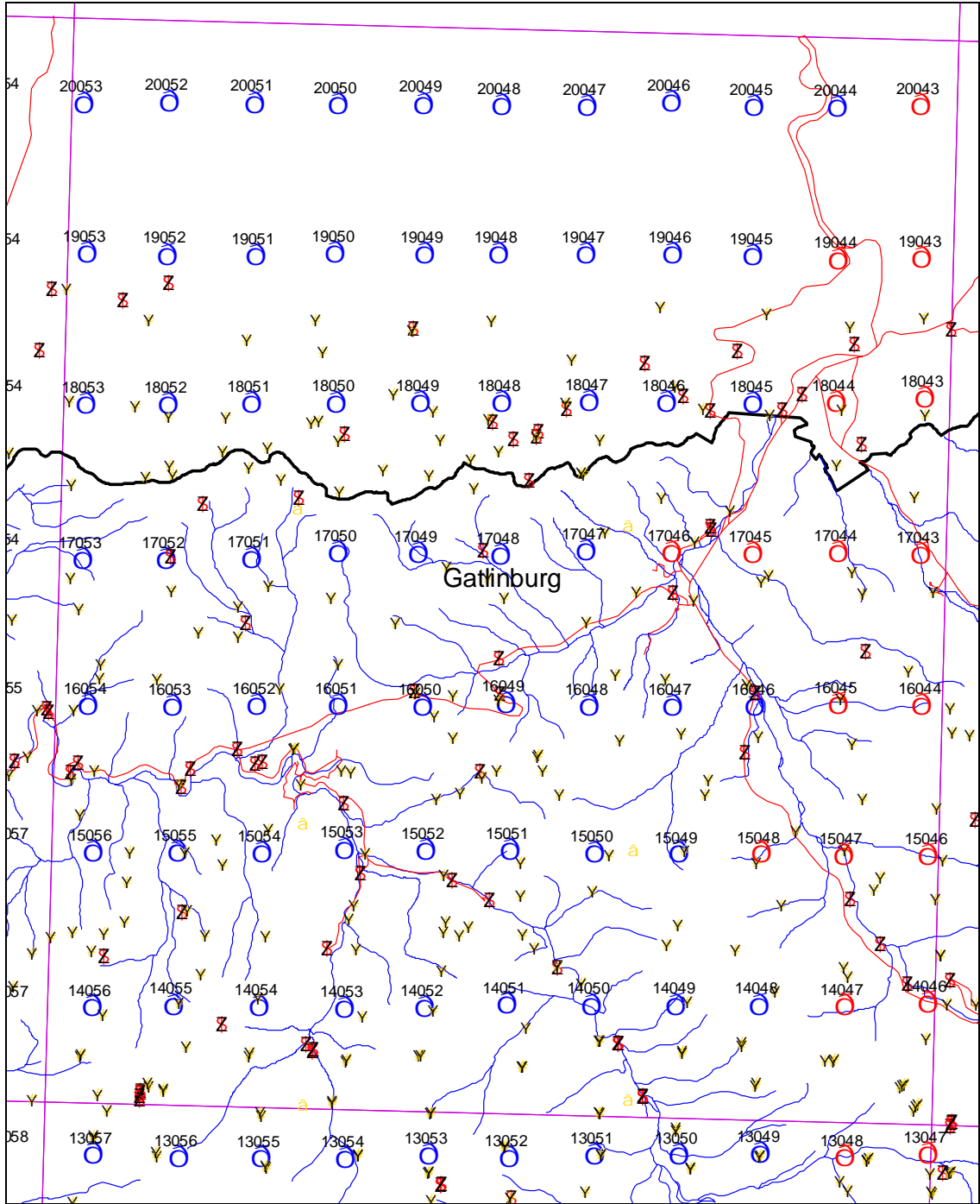


Figure 4-8. Distribution of photo centers, GCPs and pass points in the Gatlinburg Quadrangle. There are 66 photos, 45 GCPs and 208 pass points in this Quadrangle. Planimetric error at GCPs was ± 6.3 m.

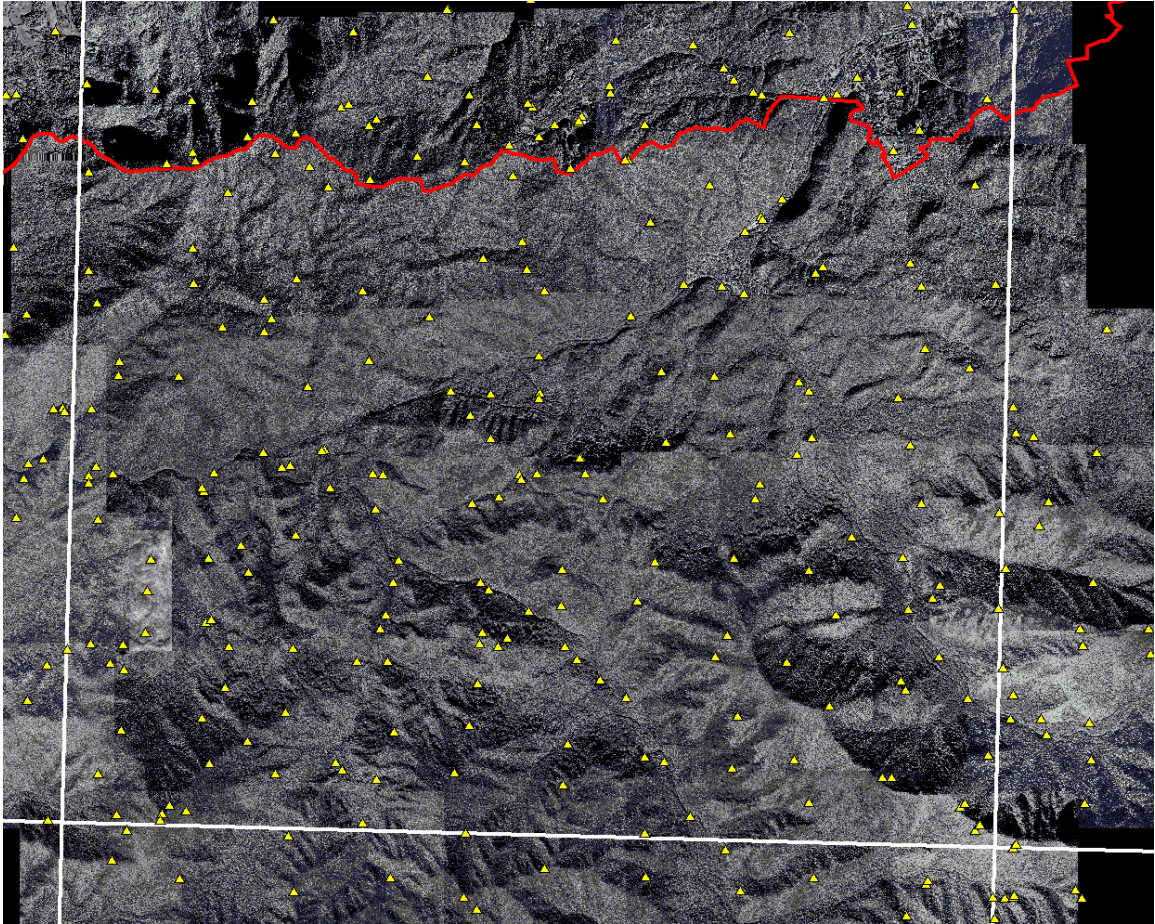


Figure 4-9. Mosaic of approximately 25 large-scale aerial photos for the Gatlinburg Quadrangle.



Figure 4-10. Portion of photo mosaic from the Kinsel Springs Quadrangle.

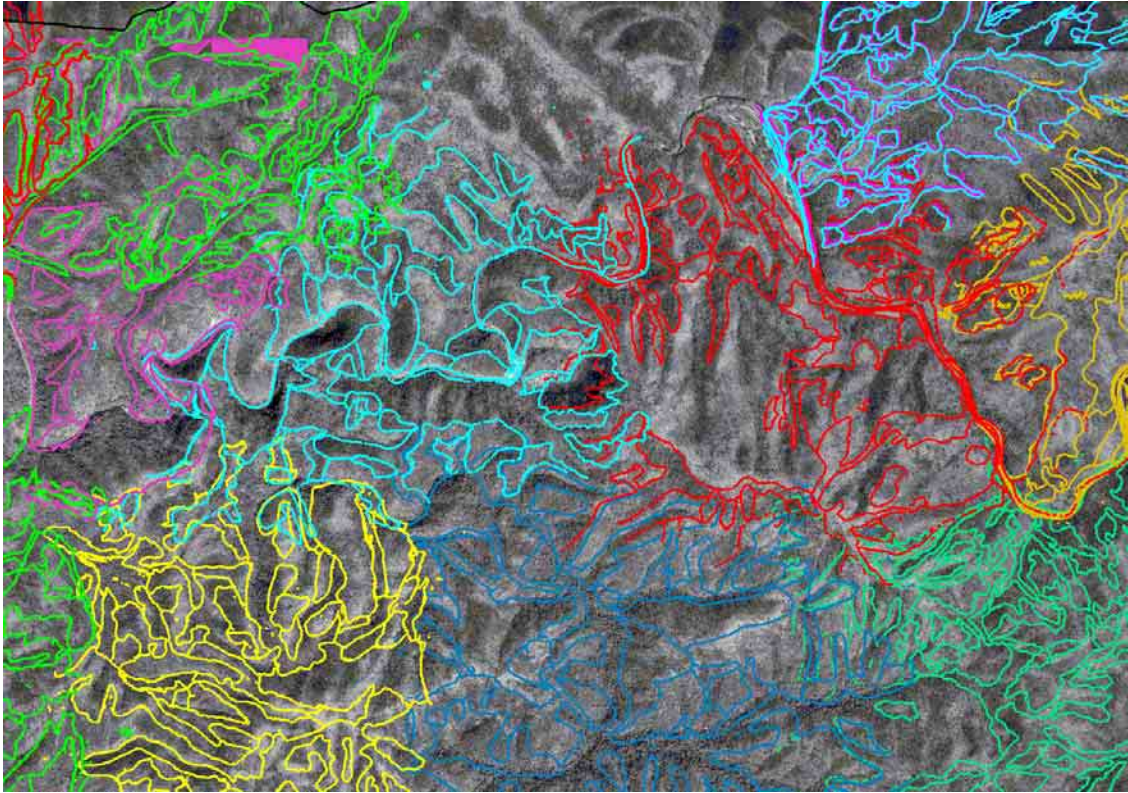


Figure 4-11. The raw vectors for vegetation communities in this portion of the Wear Cove Quadrangle were converted directly from the overlays and displayed in register with the DOQQ. The quality of the fit can be assessed by examining the polygons in relation to details and patterns in the underlying image. Each color represents data from different photographs. Differences between adjacent photos are resolved during the editing and edge-matching procedure in ARC/INFO.

vegetation communities in this portion of the Wear Cove Quadrangle were converted directly from the overlays and displayed in register with the DOQQ. The quality of the fit can be assessed by examining the polygons in relation to details and patterns in the underlying image. Each different line color in the Figure represents vector data from different photographs. It can be seen that there is excellent agreement in both position and shape of the polygons when compared to the underlying DOQQ. Similar results can be seen for Calderwood and Mount Guyot Quadrangles in Figures 4-12 and 4-13.

Where present, differences between polygons derived from adjacent photos are resolved during the editing procedure in ARC/INFO. The program, ARCEDIT, is employed to clean up and close polygons associated with vegetation classes. The individual photo coverages are then edge-matched with the data from adjacent photographs and finally merged into a single vegetation coverage (Figure 4-14). In the last process each polygon in the coverage is given attributes according to the annotation marked on the overlay by the photo interpreter. Up to three levels of attributes are assigned according to the dominant, secondary and tertiary vegetation types. Generally, colors in the final maps are based on the dominant vegetation type (Figure 4-15).

After the individual maps are completed, they are integrated into the overall GIS database by edge-matching between quadrangles. This editing process insures continuous and consistent vegetation polygons that, when complete, will form a seamless database for the entire Park. Figure 4-16 illustrates the portion of the database where the Wear Cove, Gatlinburg, Thunderhead Mountain and Silers Bald Quadrangles meet.

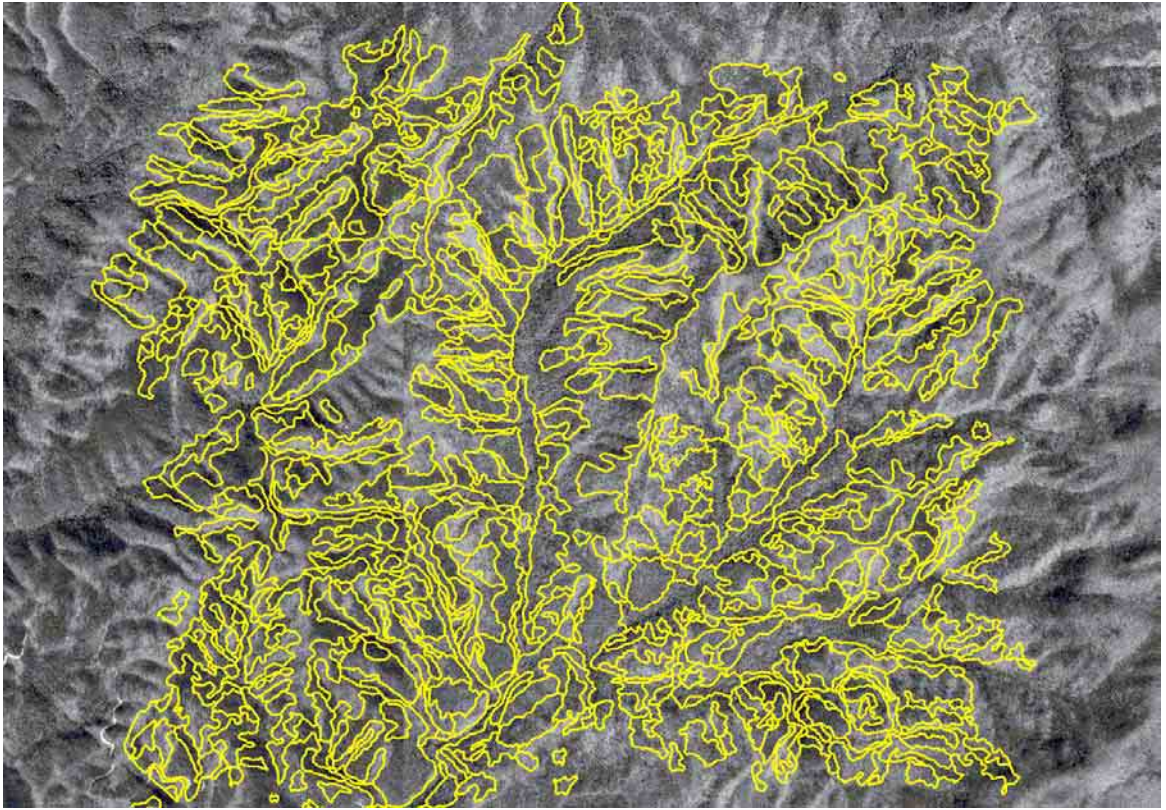


Figure 4-12. The raw vectors corresponding to four photographs displayed over the DOQQ in the Calderwood Quadrangle.

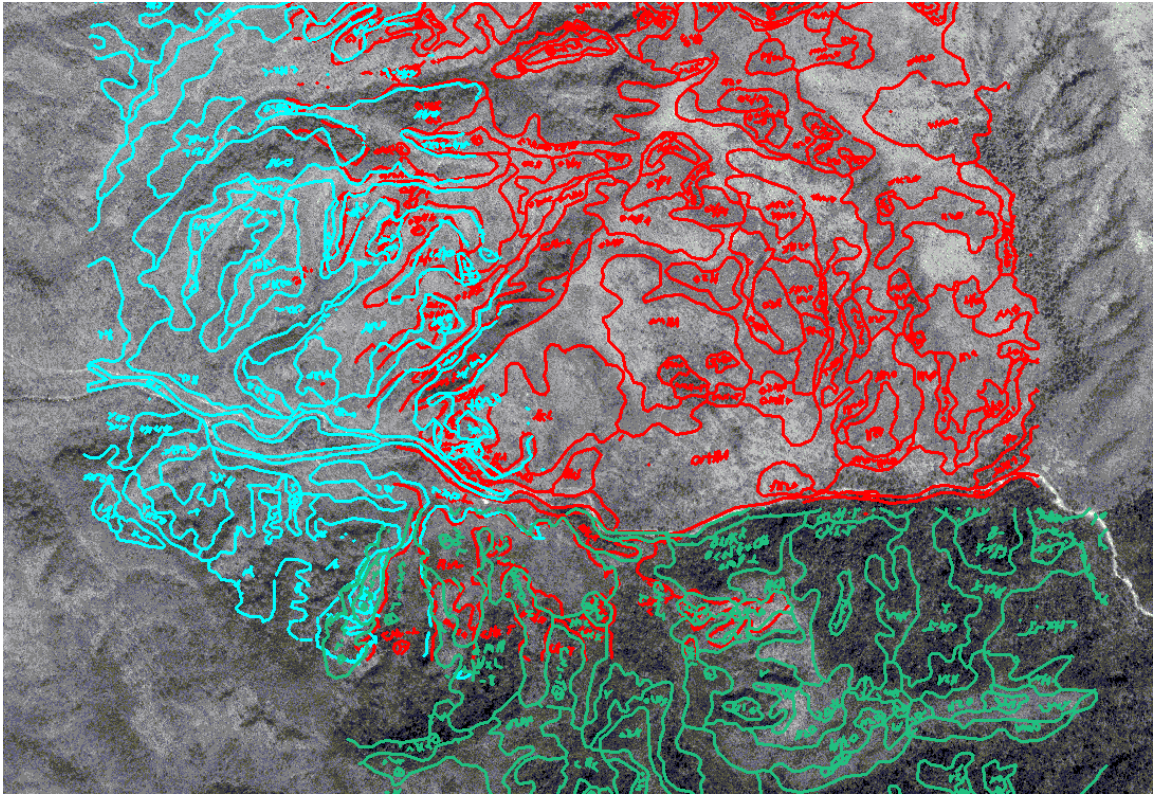


Figure 4-13. The raw vectors displayed over the DOQQ in the Mount Guyot Quadrangle.

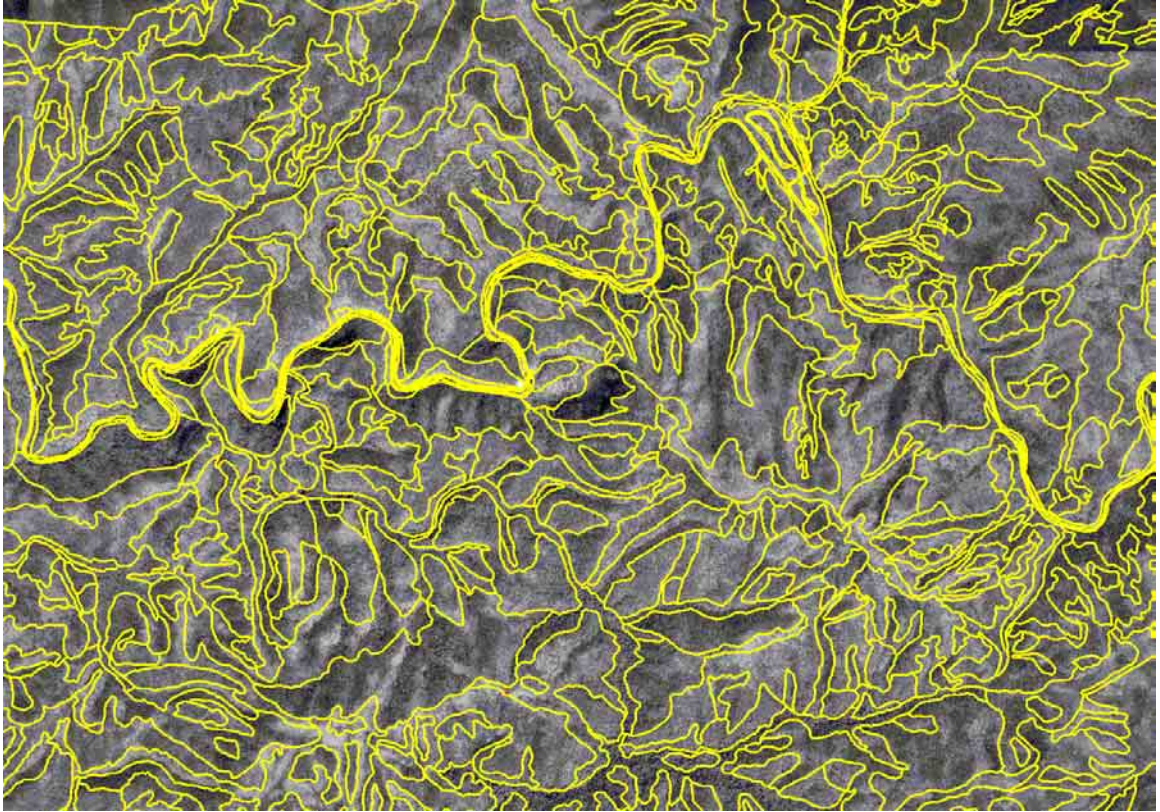


Figure 4-14. Wear Cove vegetation coverage after editing and resolving differences between adjacent photos.



Figure 4-15. Wear Cove vegetation map after final editing. Colors correspond to the dominant vegetation type in each polygon.

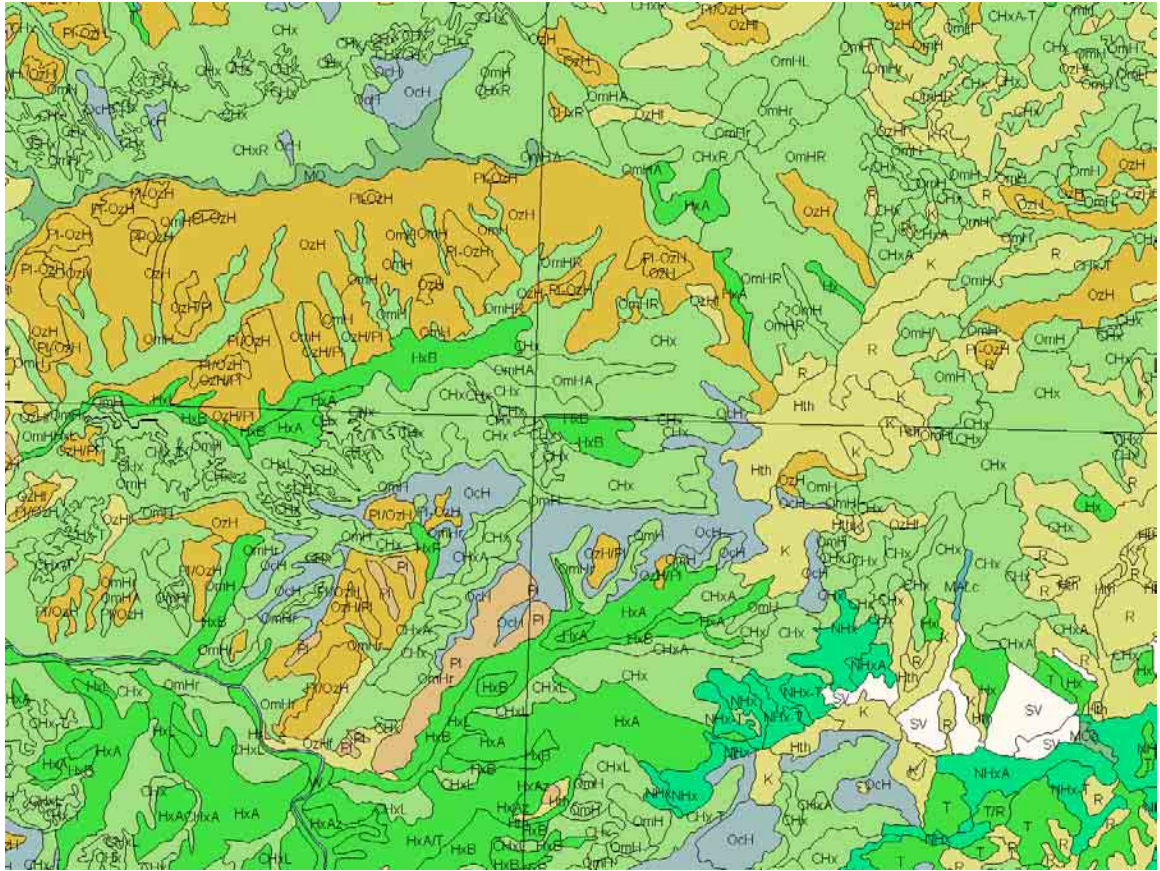


Figure 4-16. Portion of the completed Great Smoky Mountains National Park vegetation map including the junction between Wear Cove (upper left), Gatlinburg (upper right), Thunderhead Mountain (lower left), Silers Bald (lower right) Quadrangles. Attributes correspond to the dominant vegetation type.

Examples of the final maps for Calderwood, Gatlinburg and Thunderhead Mountain are presented as Figures 17 to 19.

At this writing, vegetation mapping is complete or nearly complete for 20 of the 24 quadrangles within the Great Smoky Mountains National Park. Two of the maps were produced by ESRI/AIS over a five year period and the remaining 17 by the CRMS in just three years. Most of this accelerated production has been made possible by the use of softcopy photogrammetric methods. Indeed, the project could not have been completed without analytical aerotriangulation to extend a sparse network of ground control into the much more dense set of points required to orthorectify the aerial photographs and associated vegetation overlays.

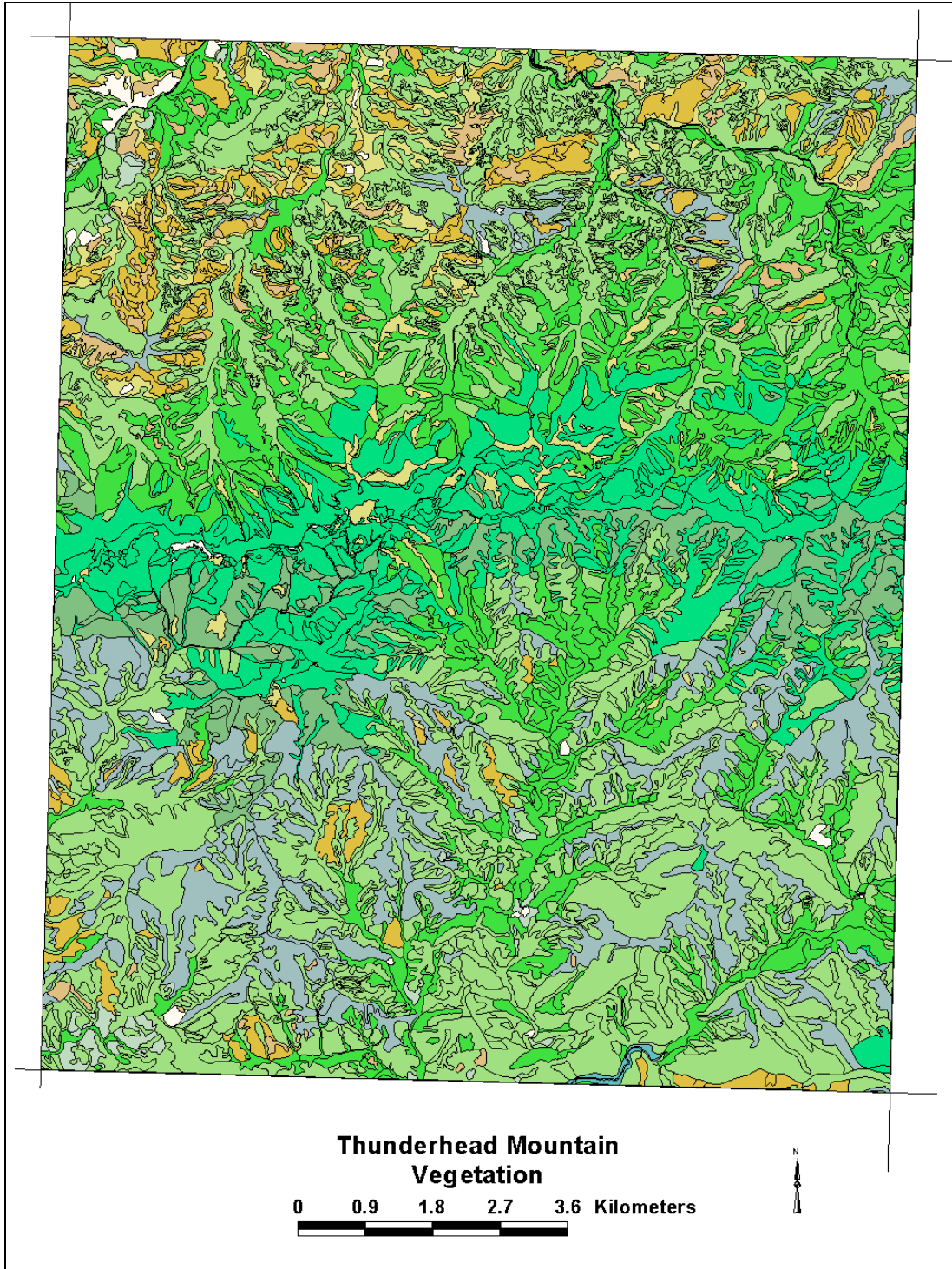


Figure 4-19. The full Thunderhead Mountain vegetation map. Attributes have been omitted for clarity.

CHAPTER 5

SUMMARY AND CONCLUSION

Summary

The Great Smoky Mountains National Park is the most popular national park in the eastern United States with an average of 9.1 million visitors per year. As one of only 43 International Biosphere Reserves in the United States, this rugged region of 209,000 ha in the southern Appalachian Mountains is also the most biologically diverse area in North America. In 1999, the Center for Remote Sensing and Mapping Science at The University of Georgia entered into a cooperative agreement with the U.S. National Park Service to create a detailed vegetation database and associated map products of the Park from large-scale, color-infrared aerial photographs recorded in the fall and spring of 1997 and 1998. This database and related map products were to be provided in digital format suitable for use (by the Park's GIS laboratory) with ESRI ARC/INFO and ArcView GIS software.

Because of the near-total tree canopy cover and the lack of roads and cultural features within the Park boundaries, the identification/location of features that could serve as GCPs for the almost 1000 aerial photos was nearly impossible. Furthermore, terrain relief in the Park reaching from 250 m to 2025 m AMSL caused significant displacements in the aerial photographs that made it very difficult to convert overlays with annotated vegetation polygons into the map coordinate system to a high degree of

accuracy. Consequently, the objectives of this dissertation were: 1) to evaluate methods for control extension and rectification of the aerial photographs and overlays that involve the use of analytical aerotriangulation and softcopy photogrammetric techniques; and 2) to accurately georeference vegetation polygons that are correct in shape and size to facilitate the construction of the GIS database.

Work for the project corresponded to 17 USGS 1:24,000-scale topographic quadrangles. The 1:12,000-scale color infrared aerial photographs were scanned at a resolution of 42 μm and saved as gray-scale TIFF images. Pass points were identified on overlapping photographs and their coordinates digitized using heads-up digitizing methods in a softcopy photogrammetry environment. Features that could serve as GCPs were then located on both the scanned aerial photographs and on USGS DOQQs. The planimetric (X, Y) coordinates of these features in the UTM coordinate system (NAD 27) were measured from the DOQQs and elevation (Z) coordinates for the GCPs were interpolated from USGS 7.5 minute Level 2 DEMs. It is estimated that the planimetric accuracy to which distinctly identifiable GCPs can be measured on the DOQQs is approximately ± 3 to 10 m. The accuracy of elevations (Z) for points at ground level is less than ± 5 m. Unfortunately, there are very few well-defined points within the Park. As a consequence, most of the GCPs used in this project were of somewhat lower confidence because of their imprecise locations and included features such as points of inflection of streams or topographic detail.

Analytical aerotriangulation techniques were employed to extend and densify the sparse network of control points to blocks of up to 88 photographs with as many as 133

GCPs and 250 pass points. Results varied according to the quality of both the GCPs and pass points. The $RMSE_{XY}$ values at GCPs ranged from ± 3.6 m to ± 24.8 m with an average value of ± 12.6 m. The coordinates of CPs were then transferred mathematically from the aerial photographs to the corresponding overlays using fiducial marks for registration and an affine polynomial transformation. The exterior orientation parameters for each of the overlays were then computed based on the extended control network. This permitted the overlays to be orthorectified to remove relief displacements and referenced to the UTM coordinate system. The corrected raster overlays were converted to vector format using the program, R2V, and the resulting polygons transferred to the ARC/INFO GIS environment. The polygons were edited to fit the USGS DOQQ, edge-matched and assigned attributes according to the vegetation types. In all, the number of pass points and GCPs obtained by aerotriangulation from 882 aerial photographs exceeded 4300. These were used to orthorectify the overlays containing over 38,000 separate vegetation polygons in 17 quadrangles.

Future Mapping of National Parks

The methods employed for creating the vegetation maps described in this dissertation have proved effective and have enabled the production of high quality maps that could not have been completed without the use of aerotriangulation and softcopy photogrammetric techniques. Point measurement and transfer is the most difficult and time-consuming part of the photogrammetric process. Care must be taken to measure and transfer every point as accurately as possible in order to obtain a high level of accuracy in

the subsequent aerotriangulation adjustment. It is unlikely that fully automated approaches to finding pass points will be successful in forested, mountainous terrain.

It is anticipated, however, that the time spent on point measurement and transfer can be reduced somewhat by taking advantage of recent improvements in computer, software and photo acquisition. New point transfer software that supports color display of aerial photographs will permit better identification of poorly defined pass points (e.g. tree tops) based on color, in addition to shape and location. Although file size remains an issue, faster computers with increased memory, larger hard disks and faster refresh rates make using large color files less troublesome.

Many of the support operations involved in this project, including point transfer, image rectification and raster-to-vector conversion operations easily can be performed with minimal training. On the other hand, the aerotriangulation software, PC GIANT, produced accurate results but was extremely difficult to learn and to use. For this reason, a photogrammetrist is needed to perform some of the more advanced procedures and to oversee the support work, especially if these techniques are adopted by other organizations. It would be desirable, in that case, to acquire more modern aerotriangulation software with a less steep learning curve, less stringent data formatting requirements, improved error analysis and clearer reporting.

Finally, the sheer volume of data for this project stems from the number of large-scale photographs. It would be possible to reduce the number of photographs that must be interpreted and controlled with aerotriangulation by using photographs of smaller scale (for example, 1:16,000 scale). This could be done with little appreciable loss of

detail, especially considering improvements in new high-resolution films. The use of airborne GPS/IMU control would greatly enhance the overall accuracy of the aerotriangulation solution while reducing the reliance on poor or marginal control points.

Additional difficulties with the aerial photographs result from their being exposed in both fall and spring. Here, the spring photos are the most problematic both for vegetation differentiation and interpretation and for pass point identification due to their uniform appearance in the color infrared aerial photographs. To prevent this in the future, all photographs should be recorded on a single date or within the same season – preferably fall so that the changing foliage colors can be used to aid in differentiating vegetation types and identifying pass points.

In mountainous regions, where relief displacements in large-scale aerial photographs have a significant impact on the mapping process, it would be advantageous to employ a camera with a focal length of 30 cm, as compared to the more traditional 15 cm. This would require doubling the flying height, which, in turn, would reduce displacements due to relief by a factor of two. Consequently, it would prove easier to control and rectify photos while maintaining the ability of the photointerpreters to discriminate vegetation types. In smaller, urban parks or those near built-up areas where few photographs are required, it might be possible to identify enough local control from DOQQs to alleviate the need for aerotriangulation. In larger parks, however, conventional aerotriangulation and airborne GPS control may be used to develop the control network to insure the accuracy and reliability of the resulting database and map products.

Conclusion

The techniques described in this dissertation for providing ground control in a rugged and remote region contributed to a significant improvement in the quality of vegetation information available for the Great Smoky Mountains National Park. Analytical aerotriangulation methods were proven to be effective for control extension and were critical for maintaining the accuracy of the map base while facilitating the transfer of detail from a large number of aerial photographs. As the management requirements of the Park evolve to accommodate applications such as vegetation mapping, fire control and habitat identification, the digital GIS database produced as a result of this project will prove to be a flexible and reliable tool.

REFERENCES

- Able Software, 1999. *R2V User's Guide*, Able Software Company, Lexington, Massachusetts, 89 p.
- Ackerman, F., 1992. Operational Rules and Accuracy Models for GPS Aerial Triangulation, *International Archives of Photogrammetry and Remote Sensing*, Commission III, ISPRS Congress, Washington, DC, 29(B3): 691-700.
- Ackerman, F., 1973. Experience with Applications of Block Adjustment for Large Scale Surveys, *Photogrammetric Record*, 7(41): 499-515.
- Ackerman, F. and H. Schade, 1993. Application of GPS for Aerial Triangulation, *Photogrammetric Engineering and Remote Sensing*, 59(11): 1625-1632.
- Adkins, K.F. and C. J. Merry, 1994. Accuracy Assessment of Elevation Data Sets Using the Global Positioning System, *Photogrammetric Engineering and Remote Sensing*, 60(2): 195-202.
- Adobe Systems Incorporated, 1998. *Adobe Photoshop 5.0 User Guide*, San Jose, California, 391 p.
- American Society of Photogrammetry, 1980. *Manual of Photogrammetry*, Fourth Edition, American Society of Photogrammetry, Falls Church, Virginia, 1056 p.
- American Society for Photogrammetry and Remote Sensing, 1989. ASPRS Interim Accuracy Standards for Large-Scale Maps, *Photogrammetric Engineering and Remote Sensing*, 55(7): 1038-1040.
- American Society of Photogrammetry, 1997. *Manual of Color Aerial Photography*, Second Edition (Warren Phillipson, Ed.), American Society for Photogrammetry and Remote Sensing, Falls Church, Virginia, 700 pp.
- Anderson, J.R., E.E. Hardy, J.T. Roach and R.E. Witmer, 1976. *A Land Use and Land Cover Classification System for Use with Remote Sensor Data*, Geological Survey Professional Paper 964, U.S. Government Printing Office, Washington, DC, 28 p.
- Ayeni, O.O., 1982. Phototriangulation: A Review and Bibliography, *Photogrammetric Engineering and Remote Sensing*, 48(11): 1733-1759.
- Baltsavias, E. P., 1998. Photogrammetric Film Scanners: Current Technologies, Products, Problems and User Requirements, *Geomatics Info Magazine*, 7(12): 55-61.

- Baltsavias, E.P., 1999. On the Performance of Photogrammetric Scanners, *Photogrammetric Week '99*, D. Fritsch and R. Spiller (Eds.), Wichmann Verlag, Heidelberg, Germany, pp. 155-173.
- Baltsavias, E.P. and B. Waegli, 1996. Quality Analysis and Calibration of DTP Scanners. *International Archives of Photogrammetry and Remote Sensing*, Vienna, Austria, 31(B1): 13-19.
- Bolstad, P.V., 1992. Geometric Errors in Natural Resource GIS Data: Tilt and Terrain Effects in Aerial Photographs, *Forest Science*, 38(2): 367-380.
- Boron, A., 1996. Calibration of Digital Images Produced with the Use of UMAX 1200 SE Scanner, *International Archives of Photogrammetry and Remote Sensing*, Vienna, Austria, 31(B1): 20-25.
- Blue Marble Geographics, 1994. *The Geographic Calculator*, Gardiner, Maine, 8 pp.
- Campbell, J.T., K. Green, J.C. Rugh and D.L. Peterson, 1996. Vegetation Mapping and Inventory in the National Parks of the Pacific Northwest, In *Digital Photogrammetry: An Addendum to the Manual of Photogrammetry*, (C.W. Greve, ed.), American Society for Photogrammetry and Remote Sensing, Bethesda, Maryland, pp. 180-182.
- Combs, R.G. and P.V. Bolstad, 1995. Positional Accuracy in a Natural Resource Database: Comparison of a Single-Photo Resection versus Affine Registration, *1995 Annual Convention and Exposition Technical Papers*, Charlotte, North Carolina, February 27 - March 2, Vol. 3, pp. 563-569.
- Cook, A.E. and J.E. Pinder, 1996. Relative Accuracy of Rectifications Using Coordinates Determined from Maps and the Global Positioning System, *Photogrammetric Engineering and Remote Sensing*, 62(1):73-77.
- Corbley, K., 1996. San Francisco Hills Challenge Orthorectification Process, *EOM*, 5(1): 29-31.
- Cox, W.E., 2001. *Great Smoky Mountains: The Story behind the Scenery*, KC Publications, Las Vegas, Nevada, 48 pp.
- Dalby, L. and E. Blaty, 2001. *Arkansas Mandeville SW Digital Ortho Quarter Quadrangle: National Standard for Spatial Data Accuracy Report*, July 23, 2001, 16 pp., <http://www.gis.state.ar.us/SGIC/ADOP/assess.htm>, accessed March 25, 2002.

- Dalby, L. and T. Rea, 2001. *Arkansas Warren NW Digital Ortho Quarter Quadrangle: National Standard for Spatial Data Accuracy Report*, August 20, 2001, 14 p., <http://www.gis.state.ar.us/SGIC/ADOP/assess.htm>, accessed March 25, 2002.
- Defense Mapping Agency, 1991. *Department of Defense World Geodetic System 1984, Its Definition and Relationships with Local Geodetic Systems* (Second Edition), DMA Technical Report 8350.2, Fairfax, Virginia, 175 p.
- Doren, R., K. Rutchey and R. Welch, 1999. The Everglades: A Perspective on the Requirements and Applications for Vegetation Map and Database Products, *Photogrammetric Engineering and Remote Sensing*, 65(2): 155-161.
- Doyle, F. J., 1997. Map Conversion and the UTM Grid, *Photogrammetric Engineering and Remote Sensing*, 63(4): 367-370.
- Dukes, R., 2001. *A Geographic Information Systems Approach to Fire Risk Assessment in Great Smoky Mountains National Park*, Masters Thesis, The University of Georgia, Athens, Georgia, 131 p.
- Eden, H.A., 1973. Point Transfer from One Photograph to Another, *Photogrammetric Record*, 7(41): 531-537.
- Elassel, A.A., 1976. *General Integrated Analytical Triangulation*, USGS Topographic Division, Reston, Virginia, 68 p.
- Environmental Systems Research Institute, 1998. *ESRI Shapefile Technical Description White Paper*, Environmental Systems Research Institute, Redlands, California, 34 p.
- Environmental Systems Research Institute and Aerial Information Systems (ESRI/AIS), 1998. *Photointerpretation and Map Generation Procedures at Rock Creek Park, Washington, DC*, Report submitted to the USGS-NPS Vegetation Inventory and Mapping Program, National Park Service, October 1, 1998, 24 p.
- Environmental Systems Research Institute and Aerial Information Systems (ESRI/AIS), 2000. *Photo Interpretation Report: Great Smoky Mountains National Park: Cades Cove and Mount Le Conte Topographic Quadrangles Pilot Study Area*, Report submitted to the USGS-NPS Vegetation Inventory and Mapping Program, National Park Service, July 1, 2000, 29 p.
- LaserSoft Imaging, 1999. *Silverfast 4 Quickstart Manual for the Epson Expression 836XL*, LaserSoft Imaging, Inc., Longboat Key, Florida, 28 p.
- Erdas, Inc., 2001. *Erdas Imagine OrthoBASE Users Guide*, Atlanta, Georgia, 548 p.

- Florida Biological Diversity Project (FBDP), 1996. *Florida Biological Diversity Project (Newsletter)*, Fall issue, Florida Cooperative Fish and Wildlife Research Unit, University of Florida, Gainesville, Florida, 7 p.
- Federal Geographic Data Committee (FGDC), 1998. *Geospatial Positioning Accuracy Standards, Part 3: National Standard for Spatial Data Accuracy (NSSDA)*, Report # FDGC-STD-007.3-1998, U.S. Geological Survey, Reston, Virginia, 25 p.
- Garbrecht, J. and P. Starks, 1995. Note on the use of USGS Level 1 7.5-Minute DEM coverages for landscape drainage analyses, *Photogrammetric Engineering and Remote Sensing*, 61(5): 519-522.
- GPA Associates, Inc., 1994. *PC Giant User's Manual*, 138 p.
- Hammond, Jensen, Wallen and Associates (HJW), 1998. Cover photograph. *Photogrammetric Engineering and Remote Sensing*, 64(4): Front cover.
- Harris, W.D., G.C. Tewinkel and C.A. Whitten, 1962. Analytical Aerotriangulation in the Coast and Geodetic Survey, *Photogrammetric Engineering*, 28(1): 44-69.
- Harris, W.D., 1962. Report on Analytic Aerotriangulation, *Photogrammetric Engineering*, 28(3): 403-410.
- Houk, R., 2000. *Great Smoky Mountains National Park: The Range of Life*, Great Smoky Mountains Natural History Association, Gatlinburg, Tennessee, 47 p.
- Hop, K.D., 2001. Personal Communication (July 21).
- Hurn, J., 1989. *GPS: A Guide to the Next Utility*, Trimble Navigation, Sunnyvale, California, 76 p.
- Hurn, J., 1993. *Differential GPS Explained*, Trimble Navigation, Sunnyvale, California, 56 p.
- Jensen, J. R., 1996. Issues Involving the Creation of Digital Elevation Models and Terrain Corrected Orthoimagery Using Softcopy Photogrammetry, In *Digital Photogrammetry: An Addendum to the Manual of Photogrammetry*, (C.W. Greve, ed.), American Society for Photogrammetry and Remote Sensing, Bethesda, Maryland, pp. 167-179.
- Jordan, T.R., 1981. *Measurement of Stream Channel Erosion Using Non-Metric Close Range Photogrammetry*, Master's Thesis, The University of Georgia, Athens, Georgia, 114 p.

- Kaiser, J., 1999. Great Smokies Species Census Under Way, *Science*, 284(5421): 1747-1748.
- Keller, M. and G.C. Tewinkel, 1967. *Block Analytic Aerotriangulation*, Technical Bulletin #35, U.S. ESSA, Coast and Geodetic Survey, November 1967, Rockville, Maryland, 101 p.
- Kemp, S. and K. Voorhis, 1993. *Trees of the Smokies*, Great Smoky Mountains Natural History Association, Gatlinburg, Tennessee, revised 1998, 125 p.
- Kletzu, R., 1996. GPS Aided Photogrammetry, In *Digital Photogrammetry: An Addendum to the Manual of Photogrammetry*, (C.W. Greve, ed.), American Society for Photogrammetry and Remote Sensing, Bethesda, Maryland, pp.71-73.
- Kodak, 1992. *Kodak Data for Aerial Photography*, Kodak Publication AS-29, Kodak Aerial Systems, Eastman Kodak Company, Rochester, New York, 222 p.
- Kolbl, O., 1996. Scanning and State-of-the-Art Scanners: Photogrammetric Scanners. In *Digital Photogrammetry: An Addendum to the Manual of Photogrammetry*, (C.W. Greve, ed.), American Society for Photogrammetry and Remote Sensing, Bethesda, Maryland, pp. 3-37.
- Kraus, K., 1993. *Photogrammetry: Volume 1 – Fundamentals and Standard Processes*, Fourth Edition, Ferd. Dummler Verlag, Bonn, Germany, 397 p.
- Light, D. L., 1992. The New Camera Calibration System at the U.S. Geological Survey, *Photogrammetric Engineering and Remote Sensing*, 58(2): 185-188.
- Light, D. L., 1993. The National Aerial Photography Program as a Geographic Information System Resource, *Photogrammetric Engineering and Remote Sensing*, 59(1): 61-65.
- Lillesand, T.M. and R.W. Keifer, 2000. *Remote Sensing and Image Interpretation, Fourth Edition*, John Wiley and Sons, New York, 724 p.
- Lo, C.P. and A.K.W. Yeung, 2002. *Concepts and Techniques of Geographic Information Systems*, Prentice Hall, Upper Saddle River, New Jersey, 492 p.
- Lucas, J.R., 1987. Aerotriangulation without Ground Control, *Photogrammetric Engineering and Remote Sensing*, 53(3): 311-314.
- MacKenzie, M.D., 1988. Remote Sensing of the Deciduous Vegetation of Great Smoky Mountains National Park, *Technical Papers of 1988 ACSM-ASPRS Annual Convention*, St. Louis, Missouri, March 13-18, Vol. 4, pp. 212-221.

- MacKenzie, M.D., 1991. *Vegetation Map of Great Smoky Mountains National Park based on Landsat Thematic Mapper Data: Accuracy Assessment and Numeric Description of Vegetation Types*, National Park Service Cooperative Studies Unit, The University of Tennessee, Knoxville, 11 p.
- MacKenzie, M.D., 1993. *The Vegetation of Great Smoky Mountains National Park: Past, present, and future*, Ph.D. Dissertation, The University of Tennessee, Knoxville, Tennessee, 154 p.
- Madden, M. and T.R. Jordan, 2001. Spatiotemporal Analysis and Visualization for Environmental Studies, *International Archives of Photogrammetry and Remote Sensing*, 34(4/W5): 71-72.
- Maune, D.F., 1996. Introduction to Digital Elevation Models (DEM), In *Digital Photogrammetry: An Addendum to the Manual of Photogrammetry*, (C.W. Greve, ed.), American Society for Photogrammetry and Remote Sensing, Bethesda, Maryland, pp. 131-134.
- Merchant, D.C., 1993. GPS Controlled Aerial Photogrammetry, *Photogrammetric Engineering and Remote Sensing*, 59(11): 1633-1636.
- Merchant, D.C., 1994. Airborne GPS-Photogrammetry for Transportation Systems, *Proceedings of the ASPRS/ACSM Annual Convention*, Baltimore, pp. 392-395.
- Moffit, F.H. and E.H. Mikhail, 1980. *Photogrammetry*, Harper and Row, Publishers, New York, 648 p.
- Moore, H.L.A., 1988. *The Roadside Guide to the Geology of the Great Smoky Mountains National Park*, University of Tennessee Press, Knoxville, Tennessee, 178 p.
- Mostafa, M.M.R. and J. Hutton, 2001. Airborne Kinematic Positioning and Attitude Determination without Base Stations, *Proceedings, International Symposium on Kinematic Systems in Geodesy, Geomatics and Navigation (KIS 2001)*, Banff, Alberta, Canada, June 4-8.
- National Climatic Data Center (NCDC), 2002. <http://lwf.noaa.gov/oa/ncdc.html>, updated March 28, 2002, viewed March 31, 2002.
- National Park Service, 1981. *Handbook 112: Great Smoky Mountains*, U.S. Department of Interior, National Park Service, Division of Publications, Washington, DC, 128 p.
- National Park Service, 1994. *Great Smoky Mountains National Park, North Carolina/Tennessee*, 22 x 30 cm. U.S. Department of Interior, Washington, DC, Government Printing Office, 1994 – 301-085/80187.

- National Park Service, 2000. National Park Service and Geographic Information Systems, http://www.nps.gov/gis/NPS_Overview.html, updated December 17, 2000, viewed March 25, 2002.
- National Park Service, 2001. *Great Smoky Mountains Trail Map*, 55 x 40 cm, scale ~1:169,000, U.S. Department of Interior, Washington, DC, Government Printing Office, 2001 – 472-470/00431.
- Newby, P.R.T., 1996. Digital Images in the Map Revision Process, *ISPRS Journal of Photogrammetry and Remote Sensing*, 51: 188-195.
- Nodvin, S.C., J.S. Rigell and S.M. Twigg, 1993. *An indexed reference database of the Great Smoky Mountains, North Carolina and Tennessee*, National Park Service Technical Report NPS/SERGRSM/NRTR-93/08, National Biological Survey-Cooperative Park Studies Unit, The University of Tennessee, Knoxville, Tennessee, 161 p.
- Novak, K., 1992. Rectification of Digital Imagery, *Photogrammetric Engineering and Remote Sensing*, 58(3): 339-344.
- Oimoen, D.C., 1987. Evaluation of a Tablet Digitizer for Analytical Photogrammetry, *Photogrammetric Engineering and Remote Sensing*, 53(6): 601-603.
- Ormsby, T., E. Napoleon, R. Burke, C. Groessl and L. Feaster, 2001. *Getting to Know ArcGIS Desktop*, ESRI Press, Redlands, California, 538 p.
- Positive Systems, 2001. *DIME Users Manual*, 153 p.
- Rutchev, K. and L. Vilchek, 1994. Development of an Everglades Vegetation Map using a SPOT Image and the Global Positioning System, *Photogrammetric Engineering and Remote Sensing*, 60(6): 767-775.
- Rutchev, K. and L. Vilchek, 1999. Air Photo Interpretation and Satellite Imagery Analysis Techniques for Mapping Cattail Coverage in a Northern Everglades Impoundment, *Photogrammetric Engineering and Remote Sensing*, 65(2): 185-191.
- R-WEL, Inc., 2000. *Desktop Mapping System Users Guide*, Version 4.2, Athens, Georgia, 389 p.
- Schwarz, C.R. (editor), 1989. *North American Datum of 1983, NOAA Professional Paper NOS 2*, National Geodetic Information Center, Rockville, Maryland, 256 p.

- Shenk, T., 1999. *Digital Photogrammetry, Volume 1*, TerraScience, Laurelville, Ohio, 428 p.
- Slama, C., C., H. Ebner and L. Fritz, 1980. Chapter IX: Aerotriangulation, *Manual of Photogrammetry*, Fourth Edition, American Society of Photogrammetry, Falls Church, Virginia, 1056 p.
- Snyder, J.P., 1987. *Map Projections – A Working Manual*, U.S. Geological Survey Professional Paper 1395, 383 p.
- Stevens, M., 2000. *AeroSys for Windows User's Manual*, 186 p.
- Tayman, W.P., 1984. User Guide for the USGS Aerial Camera Report of Calibration, *Photogrammetric Engineering and Remote Sensing*, 50(5): 577-584.
- Trimble Navigation Limited, 2002. All About GPS, <http://www.trimble.com/gps>, accessed April 7, 2002.
- U.S. Bureau of the Budget, 1947. *United States Map Accuracy Standards*, U.S. Geological Survey, Reston, Virginia, 1 p.
- U.S. Geological Survey, 1989. *North American Datum of 1989, Map Data Conversion Tables*, U.S. Geological Survey Bulletin 1875, United States Government Printing Office (three volumes).
- U.S. Geological Survey, 1990. *Digital Elevation Models Data Users Guide*, U.S. Geological Survey, Reston, Virginia, 51 p.
- U.S. Geological Survey, 1991a. *Standards for 1:12,000-scale Orthophoto Quarter-Quadrangles: National Mapping Program Technical Instructions*, U.S. Geological Survey, Reston, Virginia, 18 p.
- U.S. Geological Survey, 1991b. *Draft Standards for 1:24,000-scale Orthophoto Quarter-Quadrangles: National Mapping Program Technical Instructions*, U.S. Geological Survey, Reston, Virginia, 18 p.
- U.S. Geological Survey, 1994. *Draft Data Users Guide for Digital Orthophotos*, U.S. Geological Survey, Reston, Virginia.
- U.S. Geological Survey, 2000. *USGS Project and NAPP Camera Database Files*, Optical Science Laboratory, Reston, Virginia, <http://mac.usgs.gov/mac/tsb/osl/dbfiles.html>, updated June 22, 2000, accessed March 27, 2002.

- U.S. Geological Survey, 2001a. USGS-NPS Vegetation Mapping Program.
<http://biology.usgs.gov/npsveg/standards.html>, updated June 26, 2001, accessed March 2, 2002.
- U.S. Geological Survey, 2001b. *Digital Orthophoto Quadrangles*, U.S. Geological Survey, Fact Sheet 057-01, Reston, Virginia,
<http://mac.usgs.gov/mac/isb/pubs/factsheets/fs05701.html>.
- U.S. Geological Survey, 2001c. Overview of the USGS Digital Raster Graphic Program,
http://mcmcweb.er.usgs.gov/drg/drg_overview.html.
- Walker, S.L., 1991. *Great Smoky Mountains: The Splendor of the Southern Appalachians*, Elan Publishing, Charlottesville, Virginia, 63 p.
- Welch, R., 1989. Desktop Mapping with Personal Computers, *Photogrammetric Engineering and Remote Sensing*, 55(11): 1651-1662.
- Welch, R., 1992. Photogrammetry in Transition - Analytical to Digital, *Geodetical Info Magazine*, 6(7): 39-41.
- Welch, R., 1993. Low Cost Softcopy Photogrammetry, *Geodetical Info Magazine*, 7(12): 55-57.
- Welch, R. and A. Homsey, 1996. Datum Shifts for UTM Coordinates, *Photogrammetric Engineering and Remote Sensing*, 63(4): 371-375.
- Welch, R. and T.R. Jordan, 1983. Analytical Non-Metric Close Range Photogrammetry for Monitoring Stream Channel Erosion, *Photogrammetric Engineering and Remote Sensing*, 49(3): 367-374.
- Welch, R., and T.R. Jordan, 1996a. Using Scanned Air Photographs, In *Raster Imagery in Geographic Information Systems*, (S. Morain and S.L. Baros, eds.), Onward Press, Santa Fe, New Mexico, 493 pp.
- Welch, R., and T.R. Jordan, 1996b. Digital Orthophoto Production in a Desktop Environment, *GIM Magazine*, 10(7): 26-27.
- Welch, R., T.R. Jordan and M. Ehlers, 1985. Comparative Evaluations of the Geodetic Accuracy and Cartographic Potential of Landsat-4 and Landsat-5 Thematic Mapper Image Data, *Photogrammetric Engineering and Remote Sensing*, 51(9): 1249-1262.

- Welch, R., T.R. Jordan and M. Madden, 2000. GPS Surveys, DEMS and Scanned Aerial Photographs for GIS Database Construction and Thematic Mapping of Great Smoky Mountains National Park, *International Archives of Photogrammetry and Remote Sensing*, 33(B4/3): 1181-1183.
- Welch, R., M. Madden and R. Doren, 1999. Mapping the Everglades, *Photogrammetric Engineering and Remote Sensing*, 65(2): 163-170.
- Welch, R., M. Madden and R. Doren, 2002. Maps and GIS Databases for Environmental Studies of the Everglades, Chapter 9, *In*, (James W. Porter and Karen G. Porter, eds.) *The Everglades, Florida Bay, and Coral Reefs of the Florida Keys: An Ecosystem Sourcebook*, CRC Press, Boca Raton, Florida, pp. 259-279.
- Welch, R., M. Remillard and R.F. Doren, 1995. GIS Database Development for South Florida's National Parks and Preserves, *Photogrammetric Engineering and Remote Sensing*, 61(11): 1371-1381.
- Wells, D.E., N. Beck, D. Delikaraoglou, A. Kleusberg, E.J. Krakiwsky, G. Lachapelle, R.B. Langley, M. Nakiboglu, K.P. Schwartz, J.M. Tranquilla and P. Vanicek, 1986. *Guide to GPS Positioning*, Canadian GPS Associates, Fredricton, New Brunswick, Canada, 492 p.
- White, P. and J. Morse, 2000. The Science Plan for the All Taxa Biodiversity Inventory in Great Smoky Mountains National Park, North Carolina and Tennessee, Discover Life in America, Gatlinburg, Tennessee, http://www.discoverlife.org/sc/science_plan.html, accessed February 17, 2002.
- Whittaker, R.H., 1956. Vegetation of the Great Smoky Mountains, *Ecological Monographs*, 26(1): 1-69.
- Wolf, P.R. and B.A. DeWitt, 2000. *Elements of Photogrammetry with Applications in GIS*, Third Edition, McGraw Hill, New York, 608 p.

APPENDIX A

Camera Calibration Data For Wild RC 20 Camera #5132

Camera type: Wild RC20 with FMC
Camera Serial Number: 5132
Lens Type: Universal Aviogon A4-F
Lens Serial Number: 13162
Calibrated Focal Length: 153.4845 mm
Calibration Date: 8/1/1993
Owner: EarthData, Inc. (Maryland)

Radial Lens Distortion

Angle off-axis (degrees)	Distortion (mm)
7.5	0.000
15	-0.002
22.5	-0.003
30	-0.004
35	0.000
40	0.005

Fiducial Mark Coordinates

Fiducial #	X coordinate	Y coordinate
1	-106.0062	-106.0065
2	105.993	105.9941
3	-106.0051	105.9927
4	-105.9991	-106.0065
5	-110.0066	-0.0057
6	109.9959	-0.0035
7	-0.0054	109.9932
8	0.0001	-110.0064

Radial Distortion Coefficients:

R0 = 0.059655
R1 = -4.4 E-06
R2 = -2.3 E-11
R3 = 8.35 E-16

Principal Point Offset (x): -0.002
Principal Point Offset (y): -0.002

APPENDIX B

List of USGS Topographic Quadrangles, Abbreviations, Revision Date, DRG Name

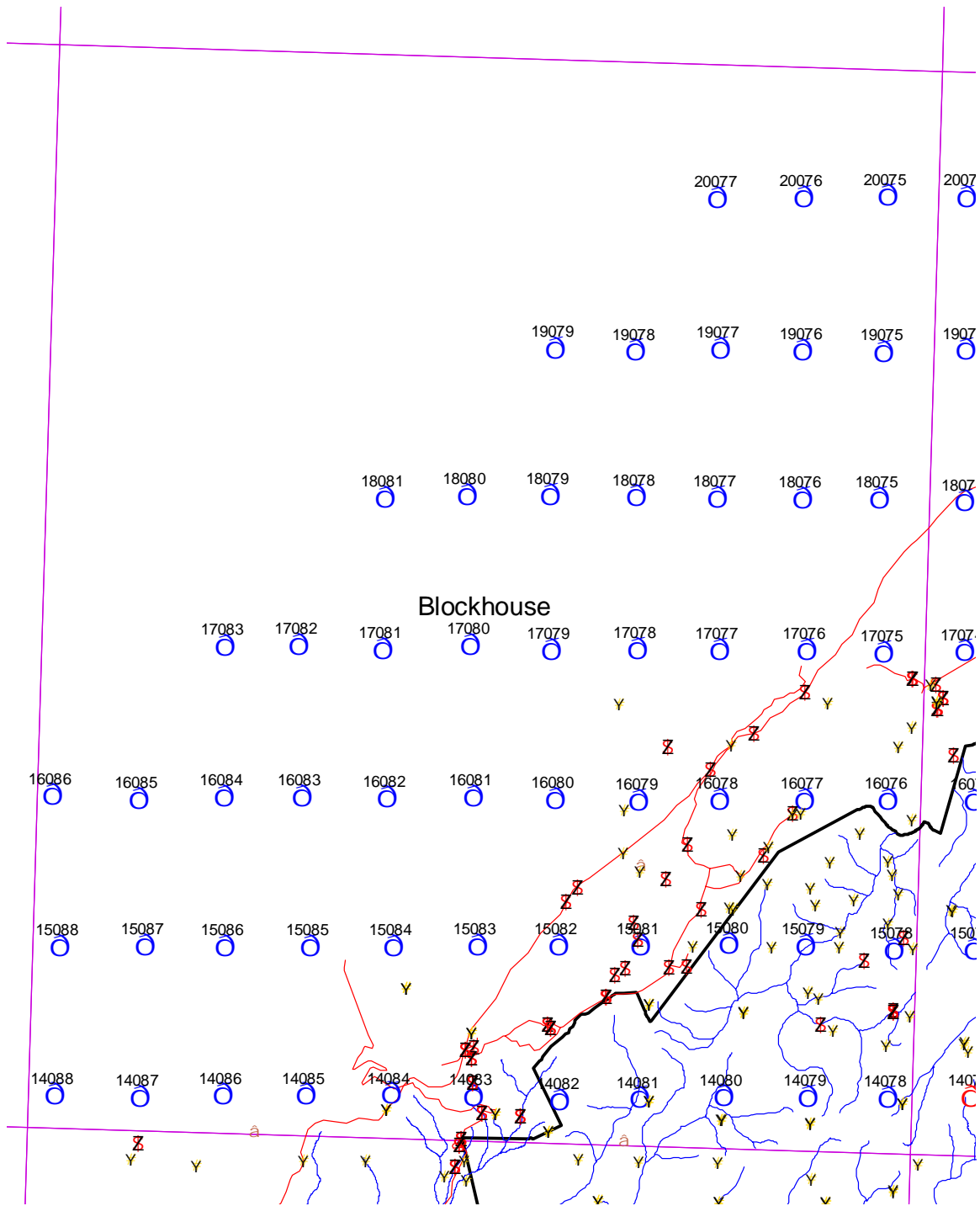
Quadrangle Name	Abbreviation	Revision Date*	USGS Index Number
Blockhouse	BLOC	1966	o35083f8
Bryson City	BRCI	1961 / 1978	o35083d4
Bunches Bald	BUBA	1964 / 1976	o35083e2
Cades Cove	CACO	1964 / 1976	o35083e7
Calderwood	CALD	1964	o35083e8
Clingmans Dome	CLDO	1964	o35083e4
Cove Creek Gap	COCR	1967	o35083f1
Dellwood	DELL	1941 / 1979	o35083e1
Fontana Dam	FODA	1961 / 1978	o35083d7
Gatlinburg	GATL	1979	o35083f5
Hartford	HART	1940 / 1968	o35083g2
Jones Cove	JOCO	1940 / 1978	o35083g3
Kinzel Springs	KISP	1953 / 1978	o35083f7
Luftee Knob	LUKN	1964	o35083f2
Mount Guyot	MOGU	1964	o35083f3
Mount Leconte	MOLE	1964	o35083f4
Noland Creek	NOCR	1961 / 1978	o35083d5
Silers Bald	SIBA	1964	o35083e5
Smokemont	SMOK	1964 / 1987	o35083e3
Tapoco	TAPO	1940 / 1978	o35083d8
Thunderhead Mountain	THMO	1964	o35083f6
Tuskegee	TUSK	1961 / 1987	o35083d6
Waterville	WATE	1940 / 1968	o35083g1
Wear Cove	WECO	1953 / 1974	o35083f6

* Revision date indicates the year of publication and, where appropriate, the year the quadrangle was either photo inspected or photo revised.

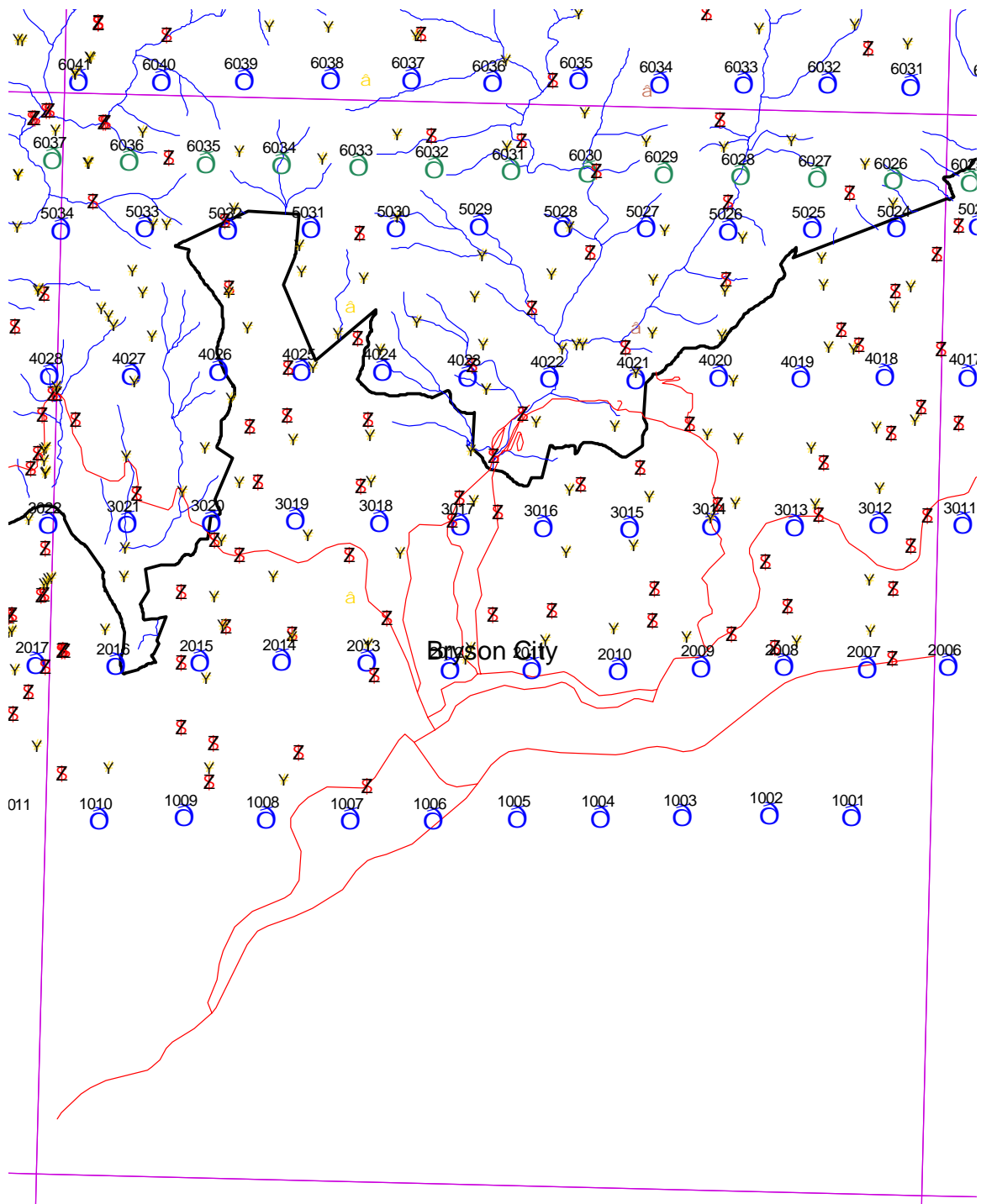
APPENDIX C

Photo Center, GCP and Pass Point Maps

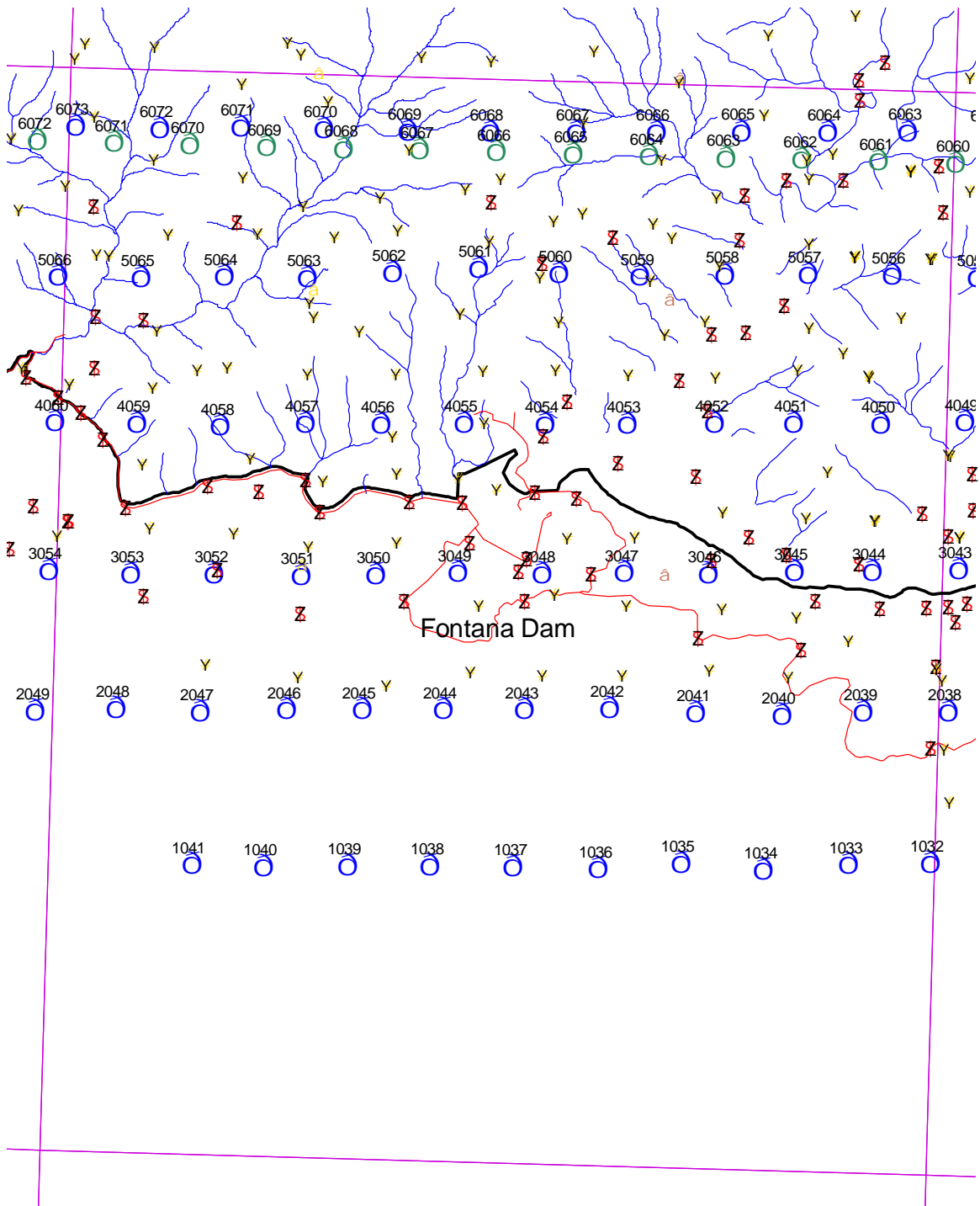
- C-1 Blockhouse
- C-2 Bryson City
- C-3 Fontana Dam
- C-4 Hartford
- C-5 Jones Cove
- C-6 Kinsel Springs
- C-7 Luftee Knob
- C-8 Mount Guyot
- C-9 Noland Creek
- C-10 Tapoco
- C-11 Thunderhead Mountain
- C-12 Tuskegee
- C-13 Waterville
- C-14 Wear Cove



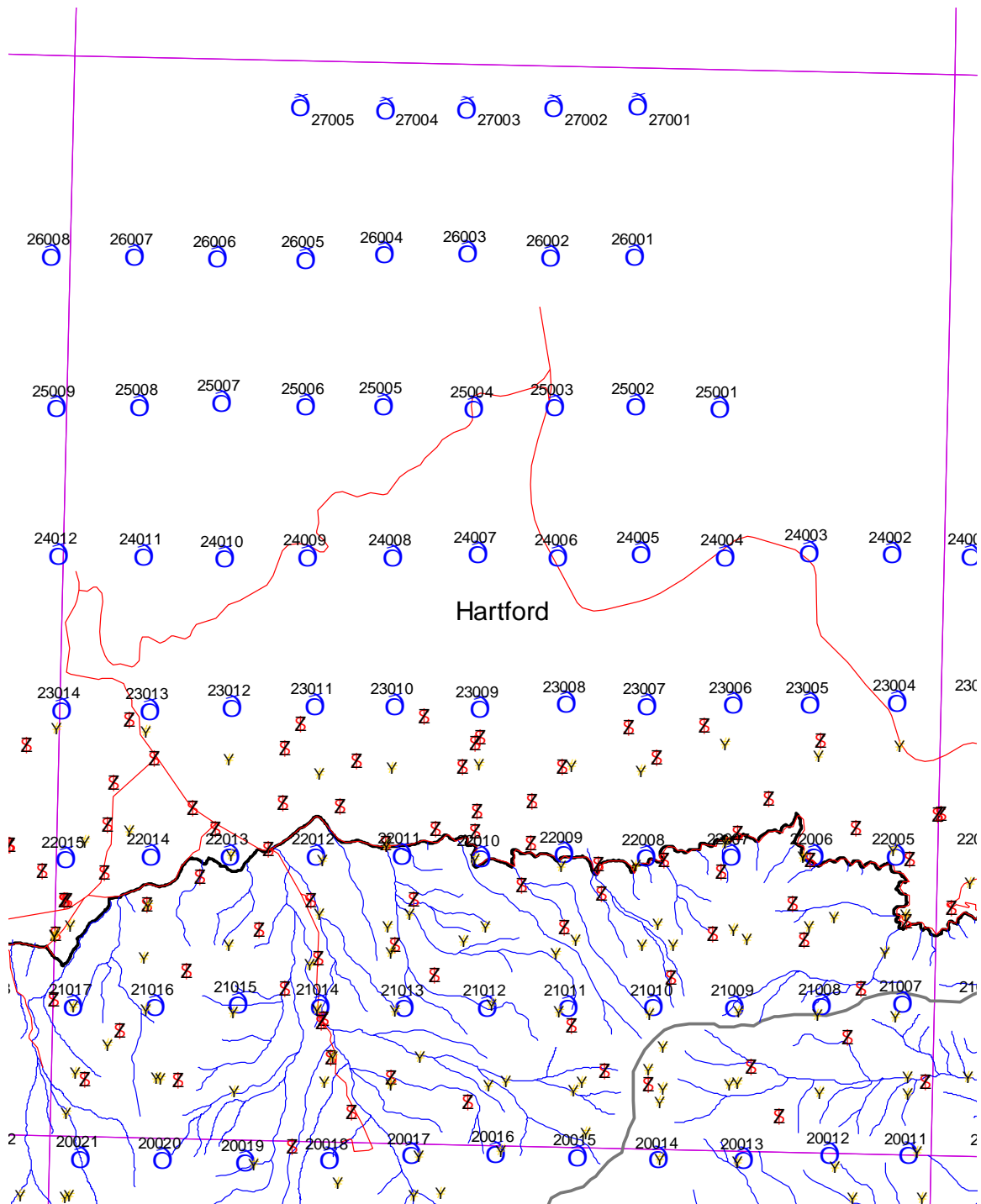
Appendix C-1. Photo centers, GCP and pass point distribution in the Blockhouse Quadrangle. There are 19 photos, 33 GCPs and 76 pass points in this quadrangle.



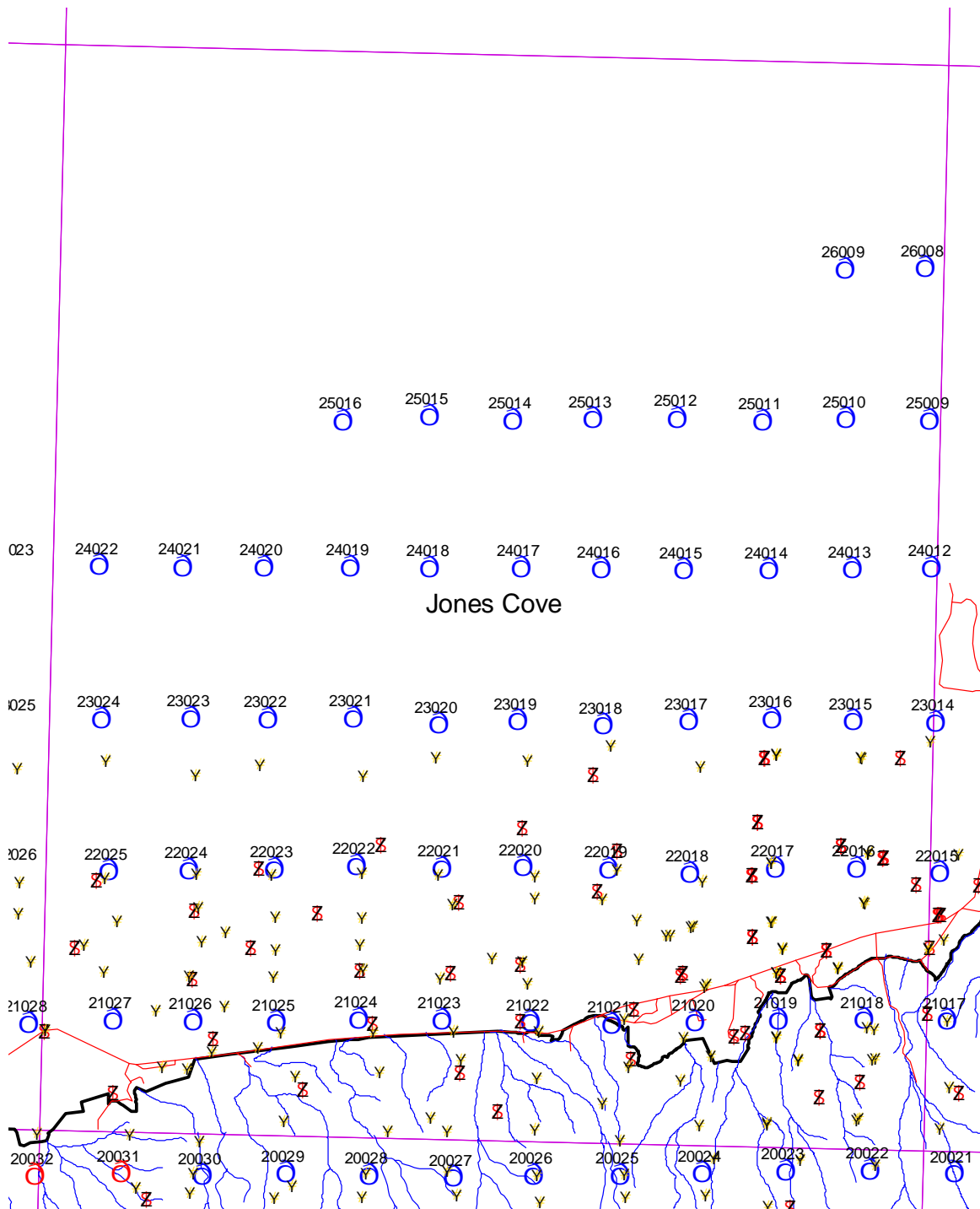
Appendix C-2. Photo centers, GCP and pass point distribution in the Bryson City Quadrangle. There are 43 photos, 76 GCPs and 150 pass points in this quadrangle.



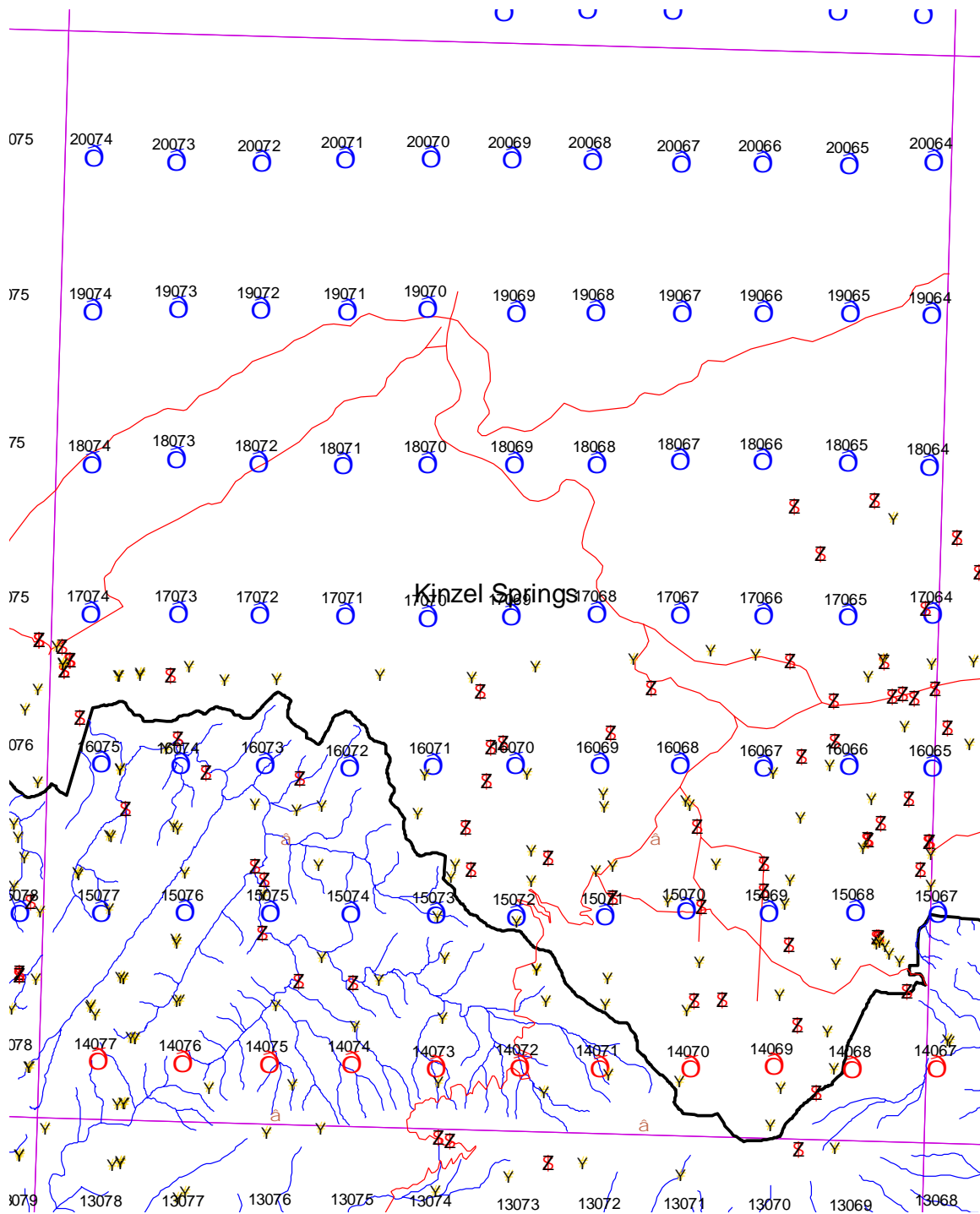
Appendix C-3. Photo centers, GCP and pass point distribution in the Fontana Dam Quadrangle. There are 42 photos, 57 GCPs and 120 pass points in this quadrangle.



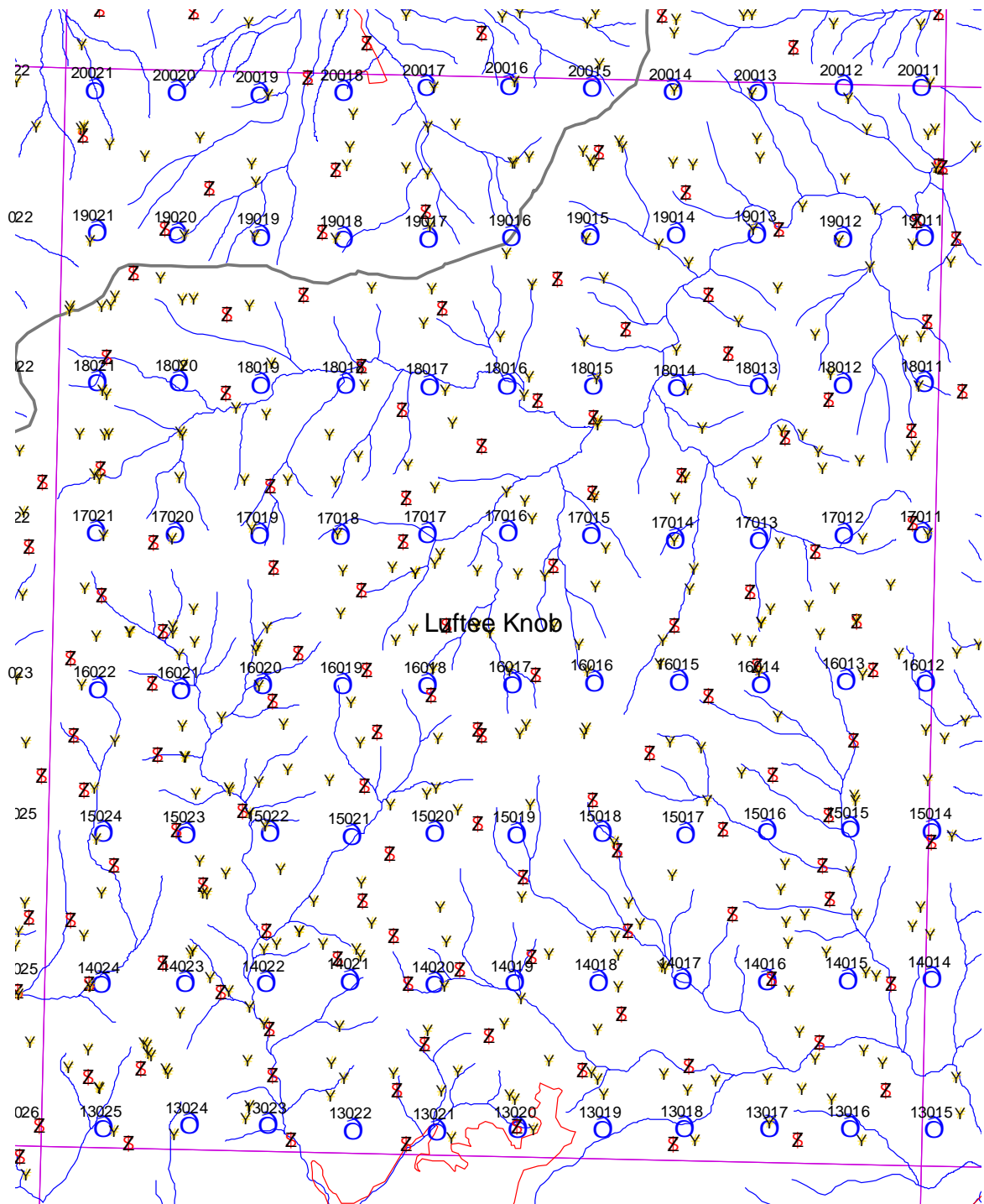
Appendix C-4. Photo centers, GCP and pass point distribution in the Hartford Quadrangle. There are 61 photos, 117 GCPs and 243 pass points in this large block that includes all of the photos from Waterville and flight lines 19 from Luttee Knob and Cove Creek Gap Quadrangles.



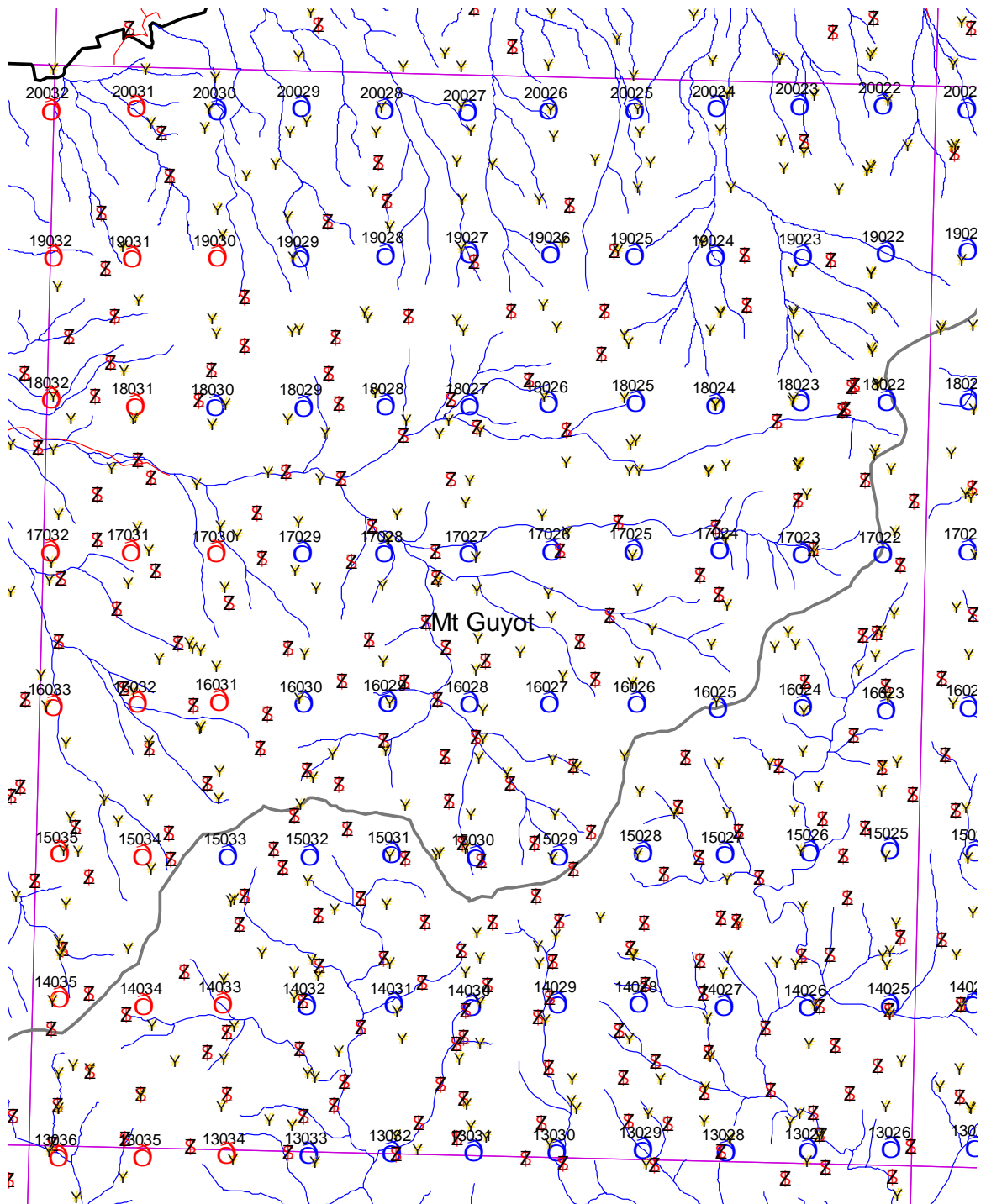
Appendix C-5. Photo centers, GCP and pass point distribution in the Jones Cove Quadrangle. There are 41 photos, 48 GCPs and 151 pass points in this block that also includes flight line 19 from the Mt Guyot Quadrangle.



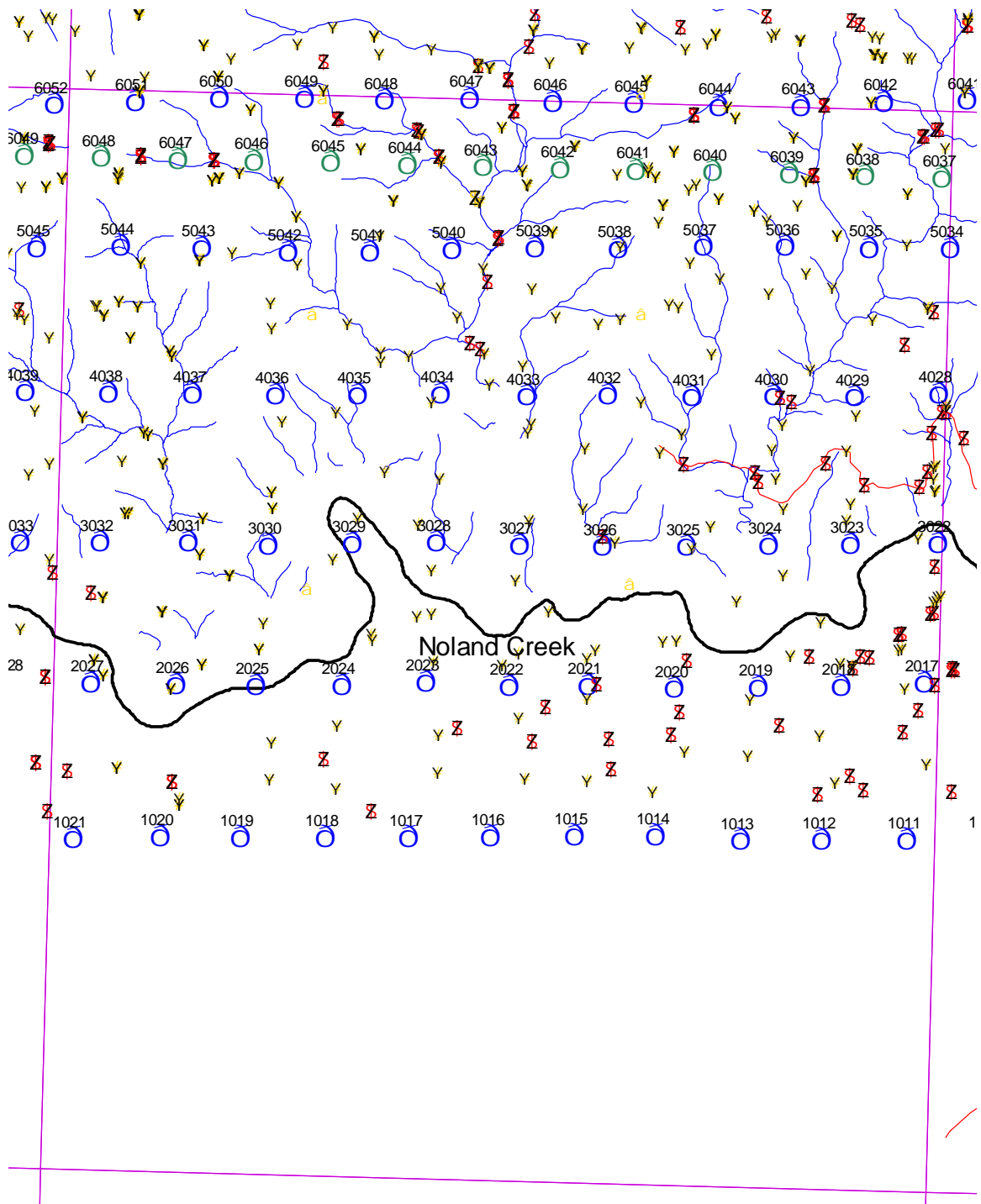
Appendix C-6. Photo centers, GCP and pass point distribution in the Kinsel Springs Quadrangle. There are 30 photos, 42 GCPs and 99 pass points in this quadrangle.



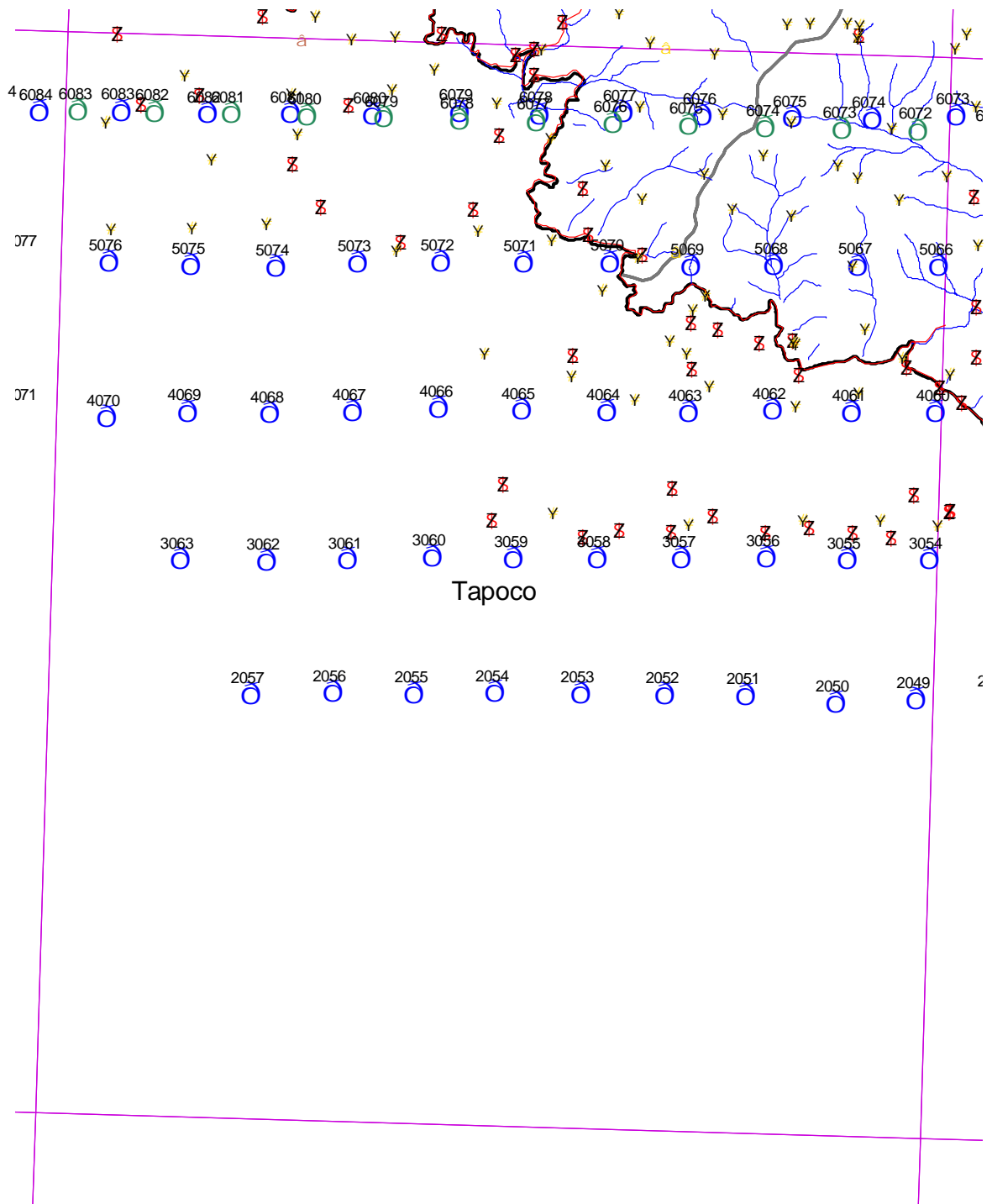
Appendix C-7. Photo centers, GCP and pass point distribution in the Luftee Knob Quadrangle. There are 61 photos, 97 GCPs and 264 pass points in this quadrangle. Photos in flight lines 19 and 20 were included in the solution for Hartford/Waterville and the northern portion of Cove Creek Gap.



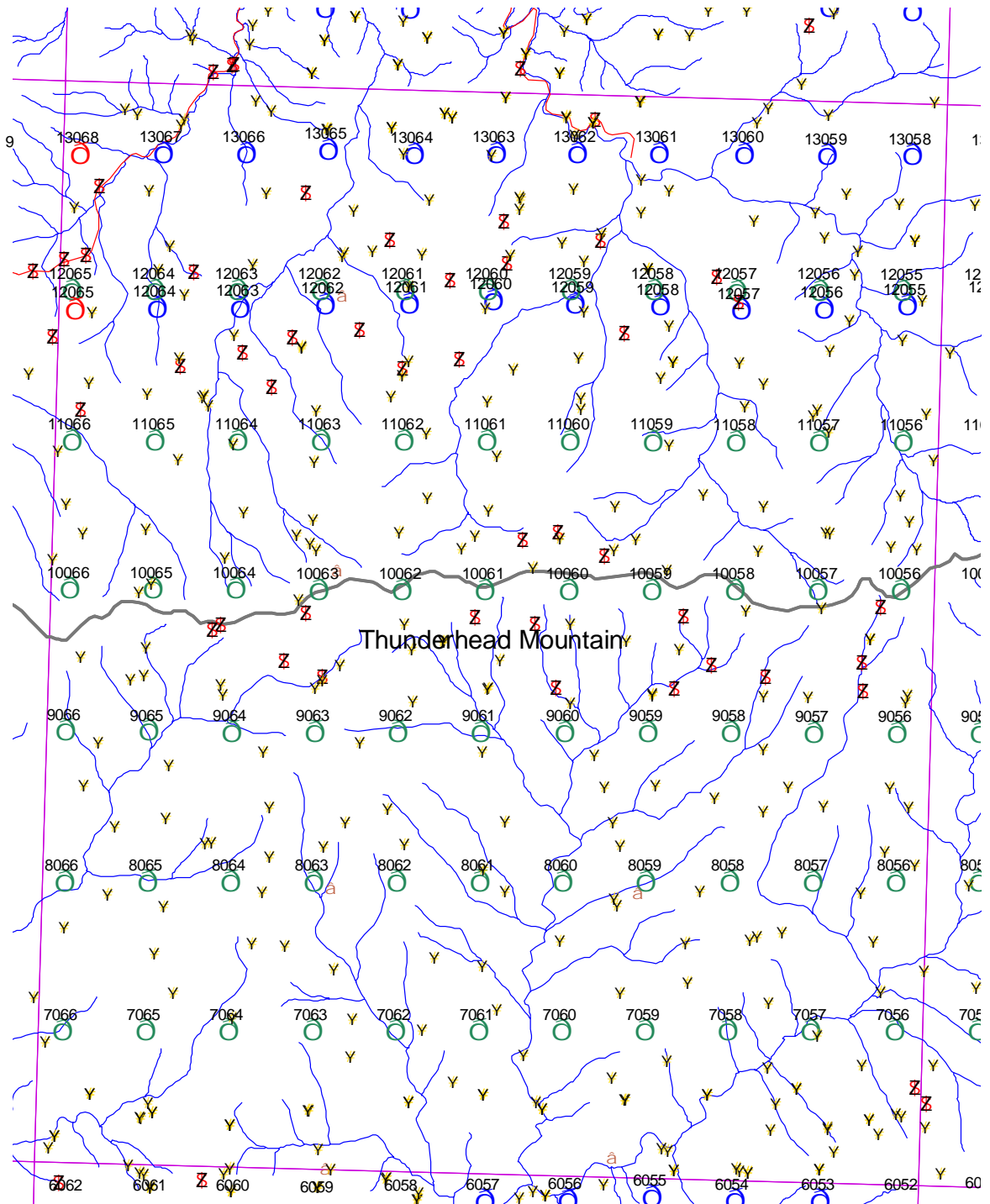
Appendix C-8. Photo centers, GCP and pass point distribution in the Mount Guyot Quadrangle. There are 77 photos, 133 GCPs and 365 pass points in this quadrangle. Photos from flight lines 19 and 20 were included with Jones Cove.



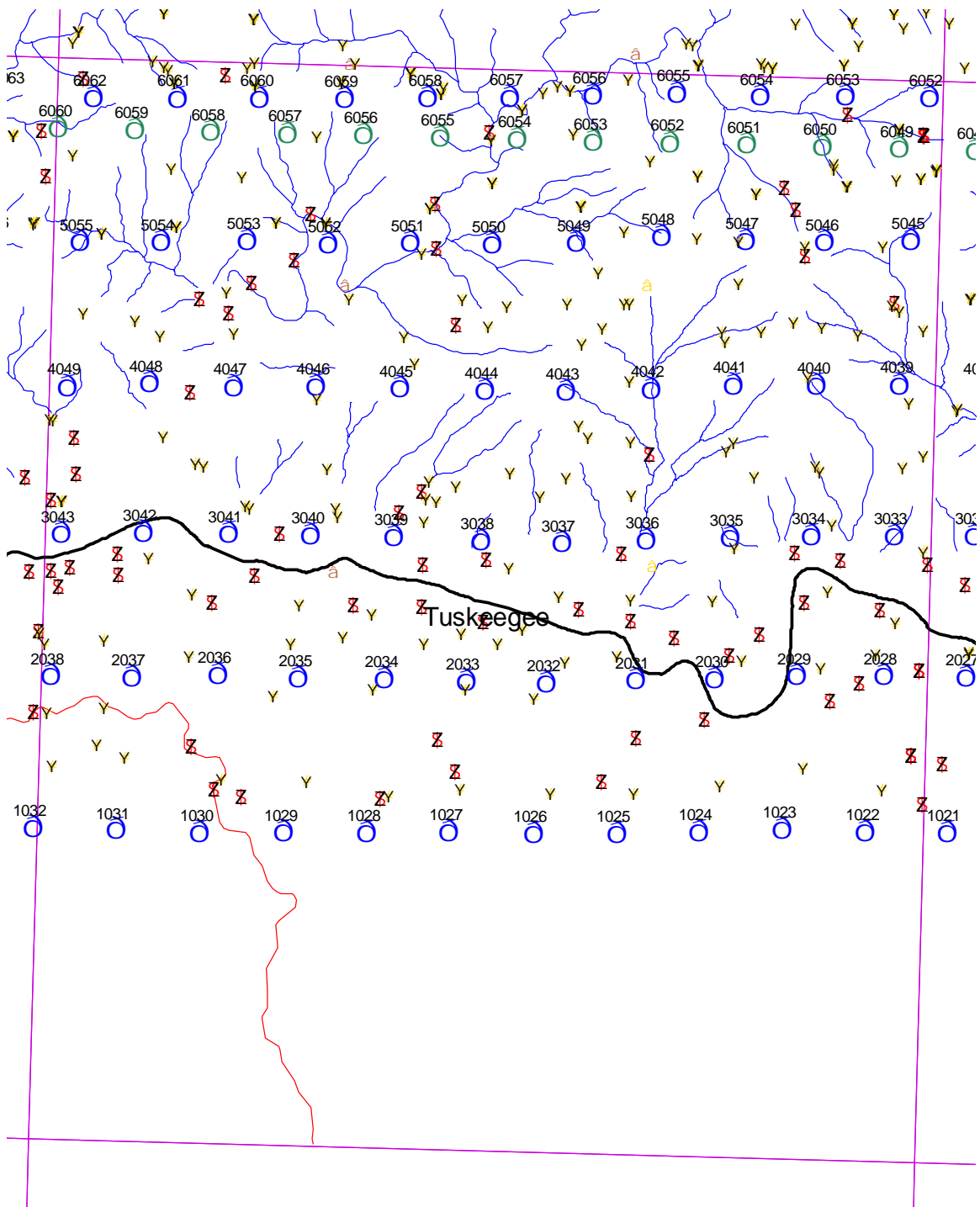
Appendix C-9. Photo centers, GCP and pass point distribution in the Noland Creek Quadrangle. There are 49 photos, 41 GCPs and 194 pass points in this quadrangle.



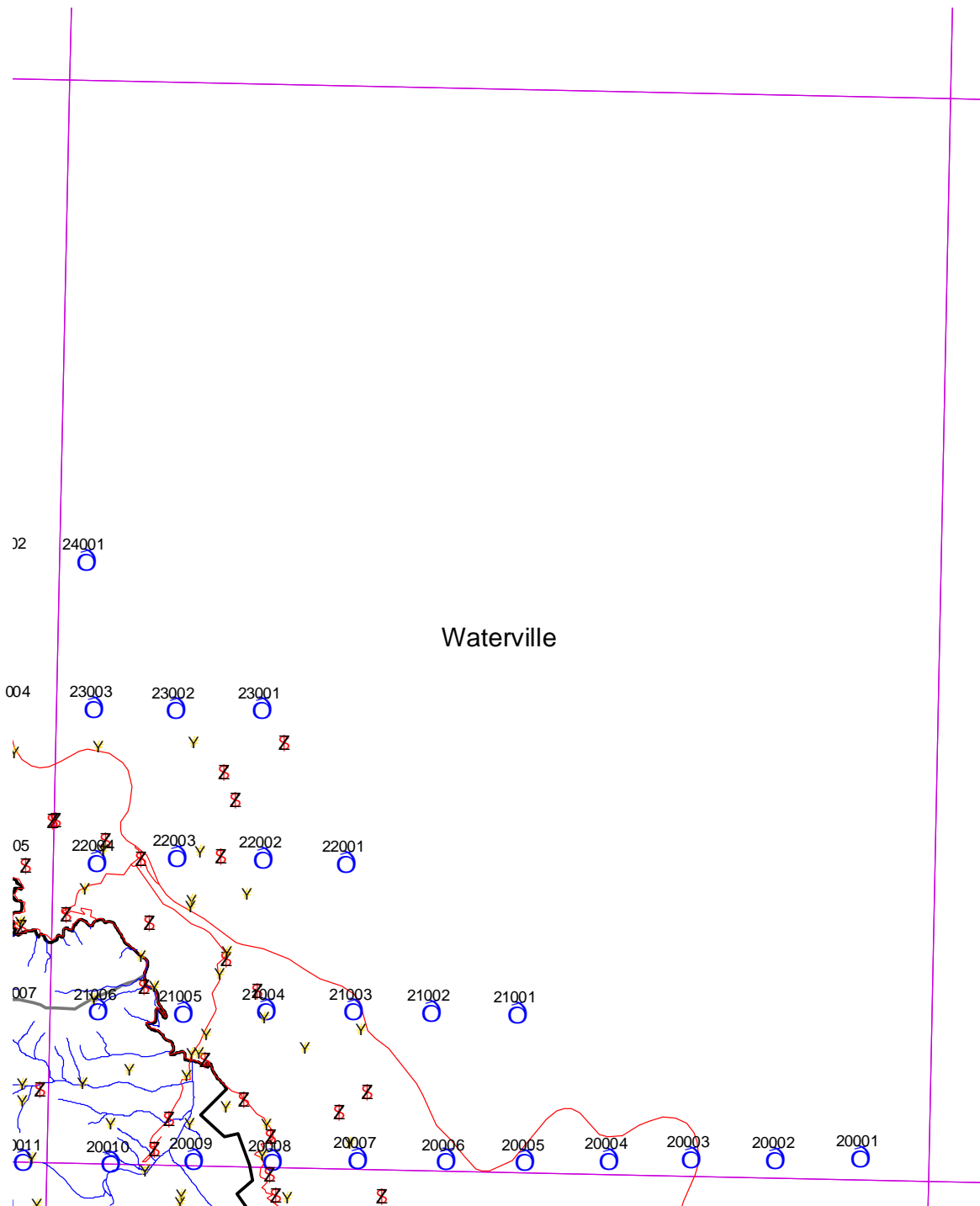
Appendix C-10. Photo centers, GCP and pass point distribution in the Tapoco Quadrangle. There are 19 photos, 37 GCPs and 60 pass points in this quadrangle.



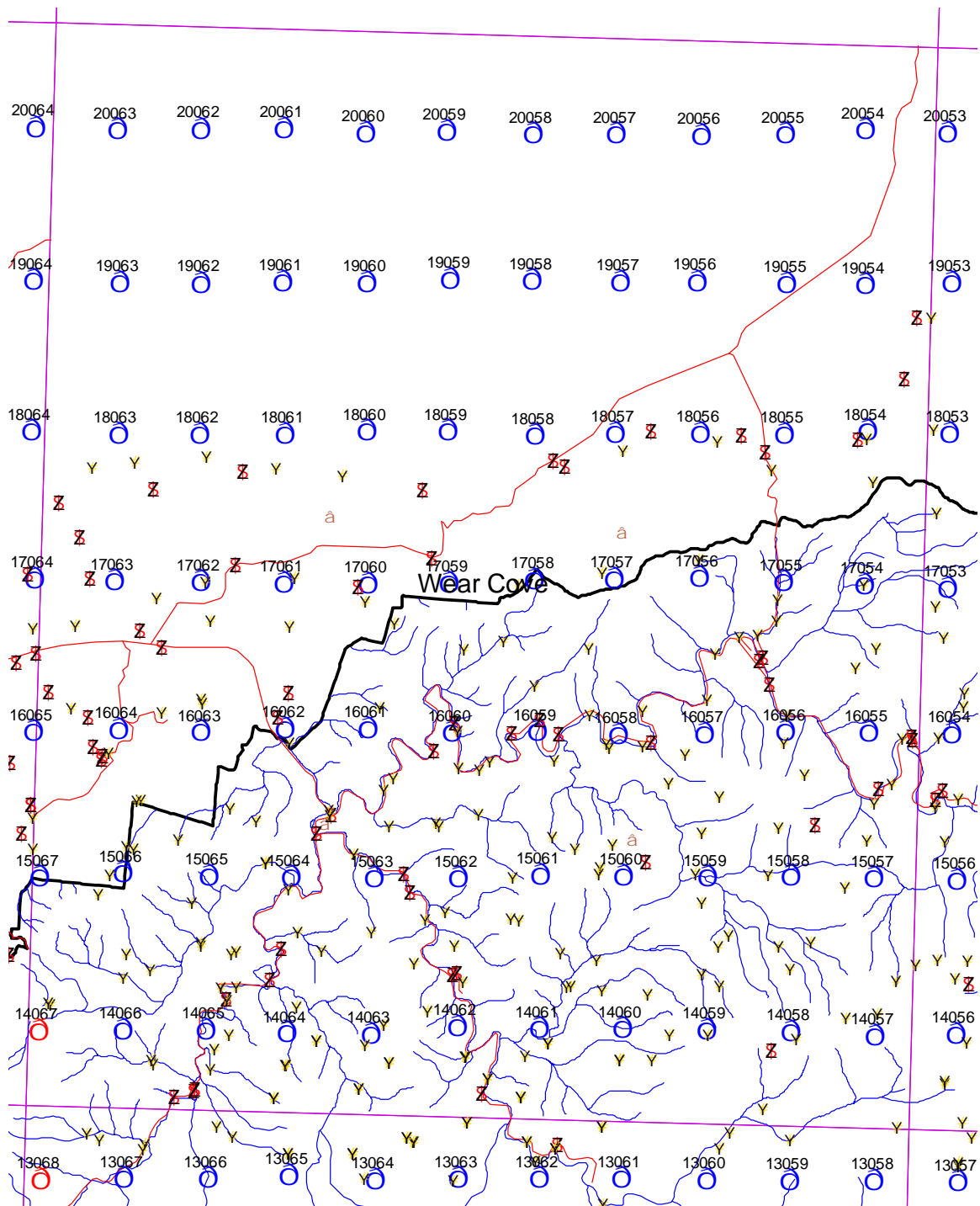
Appendix C-11. Photo centers, GCP and pass point distribution in the Thunderhead Mountain Quadrangle. There are 83 photos, 93 GCPs and 254 pass points in this quadrangle.



Appendix C-12. Photo centers, GCP and pass point distribution in the Tuskegee Quadrangle. There are 61 photos, 92 GCPs and 180 pass points in this quadrangle.



Appendix C-13. Photo centers, GCP and pass point distribution in the Waterville Quadrangle. There are 61 photos, 117 GCPs and 243 pass points in this large block that includes all of the photos from Waterville and flight lines 19 from Luttee Knob and Cove Creek Gap Quadrangles.



Appendix C-14. Photo centers, GCP and pass point distribution in the Wear Cove Quadrangle. There are 58 photos, 74 GCPs and 235 pass points in this quadrangle.